Thesis

On

Effect of Isothermal Annealing on Microstructural Morphology of Martensite in a Super Martensitic Stainless Steel subjected to different prior conditions

Submitted in partial fulfilment of the requirement for the award of degree

of

Master of Engineering

in

(PRODUCTION AND INDUSTRIAL ENGINEERING)

Submitted by:

Jasdeep

Roll No. 801182012

Under the guidance of

Dr. Tarun Nanda
Assistant Professor,
MED, TU, Patiala

Dr. B. Ravi Kumar
Principle Scientist (E-II)
MST Division, NML
Jamshedpur

DEPARTMENT OF MECHANICAL ENGINEERING

THAPAR UNIVERSITY

Patiala - 147004, Punjab, India

July, 2013

DECLARATION

I hereby declare that the thesis report entitled '***Effect of Isothermal Annealing on Microstructural Morphology of Martensite in a Super Martensitic Stainless Steel subjected to different prior conditions***' is an authentic record of my thesis carried out as requirement for the award of degree of M.E (Production and Industrial Engineering) at Thapar University, Patiala under the supervision of Dr. Tarun Nanda, Assistant Professor, Thapar University, Patiala and Dr. B. Ravi Kumar, Principle Scientist (E-II), MST Division, National Metallurgical Laboratory (NML), Jamshedpur, during 4th semester, Jan-July 2013.

The matter presented in this report has not been submitted in any other University/Institute for award of Masters of Engineering or any other degree.

Date: 22/7/13

Jasdeep

i

CERTIFICATE

This is to certify that the thesis entitled, **Effect of Isothermal Annealing on Microstructural Morphology of Martensite in a Super Martensitic Stainless Steel subjected to different prior conditions** being submitted by Jasdeep (Regd. No. 801182012), in partial fulfillment of the requirements for the award of degree of Master of Engineering (Production and Industrial Engineering) of Mechanical Engineering Department, Thapar University, Patiala, is a record of candidate's own work carried out by him under our supervision. To the best of our knowledge, the contents of this thesis do not form a basis for the award of any previous degree to anyone else.

Dr. Tarun Nanda
Assistant Professor,
MED, TU, Patiala

Dr. B. Ravi Kumar
Principle Scientist (E-II)
MST Division, NML, Jamshedpur

(Countersigned by)

Dr. Ajay Batish
Professor and Head
MED, TU, Patiala

Dr. S.K. Mohapatra
Dean of Academics Affairs
TU, Patiala

ii

ACKNOWLEDGEMENT

I would like to express my deep sense of gratitude to **Dr. B. Ravi Kumar**, Principle Scientist (E_2), Material Science and Testing division, National Metallurgical Laboratory (NML), Jamshedpur for his invaluable suggestions, excellent supervision, constant encouragement and critical discussion throughout the research work.

I express my deep sense of gratitude and a very sincere thanks to my guide **Dr. Tarun Nanda** Assistant Professor, Mechanical engineering department, Thapar University, Patiala for his indefatigable guidance and full support which helped me in the accomplishment of this project. I am highly indebted to them for their painstaking efforts and invaluable suggestions during the period of work.

I offer special regards to **Dr. B. Ravi Kumar**, Scientist (E_2), Material Science and Testing division, National Metallurgical Laboratory (NML), Jamshedpur for providing his immense support in performing the experimental work throughout my stay at NML, Jamshedpur.

The greatest thanks go to my **Parents** for their infinite support. Above all, I express my indebtedness to the "ALMIGHTY" for all His blessing and kindness.

Jasdeep

ABSTRACT

A ternary Fe–Cr–Ni super martensitic stainless steel alloy has been investigated during isothermal annealing after subjecting it to different prior conditions. The difference in morphology has been observed for the deformed and annealed martensite after isothermal annealing. The as-received hot rolled plate of martensitic microstructure was cold rolled to 80% thickness reduction. The phase transformation studies by X-ray diffraction analysis of hot and cold rolled specimens showed presence of retained austenite in air cooled as well as in water quenched state after solution annealing/austenizing temperature of 1060°C; showing austenite retention at room temperature, thus justifying its composition. Critical temperatures (A_s, A_f and M_s) were established from empirical relations and were validated with literature. Isothermal annealing was carried out on cold rolled and cold rolled annealed samples between A_s and A_f for different time periods ranging from 1 min to 2.5 min. The recrystallisation behaviour and microstructural morphology changes in cold rolled and cold rolled annealed material was studied in detail by Electron Back Scatter Diffraction (EBSD), and further supported by X-ray Diffraction analysis and hardness values measured by Vickers's hardness. The morphology of martensite changed entirely from lath martensite to equiaxed grains in cold rolled samples while cold rolled annealed samples showed both morphologies (i.e. equiaxed and typical martensitic lath) at certain isothermal annealing temperatures. The tensile properties of the cold rolled and the cold rolled isothermally annealed samples were evaluated and compared. The cold rolled isothermally annealed samples provided a good combination of strength and ductility at the selected heat treatment parameters.

List of Figures

List of Acronyms

Acronym	Full Name
ASS	Austenitic Stainless Steels
ASTM	American Society for Testing of Materials
BKD	Backscatter Kikuchi Diffraction
CCT	Continuous Cooling Transformations
CR	Cold Rolled
CRSS	Critical Resolved Shear Stress
DBTT	Ductile to Brittle Transition Temperature
DSC	Differential Scanning Calorimeter
DIM	Deformation Induced Martensite
DSS	Duplex Stainless Steels
EBSP	Electron Back Scatter Patterns
EBSD	Electron Back Scattered Diffraction
ESEM	Evnviornmental Scanning Electron Microscopy
FSS	Ferritic Stainless Steels
HAZ	Heat affected zone
HT	Heat Treated
HT-XRD	High Temperature X-Ray Diffractrometry
IGSCC	Intergranular stress corrosion cracking
IPF	Inverse Pole Figure
LCT	Lower Critical Temperature
M_s	Martensite Formation Starts
MSS	Martensitic Stainless Steel
OIM	Orientation Imaging Microscopy
PHSS	Precipitation Hardening Stainless Steels
SEM	Scanning Electron Microscope
SFE	Stacking Fault Energy
SMSS	Super Martensitic Stainless Steel
SS	Stainless Steel
TEM	Transmission Electron Microscopy
TMT	Thermo Mechanical Treatment
TRIP	Transformation Induced Plasticity
UCT	Upper Critical Temperature
UFG	Ultrafine Grained
UTS	Ultimate Tensile Strength
VOD	Vaccum Oxygen Decarburization
YS	Yield Strength
XRD	X-Ray Diffraction

Table of Contents

CHAPTER 1
INTRODUCTION

1.1 GENERAL

History places the discovery of stainless steels to the period of 1900-1915. The first commercial production of stainless steel was in June, 1920 at Brown Bayley's Steel Works in Sheffield, England. The first alloy contained 0.07% carbon and 11.7% chromium (McDowell et al., 1966). Stainless Steels are an imperative class of alloys whose importance can be manifested from plenitude of applications in which they are used, which are so diverse in itself that they vary from low end applications like utensils and furniture to very sophisticated ones such as space vehicles (Lo et al., 2009). In fact, the omnipresence of steels makes it impossible to enumerate their applications. Stainless steels have become important engineering materials due to their high strength and corrosion resistance and have made their presence inevitable in a wide range of applications (Yeddu et al., 2012). The word 'steel' means that iron is bulk constituent and stainless means that resistance to staining, corrosion or rusting even in severest of environment to which other steels might have failed. The battle against corrosion had been tried to be won in many other ways which are surface treatments such as plating, painting surfaces and many types of coatings but to no vain, as these surfaces need to be maintained every now and then. Another method which fascinated every metallurgist was alloying addition as it not only combats corrosion at surface but also within iron alloy's entire surface. This concept of alloying gave birth to new important class of alloys known as stainless steels (McDowell et al., 1966; Pickering, 1976).

Stainless steel is not an alloy having single composition but a large group of special alloys. Stainless steels are mainly characterized by being an iron base alloy containing more than about 11% Chromium (McDowell et al., 1966; Sedriks, 1996). The minimum 11% wt. chromium imparts stainless steels with remarkable resistance against chemical attacks; this phenomenon is commonly referred to as 'passivity'. The reason for good corrosion resistance of stainless steels is that they form a very thin, invisible surface film in oxidising environments. This film is an oxide that protects the steel from attack in aggressive environments (Sedriks, 1996). In more scientific manner, it can be said that when chromium is alloyed with iron, it changes the passivating potential of iron to much higher values and thus drastically lowers the critical current density (I_{crt}) required for passivation. As a consequence, at such a low value of $I_{crt,}$ self-passivation occurs. But this passivating film on

stainless steels is attacked under reducing conditions and Cl^- ions are destructive to passive films (Raghvan, 2006).

Along with good corrosion resistance, stainless steels also possess good strength at elevated temperatures which enlarges their field of application. Stainless steels provide good aesthetic look due to their provision of retention of beauty for quite long period. Even though their cost is many times to carbon steels but the properties they can provide makes them economically justified.

Stainless steels possess good fabricating characteristic. Stainless Steels are used extensively in food and beverage industry because they never show corrosion or rusting hence chances of contamination are minimal. Stainless steels resist destructive action of acids present in food too. Stainless steel is without equal in dairy industry which is responsible for protecting delicate flavour of milk and delivering uncontaminated milk and milk products such as cheese, butter, and ice cream. Corrosion resistance is the key to success of stainless steels in diary industry as it doesn't add to or subtract from flavour. Stainless steel is also used for sutures and plates which are either permanently or temporarily placed within human body. Automobile industry is the biggest consumer of stainless steel which normally takes 20 to 25% of its total production, mostly used for making trims or moldings. Other automotive uses of stainless steel include windshields wiper arms, hub caps, radio antennas, wheel rings, exhaust pipe extensions etc. Kitchen is the biggest consumer of stainless steel in home which is used for making cooking utensils, pots and pans, pressure cookers, roasting pans etc.

Application list of stainless steel is too large and with addition of new alloys everyday into this group it keeps on extending. Other applications of stainless steels are in soft drink industry, brewing industry, chemical industry etc. (McDowell et al., 1966; Singh, 2008; Lo et al., 2009).

1.2 CLASSIFICATION OF STAINLESS STEELS

Each one grade of stainless steel has some specific properties which makes it suitable for particular applications. Today, more than 180 different alloys can be recognized as belonging to stainless steel group and each year new ones and modification of existing ones appears. In some stainless steels, chromium content increases up to 30% and many other alloys are added to provide specific properties or ease of fabrication. For example nickel, nitrogen and molybdenum are added to help chromium in providing enhanced corrosion resistance properties; carbon, titanium, aluminium, copper are added for strength; sulphur and selenium

are added for machinability. Nickel also results in improved formability and toughness (Sedriks, 1996; Ma et al., 2011).

The structure of stainless steels after rapid cooling to room temperature from 1050^{o}C is given by Schaeffler diagram which is strictly not an equilibrium diagram. Three main type of structures exist in stainless steels i.e. ferritic, austenitic and martensitic (Sedriks, 1996). Depending on the properties, stainless steels may be characterized into several main classes (Pickering, 1976; Lo et al., 2009) as discussed below:

[1] Austenitic Stainless Steels (ASS)

[2] Ferritic Stainless Steels (FSS)

[3] Martensitic Stainless Steels (MSS)

[4] Precipitation Hardening Stainless Steels (PHSS)

[5] Duplex Stainless Steels (DSS)

[6] Mn-N substituted Austenitic Stainless Steels

Table 1.1 presents the composition, room temperature microstructure, characteristic properties and applications of the main type of stainless steels.

Table 1.1 Property Based Classification of Stainless Steels (McDowell et al., 1966; Pickering, 1976; Pickering, 1978; Sedriks, 1996; Gunn, 1997; Callister, 2007; Singh, 2008)

Type of Stainless Steel	Composition and Room Temperature Microstructure	Characteristics
AUSTENITIC STAINLESS STEEL	**COMPOSITION** Cr:-16-26% Ni:-6-22% Mo:-2.6% C<0.1% + other alloying elements **EXAMPLE** AISI 304 (C = 0.08% max; Cr = 18-20, Mn=2.0%, Ni = 8-12%) **MICROSTRUCTURE** Austenitic (FCC)	**PROPERTIES** • Very good corrosion resistance • Great formability due to FCC structure • Moderate strength but high strength with good ductility can be achieved by grain refinement cold and hot working (Tensile Strength:-490-860; Yield Strength:-205-575) • Very low stacking fault energy (SFE) value.so work hardened to large extent • Non-magnetic in nature • High thermal expansion than mild steels • Elongation in 50mm: 30-60% **APPLICATIONS** • Petrochemical industries, food industry, medical applications, paper making, marine environment etc. L**IMITATIONS** • Thermal conductivity is near half of mild steels • Difficult to machine unless they contain S and Se
FERRITIC STAINLESS STEEL	**COMPOSITION** Cr:-11.5-27% Ni:-0% Mn:-0.3-1.25% Si:-0.2-1% C:-O.12%	**PROPERTIES** • High Strength (Yield Strength:-205-575MPa; Tensile strength:-490-860MPa) • Cheaper than austenitic stainless steels (as expensive Ni is not added) • Excellent hot ductility (elongation in 50mm: 10-25%) • Magnetic in nature

	+other alloying elements **EXAMPLE** AISI 430 (C = .08% max; Cr = 16-18%; Mn=1.0%) **MICROSTRUCTURE** Ferritic (BCC)	• Higher thermal conductivity and lower thermal expansion than austenitic stainless steels **APPLICATIONS** • Heat treatment furnaces, boiler tubing, lining and tubing of vessels used in petroleum industries, nut and bolt etc **LIMITATIONS** • Cannot be strengthen by heat treatment • Get corroded in chloride and sulphur dioxide environment • Grain-refinement is difficult • Start coarsening rapidly at 600^{o}C (Compared to austenite at 900^{o}C) • Intergranular corrosion in heat effected zone • Embrittlement (400-500^{o}C) • Corrosion resistance, formability and toughness are lower than austenitic stainless steels
MARTENSITIC STAINLESS STEEL	**COMPOSITION** Cr:-11.5-18% Ni:-0-4% C:-0.1-1.2% + other alloying elements (like Mo, Nb, N, P etc) **EXAMPLE** AISI 403 (C = 0.15% max, Cr = 11.5-13%, Mn = 1.0%) **MICROSTRUCTURE** Martensite + delta ferrite + undissolved carbides (BCT)	**PROPERTIES** • Hardened and stronger than all type of steels except precipitation hardening steels and are hardenable by heat treatment • Excellent mechanical properties mainly strength (Tensile Strength:-480-1000MPa; Yield Strength:-275-860MPa) • Elongation in 50mm : 14-30% • Combination of good strength and ductility can be achieved by tempering at optimum tempering parameters and quenching treatment • Moderate corrosion resistance • Magnetic in nature • Can be cold worked without difficulty (especially with low carbon content) **APPLICATION** • Tool making for high hardness, pressure vessels, steam generators, mixer blades, cutting tools, SURGICAL stainless steels etc. **LIMITATIONS** • Low/ moderate corrosion resistance due to low chromium and nickel content • Difficult to machine (sulphur and selenium are added to improve machinability but at expense of corrosion resistance)
DUPLEX STAINLESS STEEL	**COMPOSITION** Cr:-2.5-7% Ni:-23-30% + other alloys (Ti, Mo, Si, Mn, etc.) **EXAMPLE** AISI 329 (C = 0.2% max; Cr = 23-28%, Mn=1.0%, Ni = 2.5-5%) **MICROSTRUCTURE** Ferrite + Austenite (BCC+ FCC)	**PROPERTIES** • Higher mechanical strength (Tensile Strength:- 680-900 MPa; Yield Strength:- 410-900 MPa) • Lower ductility as compared to austenitic stainless steels (elongation in 50mm: 10-48%) • Super-plasticity • Freedom from trans granular stress corrosion cracking (As the ferrite phase I immune to this type of failure) • Good weldability • Good corrosion resistance (similar to austenitic stainless steels) • Not suffer from intergranular corrosion **APPLICATIONS** • The duplex steels are used in powder industry feedwater heaters and flue-gas scrubers, in oil and gas production equipment; in chemical industry heat exchangers and pressure vessels, tanks, valves and shafting; as linear for oceangoing tankers and chemical transport barges; and as tanks and piping in breweries **LIMITATIONS** • **S**uffer from both type of embrittlement effects, 475^{o}C embrittlement as well as due to formation of sigma phase • Non-heat treatable

PRECIPITATION HARDENABLE STAINLESS STEEL	**COMPOSITION** Cr upto 17% C<0.1% + Other alloying elements **EXAMPLE** 17-4P H (C = 0.04% max; Cr =16%, Mn = 0.3%, Ni = 4.2%, Cu = 3.4%) **MICROSTRUCTURE** Austenite + Martensite (FCC + BCT)	**PROPERTIES** • Precipitation-hardening stainless steels are chromium-nickel alloys that can be hardened by an ageing treatment • high strength by precipitation hardening of the martensitic structure • Hardenable by heat treatment • Very high strength (Tensile Strength:-895-1100MPa; Yield Strength:- 276-1000MPa) • Elongation in 50mm : 10-35% **APPLICATIONS** • Extensive use in aerospace and high-technology industries **LIMITATIONS** • Expensive • Difficult to hot process • Restricted for use to high strength to weight ratio applications (Such as the high-temperature power plants)

1.3 MARTENSITIC STAINLESS STEELS

Martensitic Stainless Steels (MSS) consist mainly of 11.5-18% Cr, 0-4% Ni, and 0.1-1% C. Mo, V, Nb, Al and Cu are sometimes added (Sedriks, 1996). These steels have an austenitic structure at elevated temperatures in the range of 550-1000^{o}C which transforms into a martensitic structure by suitable cooling to room temperature. Depending on the composition and processing history, martensitic stainless steels consist of martensite, un-dissolved carbides and δ-ferrite (Isfahany et al., 2011). Heat treatment plays an influential role in determining the properties of MSS (Choi et al., 2007; Zheng et al., 2010; Leem at al., 2001; Ma et al., 2011; Ma et al., 2012a).MSS have complicated structure which requires careful heat treatment to avoid carbide precipitation and δ-ferrite formation and to ensure complete transformation to homogeneous martensitic structure and not to ferrite during cooling stages (Park and Park, 2007). The composition of MSS, austenizing temperature and cooling rate decides the temperature at which martensite formation starts (M_s). Increasing the austenizing temperature and the cooling rate results in lowering M_s temperature or increasing retained austenite content (Tsai et al., 2002; Park and Park, 2007).

Martensitic stainless steels are usually tempered to obtain an optimal combination of strength, ductility, and toughness. Tempering treatment after austenization or solution annealing is a must as it results in enhanced toughness and ductility values. Tempering at a temperature close to the lower critical temperature (LCT) results in finely distributed austenite along martensite interlath boundaries (Isfahany et al., 2011; Ma et al., 2011; Bojack et al., 2012).

The presence of retained austenite prior to tempering can lead to (Pickering, 1976; Wu et al., 2000):

- Possible distortion effect due to difference in coefficient of thermal expansion of both phases (as retained austenite transforms to martensite during tempering).
- Lower strength prior to tempering.
- Formation of fresh un-tempered martensite after tempering treatment.

The presence of retained austenite after tempering accounts for high toughness, especially the low temperature impact toughness (Song et al., 2010; Yu-rong et al., 2011; Ma et al., 2012b) but at higher operating temperatures, it has lower strength values (Klueh et al., 2005; Ma et al., 2012c). Retained austenite presence during tempering promotes re-precipitation of carbides during tempering because a large amount of carbon atoms are present in it (carbon is maximum in this phase). However, it also deteriorates pitting corrosion resistance as carbide precipitation results in chromium and molybdenum depletion zones (Park and Park, 2007). M_s temperature is the primary factor affecting the level of retained austenite in MSS and numerous empirical equations have been published to model the effect of given elements on the M_s temperature. If an alloy element lowers the M_s temperature, the retained austenite levels are increased and vice-versa (Wu et al., 2000). The volume fraction of retained austenite also depends on the quenching media (Balan et al., 1998). In general, medium carbon-contained MSSs which contain more than 0.2% wt. carbon should be heat treated (HT) and quenched at temperatures where undissolved carbides are totally dissolved into the matrix. At such high heat treatment temperatures, retention of austenite, formation of δ-ferrite and grain coarsening cannot be deserted. The microstructure of MSS consists of martensite phase, undissolved as well as re-precipitated carbides and δ-ferrite (Sedriks, 1996; Balan et al., 1998; Tsai et al., 2002; Choi et al., 2007; Wang et al., 2010; Isfahany et al., 2011). There exists an ambiguity on the effect of delta ferrite on impact properties. Some researchers believe that delta ferrite deteriorates the impact properties of material because of lack of cohesion between delta ferrite and the surrounding matrix, while others believe that it is relatively a soft phase which increases ductility and toughness of the material (Wang et al., 2010; Zheng et al., 2010). Carbides present in the microstructure present an important influence on hardness, corrosion resistance and wear characteristic. Type 410 is a classic and progenitor in commercial martensitic stainless steels and is widely used in many industries for essential parts due to its high corrosion resistance, high strength and toughness (Tsai et al., 2002). Martensitic stainless steels are used for manufacturing components with excellent mechanical properties and moderate corrosion resistance (Sedriks, 1996; Choi et al., 2007;

Park and Park, 2007; Isfahany et al., 2011). Major advantage of MSS over other elevated temperature alloys such as austenitic stainless steels and super alloys is good thermal properties (Klueh et al., 2005). MSSs can operate under both low and high temperature conditions (Isfahany et al., 2011) and their properties can be changed by heat treatment process, in accordance to application for which they are required to be used (Choi et al., 2007). MSSs are widely used in steam generators, pressure vessels, mixer blades, cutting tools, and for offshore platforms for oil extraction etc. They are also used in hydraulic turbines, valve bodies, building structures, vehicle construction, mining machines, ship building and high pressure pipes (Tsai et al., 2002; Choi et al., 2007; Park and Park, 2007; Wang et al., 2010; Zheng et al., 2010; Isfahany et al., 2011; Ma et al., 2012c; Ye et al., 2012).

In MSSs, the chromium-depleted regions around carbides precipitated at certain temperatures are thought to act as preferential sites for pitting corrosion (Sedriks, 1996; Choi et al., 2007). MSSs often suffer from poor resistance to corrosion and failure in surroundings containing H_2S, CO_2 and Cl^-(De-ning et al., 2010). The formation of brittle carbides at grain boundaries has also limited the use of high carbon martensitic stainless steels (Park et al., 2004; Yu-rong et al., 2011).

The complicated structure of MSS containing un-dissolved carbides and δ-ferrite within matrix limits their application as presence of these two deteriorates there toughness properties and corrosion resistance properties respectively.

1.4 SUPER MARTENSITIC STAINLESS STEELS

The concept of Super Martensitic Stainless Steels (SMSS) came into existence at the end of 1950's. These were known by the name of soft martensitic stainless steels due to their low carbon content. Compared with the traditional martensitic stainless steels, the strength, ductility, weldability and corrosion resistance of SMSS are greatly improved by lowering the carbon content and increasing the nickel and molybdenum contents (Park et al., 2004; Bojack et al., 2012; Ma et al., 2012c; Ye et al., 2012, Yu-rong et al., 2011). These steels are based on the Fe–Cr–Ni–Mo system with 4–6 wt% of Ni, 0.5–2.5 wt% of Mo, low amounts of carbon, nitrogen, phosphorus and sulphur (C ≤ 0.02, N, P, S ≤ 0.03) and sometimes micro-alloyed with elements of Ti, Nb, and V. Micro alloying elements of Ti, Nb and V are usually added to combine with residual carbon and nitrogen to form carbo-nitrides, thereby increasing the strength (De-ning et al., 2010; Ma et al., 2011; Yu-rong et al., 2011; Ma et al., 2012b; Ma et al., 2012c; Ye et al., 2012). Typical values of mechanical properties range within the following: 650–750 MPa of 0.2% yield strength, 880–950 MPa of ultimate tensile

strength, elongation at rupture up to 20% and impact energy up to 100 J (Ma et al., 2011). Molybdenum is added in order to improve the corrosion resistance but it is a δ-ferrite stabilizer. However, nickel needs to be added to balance the effect of molybdenum. The increased nickel content extends the gamma phase field and maintains martensitic microstructure without delta ferrite formation upon cooling (Pickering, 1976; Ye et al., 2012). SMSS properties can be changed by heat treatment. Mechanical properties of SMSS are strongly dependent on the microstructure comprising of martensite with retained austenite film occurring at martensite lath boundaries and within laths which can be obtained by heat treatment processes such as normalizing from austenite field temperature and tempering above Ac_1 temperature (Ma et al., 2011; Bojack et al., 2012). In order to get required microstructure, heat treatment process should consist of austenizing (above Ac_3) followed by cooling to ambient temperature and single or double tempering (above Ac_1) (Bojack et al., 2012). The presence of retained austenite is reported to be very effective in restoring toughness and elongation but it lowers the strength properties. The reverse austenite fraction varies with tempering temperature and time and it also depends on content of austenite stabilizing elements (De-ning et al., 2010; Yu-rong et al., 2011; Bojack et al., 2012). The normal microstructure of SMSS after normalizing and tempering comprises of tempered martensite and reverse austenite but at times some δ-ferrite also gets introduced. δ-ferrite formed is a controversial phase in steels which becomes very difficult to be removed by conventional heat treatment processes except for high temperature diffusion annealing which too can bring burning losses and severe distortion of the casting (Wang et al., 2010; Zheng et al., 2010; Yu-rong et al., 2011).

The basis of SMSS alloy design is (Pickering, 1976; Ma et al., 2012c):

- Increase in effective chromium content by reducing carbon to improve corrosion resistance and weldability
- addition of nickel to maintain martensitic microstructure without δ-ferrite formation
- addition of molybdenum to provide resistance to localized corrosion

Although SMSS has a very low carbon concentration, intergranular stress corrosion cracking (IGSCC) is still observed at heat-affected zone because of the occurrence of chromium-depleted zones caused by the precipitation of chromium carbides (Sedriks, 1996; Raghvan, 2006; Choi et al., 2007; Ma et al., 2012c).

Micro-alloying additions are adopted to enhance localized corrosion resistance and to some extent the strength values of these steels (Ma et al., 2012c). Micro-alloying elements such as

titanium have higher affinity for carbon than chromium, forming preferentially carbides of micro-alloying elements (such as TiC) at the expense of $Cr_{23}C_{6.}$ This makes the SMSS less prone to localized corrosion. Effect of other micro-alloying elements such as nitrogen and niobium is also influential in determining the corrosion resistance of SMSS (Raghvan, 2006; Ma et al., 2012c).

Due to their good corrosion resistance properties, SMSS have replaced the more expensive duplex stainless steels in many offshore applications etc. owning to the excellent combination of toughness, weldability along with good corrosion resistance. These stainless steels present an economic alternative against carbon steels and they are free from the use of coating and inhibitors (Ma et al., 2011; Bojack et al., 2012; Ma et al, 2012c; Ye et al., 2012). As a new economical low carbon MSS, SMSS have been widely used for petroleum and natural gas transmission pipelines, ship building, offshore drilling platforms, and hydraulic turbine blade industry (Ye et al., 2012). SMSS are extensively used in hydraulic turbines, valve bodies and high pressure pipes in power generation because of high strength, good toughness and corrosion resistance properties (Yu-rong et al., 2011).

Due to lower C content than MSS they show good strength, ductility, weldability and corrosion resistance. Ni enrichment leads extends the gamma phase field which helps in maintaining martensitic structure without δ-ferrite formation on cooling. The presence of retained austenite further enhances the toughness and ductility properties. Micro-alloying addition of elements such as Ti, N and Nb having higher affinity for C than Cr helps in improving localized corrosion caused due to Cr depletion or Chromium carbides formation.

1.5 HEAT TREATMENT OF MARTENSITIC STAINLESS STEELS

The main factors which affect the heat treatment of martensitic and super martensitic stainless steels are discussed as follows:

1.5.1 Effect of Austenization Temperature

The microstructure of martensitic stainless steels mainly consists of martensite, retained austenite and δ-ferrite. δ-ferrite is considered to have deleterious effect on mechanical properties while retained austenite is considered to improve toughness and ductility at the cost of strength. Austenization temperature plays a pivotal role in deciding the fraction of retained austenite at room temperature. With increase in austenization temperature, the M_s temperature lowers which facilitates austenite retention at room temperatures. The cooling

rates followed from the austenization temperature also affect the austenite fraction. Higher cooling rates result in lower M_s temperature. Hence, the M_s will be lowest for high austenization temperatures and high cooling rates (Tsai et al., 2002; Park and Park, 2007). Isfahany et al (2011) reported that the ultimate tensile strength increases with rise in austenization temperature. Even though austenite produced will tend to lower the strength values but with rise in austenization temperature, the carbides dissolve within the matrix. Carbide dissolution results in carbon saturation within the matrix and results in lattice distortion of the martensite formed on cooling from higher austenization temperature. Also, carbon saturation results in introduction of twin boundaries and more dislocations.

1.5.2 Effect of Tempering Temperature

All martensitic stainless steels hardened by formation of martensite phase need to be tempered to give useful mechanical properties. Tempering of low carbon 12% Cr steel at as high a temperature as possible is requisite to obtain optimal combination of ductility, toughness and stress corrosion resistance along with maximum possible strength (McDowell et al., 1966; Pickering, 1976; Sedriks, 1996). The general trend of hardness, toughness and corrosion rate is shown in Figure 1.1 which is characteristic of all MSS (McDowell et al., 1966). Tempering in the range, 450-600^{o}C yields poor impact resistance and corrosion resistance which is attributed to formation of precipitates in this range (Sedriks, 1996). While tempering, precipitates get formed and with rise in tempering temperature, these precipitates get coarsened (McDowell et al., 1966; Pickering, 1976; Ma et al., 2012b) which further decreases the hardness value in accordance to Figure 1.2 (Isfahany et al., 2011). Some precipitates formed during tempering produce more secondary hardening effect on comparing to others. M_2X precipitates produce a pronounced secondary hardening effect and their formation is accentuated by presence of N_2, Mo, and V (Pickering, 1976).

Tempering temperature plays a significant role in deciding strength, ductility and toughness values of MSS. Toughness/ductility and strength are contrary to each other when it comes to tempering temperatures. From published tempering curves on MSS, it is quite evident that when maximum strength is obtained at tempering below 400^{o}C, toughness/ductility values are not that good. Reverse austenite fraction formed during tempering is determinant in deciding toughness and ductility which is reported to one who help in resorting toughness and ductility but it lowers strength values (De-ning et al., 2010; Isfahany et al., 2011; Yu-rong et al., 2011; Bojack et al., 2012;). Reverse austenite is maximum at tempering temperature range of 600-650^{0}C and when it is dispersed in

martensite matrix; it can improve the mechanical properties by means of absorbing deformation work when the plastic deformation of material occurs. Presence of reverse austenite along grain boundaries prevents crack propagation along martensitic laths; relieve the stress concentration caused by dislocations and thus increases the toughness of material (Leem et al., 2001; Yu-rong et al., 2011). The increase in volume fraction of reversed austenite is caused by increase in driving force of martensite to austenite transformation with raised temperature. At lower temperatures, the thermal stability of reverse austenite is good as it is rich in austenite stabilizing elements. Thus, it becomes difficult for lesser amount of austenite formed at low temperatures to transform into martensite while cooling. At higher tempering temperature of above 650^{o}C, the austenite formed is higher but concentration of austenite stabilizing elements decreases. As a result, the higher austenite formed transforms back to martensite (Bojack et al., 2012; Isfahany et al., 2011; Leem et al., 2001; Ma et al., 2012b; Park et al., 2004; Yu-rong et al., 2011). Also the increase in quench-in-vacancies with temperature lowers the stability of austenite during cooling (Ma et al., 2012b).

Volume fraction of retained austenite also increases with increasing tempering time (Park et al., 2004).

The precipitates are formed along the martensitic laths or the prior austenite grain boundaries (Ma et al., 2012a). The formation of precipitates mainly $Cr_{27}C_6$ deplete the grain boundaries of Cr content making it vulnerable to corrosion (Raghvan, 2006; Choi et al., 2007; Ma et al., 2012a).

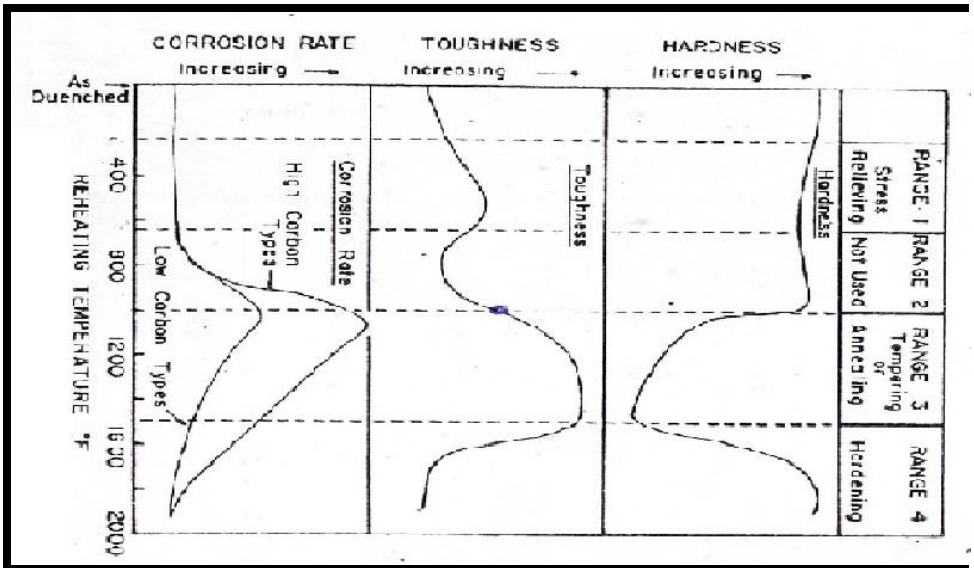

Figure 1.1 (General trend of Hardness, Toughness, and Corrosion Rate) in a 0.1C-12%Cr steels

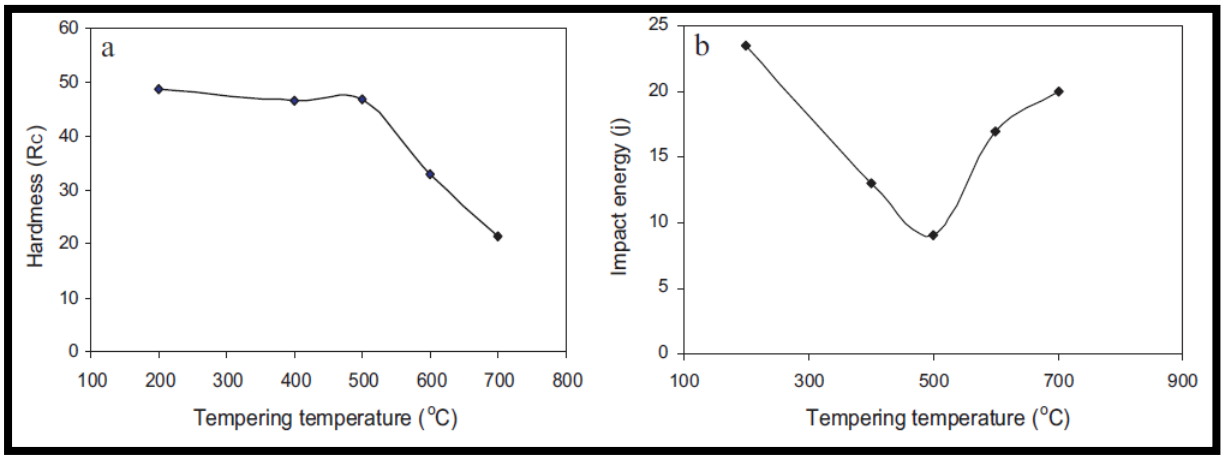

Figure 1.2 Effect of tempering on impact resistance showing minimum at maximum secondary hardening (Isfahany et al., 2011)

1.5 EFFECT OF ALLOYING ELEMENTS ON MARTENSITIC STEELS

In order to obtain maximum strength, the MSS should comprise of 100% austenitic structure at the solution-treatment temperature. Therefore, it becomes necessary to balance the constitution by adding austenite forming elements or balancing the effect of δ-ferrite forming elements (McDowell et al., 1966). The effect of elements can be well-known by Schaeffler diagram. This diagram approximately relates the metallurgical structure to composition of stainless steels. Schaeffler diagram indicates the structure obtained after rapid cooling to room temperature from austenization temperature. In establishing this diagram, alloying elements commonly found in stainless steels are regarded either as austenite stabilizer or as delta ferrite stabilizers. The relative 'potency' of each element is conveniently expressed in terms of equivalence to either nickel (austenite stabilizer) or chromium (delta ferrite stabilizer) on a weight percentage basis (Sedriks, 1996). The nickel and chromium equivalents, which form the two axes of the Schaeffler diagram, can be calculated from the following equations (Pickering, 1976; Sedriks, 1996).

% Ni equivalent = % Ni + % Co + 30(%C) + 25(%N) + 0.5(%Mn) + 0.3(%Cu)…....…Eq**1.1**

% Cr equivalent = % Cr + 2(%Si) + 1.5(%Mo) + 5(%V) + 5.5(%Al) + 1.75(%Nb) + 1.5(%Ti) + 0.75 (%W) ……...Eq**1.2**

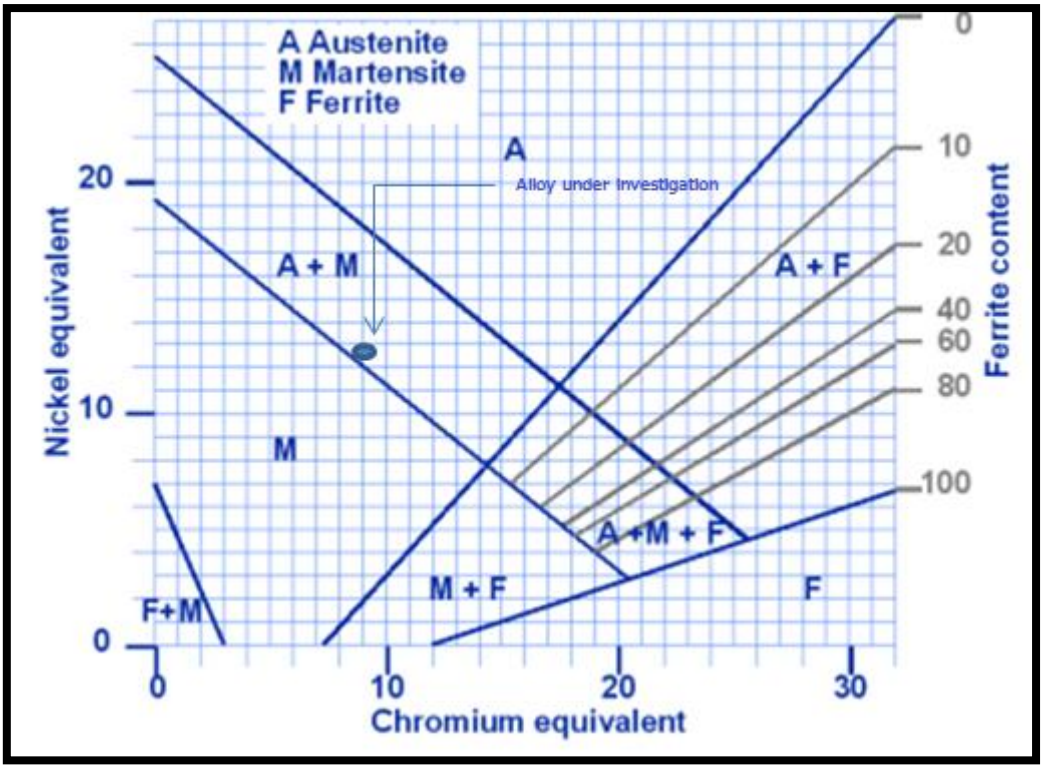

Fig 1.3 Schaeffler Diagram (Sedriks, 1996)

The volume fraction of the phases and hence the mechanical properties critically depend on the balance between the chromium and nickel-equivalents (Balan et al., 1998). The austenite stabilizing elements lower the M_s temperature during cooling and thus stabilize the austenite phase. Austenite stabilizing elements are Ni, Mn, Co, Cu, C, N, Mo, W, and Si.

The cheapest austenite forming addition is carbon, but its addition decreases the toughness and weldiability, impairs corrosion resistance and requires higher solution treatment temperature to dissolve carbides which coarsen the austenite grain size (Pickering, 1976). The M_s temperature strictly should lie above the room temperature. Carbon addition can depress it by 474^0C for every wt-% addition, followed by Mn (33^oC/wt% addition) and Ni (17^0C/wt% addition) but way behind C. The useful criterion for selecting an element is the ratio of decrease in delta ferrite wt% to decrease in M_S temperature. This ratio needs to be maximum for an element for its addition to MSS. The Ni addition also lowers the A_{C1} temperature by 30^0C per wt% addition which can lower the tempering temperature as tempering required to be carried near to Ac_1 (Isfahany et al., 2011; Ma et al., 2011; Bojack et al., 2012). Tempering needs to be carried out at as maximum temperature as possible in order to obtain an optimal combination of strength, ductility, and toughness (Pickering, 1976). Due to this shortcoming of Ni, its addition is only limited up to 3% which has been overcome or nullified in SMSS by increasing Mo (Ma et al., 2012c; Ye et al., 2012).

1.5.1 Effect of Individual Alloying Element

Cu addition has a very significant effect on mechanical properties of SMSS as it promotes the formation of reversed austenite at tempering temperature of 650^0C. It has been reported that 3 wt% Cu additions can produce a retained austenite fraction of 55.9% at a tempering temperature of 650^0C. Cu can precipitate as Cu rich nanometer phase (ε-Cu) in SMSS leading to solid solution strengthening and precipitation strengthening (Ye et al., 2012).

Addition of Nb retards reversed austenite formation and enhance strength through precipitation hardening along with improving corrosion resistance as it suppress Cr precipitates formation (Ma et al., 2011; Ma et al., 2012c).

With C addition hardness, yield strength, and tensile strength of as-received stainless steel but there impact toughness and elongation decreases with carbon content. Therefore ultra-low carbon 12Cr-Ni steels have excellent impact toughness (Zheng et al., 2010)

Addition of N can act an economical alternative for Ni addition as N too is a strong austenite stabilizer. While tempering at temperature of 550^oC, formation of Cr_2N along martensite laths and within martensite laths slightly increases strength but lowers toughness in comparison to MSS without N. Increasing tempering temperature can increase enhance fraction of retained austenite, hence restore the ductility and toughness at higher tempering temperature (Ma et al., 2012a).

Mo and W are known to increase high temperature strength via solid solution hardening, carbide formation and formation of laves phase (Klotz et al., 2008).

1.6 RELATION BETWEEN MICROSTRUCTURE AND PROPERTIES FOR SMSS

The properties of SMSS closely depends on balance between softening effect produced by retained austenite, the elimination of dislocations within the martensite matrix, hardening effect produced by precipitates and retransformation of reversed austenite to martensite (Ma et al., 2012a; Ma et al., 2012c). Generally low carbon tempered martensite exhibiting lath morphology can be seen at lower tempering temperatures. With increasing the tempering temperature the martensite laths starts coarsening which is quite obviously shows reduction in retained austenite content. Tempering treatment promotes precipitation of fine precipitates at interlath boundaries and within laths which effectively increase strength (Ma et al., 2012b). The strength and hardness of SMSS is also due to presence of tempered martensite. While tempering at higher temperatures, quenched martensite formed while solution annealing starts softening which leads to elimination of internal stresses, decrease in dislocation density, and occurrence of retained austenite (De-ning et al., 2010). This retained austenite formed having

a membraniform distribution between martensitic laths in microstructure has a good effect on toughness (De-ning et al., 2010). The toughening mechanism produced by presence of austenitic particles is explained with many models viz. crack blunting model and transformation induced plasticity model associated with transformation induced plasticity (TRIP) (De-ning et al., 2010; Ma et al., 2012b). Several studies have reported that carbide precipitation while tempering also plays a crucial role in deciding the strength properties of MSS. As precipitation of $M_{23}C_6$ precipitate gradually forms and grows or get coarsen up with increasing tempering temperature from 500^{o}C to A_{c1}. The precipitates help in providing the secondary hardening effect which can overshadow the softening effect produced by retained austenite produced while tempering. Although the relative contribution of different precipitates formed within SMSS microstructure is difficult to quantify but it is well known that well dispersed, fine scale precipitates are most effective in contributing to strength, although at cost of ductility and toughness. According to Ashby-Orowan model for precipitate strengthening, strength increment in excess of 100 MPa can be obtained even at a small precipitate fraction (<0.0005 %) when the precipitate size is approximately 5 nm (Ma et al., 2012c).

1.7 SCOPE OF THE PRESENT WORK

Super Martensitic Stainless Steels have replaced the Martensitic Stainless Steels in many applications. The excellent properties of SMSSs are due to lowered carbon content (kept below 0.07%) and increased nickel content. Benefit of increasing the nickel content is to supress δ-Fe formation. Molybdenum is also added to SMSS to catalyse the effect of chromium in corrosion resistance. Tempering at suitable temperature tends to introduction of tempered lath martensite with retained austenite present around the laths. The volume fraction of retained austenite depends on tempering temperature and its formation improves the ductility and toughness. The heat treatment/tempering should be selected judiciously in order to get suitable amount of retained austenite which can impart optimal combination of strength and ductility.

Various strategies have been suggested by different investigators for obtaining requisite amount of retained austenite in the end microstructure. Some have added silicon to widen the gap between A_s and A_f temperatures so that a good fraction of austenite can be obtained during tempering treatment (Leem et al., 2001). Some have used copper to promote formation of austenite while others have introduced multiple alloy addition concepts to introduce stable austenite during heat treatment (Ye et al., 2012). A very recent work has suggested

application of quench and partition treatment of a low carbon martensitic SS for austenite stabilisation (Tobata et al., 2012).In summary, most of the efforts have been made to stabilize austenite formed during the tempering treatment by alloy design modifications in the SMSS.

From above discussions of available literature, we observed that extensive work was related to effect of alloying elements on properties of SMSS and very much limited to retained austenite content present within their grade of stainless steels. Even though these grades of SS are heat treatable unlike their counterparts like austenitic SS but very limited work has been done by following the thermo-mechanical routes as the proposed end use of these alloys is mostly confined to as cast or thick sections. Today, achieving higher material efficiency is an important step towards encouraging their wider use or application.

For attaining our above stated objective we considered alloy consisting of principle ternary composition of Fe-Cr-Ni system. The study is mainly focussed or is an attempt to understand the effect of cold rolling and cold rolling and annealing on phase transformation, microstructural morphology changes, and recrystallization behaviour of SMSS type during isothermal annealing process and to relate it with mechanical properties.

CHAPTER 2
REVIEW OF LITERATURE

2.1 THERMALLY ACTIVATED PROCESSES

The free energy of polycrystalline materials increases during deformation by the presence of dislocations and interfaces, and the material containing these defects are thermodynamically unstable. When a material is heated, thermally activated processes such as solid state diffusion occur which result in defect removal or an alternative arrangement in configuration of lower energy (Humphreys and Hatherly, 2004). The main thermally activated processes that occur are recovery, recrystallization and grain growth.

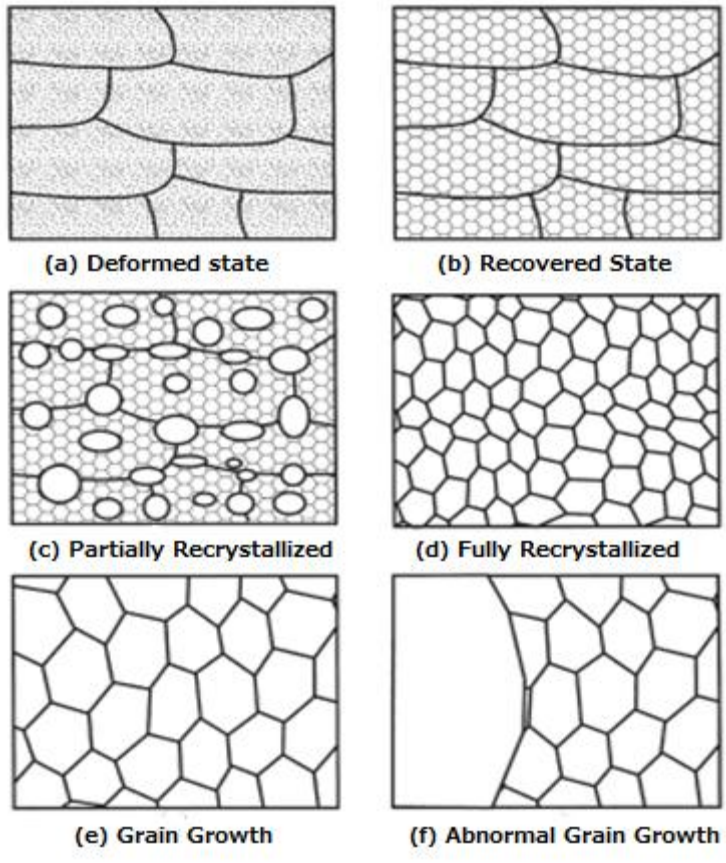

Fig. 2.1 Schematic of Recovery, Recrystallization, and Grain Growth
(Source: Humphreys and Hatherly, 2004)

2.1.1 Recovery

Recovery refers to the changes in a deformed material which partially restore material to its properties prior to deformation. Recovery is primarily due to the changes taking place in dislocation structure. During recovery, stored internal strain energy is released due to dislocation motion. It takes place in a temperature range of less than 0.3 of melting temperature (T_m). Residual stresses induced during cold working go on decreasing. Ductility, strength, and hardness remain same as were for cold worked material. During recovery, sub-grain boundaries are formed. There is some reduction in the number of dislocations, and dislocation configurations are produced having low strain energies. Also, some of the physical properties such as thermal and electrical conductivities and the like are recovered to their pre-cold worked states (Callister, 2007). The properties most affected during recovery process are those which are sensitive to point defects. The strength properties which mostly depend on dislocations are not affected at recovery point defects. During recovery, some of the stored energy is relieved by any of the recovery mechanisms, which include dislocation annihilation, dislocation rearrangement and sub-grain growth. Because the microstructural changes during recovery are subtle, recovery is generally measured indirectly by changes in resistivity etc. (Kalu and Waryoba, 2007).

Recovery is not confined to plastically deformed materials; it may even occur in any crystal into which non equilibrium, high concentration of points or line defects have been introduced as the (a well-known example in this is a material which has been quenched from a high temperatures) (Humphreys and Hatherly, 2004).

2.1.2 Recrystallization

Recrystallization is the formation of a new set of strain free and equiaxed grains that have low dislocation density and are similar to pre-cold worked conditions. Recrystallization of cold worked metals may be used to refine the grain structure. Recrystallization up to some extent is dependent on temperature and time. Every metal and alloy has specific recrystallization temperature, which lies between 0.3-0.5 of T_m. Recrystallization temperature is difficult to specify and, for steels it depends on several factors such as the steel type, the heat treatment that the steel might have been submitted to before cold working, the extent of cold working, as well as the heating rate and holding time at the annealing temperature (Padilha, 2003). In general, all variables that increase the stored energy due to deformation such as a decrease in the stacking fault energy, increase in strain, increase in strain rate and decrease in deformation temperature, cause a decrease in the recrystallization temperature (Padilha, 2003). During recrystallization, grain boundary motion occurs as the new grain

nuclei form and then grow. Sometimes impurity atoms preferentially segregate at and interact with these recrystallized grain boundaries so as to diminish their mobility. This results in decrease of recrystallization rate and raises the recrystallization temperature which may even run as high as 0.7 of T_m. During recrystallization, strength and hardness of material decreases but its ductility increases, residual stresses reduce to certain limit and then become constant. More is the prior cold work done, lower is the temperature required for recrystallization (Callister, 2007; Kalpakjain and Schmid, 2009).

The kinetics of recrystallization is superficially considered similar to phase transformation as both consist of nucleation and grain growth but nucleation in classic thermodynamic sense does not occur. Recrystallization is readily detected by metallographic methods and is evident by decrease in hardness and strength (Dieter, 1988; Habibi and Ketabchi, 2012). Although the process of recovery and recrystallization proceed the grain growth process but sometimes they even overlap each other making it cumbersome or difficult to unambiguously distinguish between these phenomenon (Habibi and Ketabchi, 2012).

In carbon steels the process of recrystallization and precipitation take place nearly at similar temperatures, therefore precipitation retards the recrystallization. Recrystallization is not much frequent in high carbon steels as they show more precipitation phenomenon (Padilha et al., 2003).

2.1.3 Grain Coarsening

Grain Growth follows recrystallization and in it the strain free grains continue to grow if the metal specimen is left at elevated temperatures. Grain growth occurs by migration of grain boundaries in such a way that smaller grains are engulfed by larger ones while showing growth. The driving force for grain growth is decrease in surface energy not the stored energy (Dieter, 1988). Boundary motion in grain growth is just a short range diffusion of atoms from one side of boundary to other and atom movement and boundary movement are in opposite direction to each other. Grain growth also depends on time and temperature. Grain growth proceeds rapidly as the temperature increases, due to enhancement in diffusion rate with rising temperature. Grain diameter (d) varies with time (t) according to relationship given in Equation 2.1 (Callister, 2007).

$$d^n - d_o^n = Kt \qquad \text{----------2.1}$$

Where, n and K are time independent constants; value of n is generally equal to or greater than 2, d_o is grain size at t=0, and d is the grain size after time period t. Grain growth is

inhibited by presence of a fine dispersion of second phase particles, which restricts grain boundary movement (Dieter, 1988).

2.2 DETERMINATION OF CRITICAL TEMPERATURES

The transformation temperatures are referred to as critical temperatures and are observed by measuring changes in heat transfer or volume as the specimen is heated or cooled. The absorption or release of heat during phase transformation produces a change in slope, or "arrest" on continuous plot of specimen's temperature versus time (Krauss, 1980). The three critical temperatures of interest are A_1 or A_{c1}, A_3 or A_{c3}, and M_s. At A_1 or A_{c1} the slowly heated specimen will start showing traces of austenite. At A_3 or A_{c3} the austenite will be completely formed.

Some empirical relations showing effect of alloying elements on critical temperature has been developed by regression analysis of a large amount of data and some of relations for stainless steels of our interest have been listed in Equations 2.3 and Equation 2.3 below (Pawlowski, 2011).

$$A_{c1} = 739\text{-}22.8C\text{-}6.8Mn+18.2Si+11.7Cr\text{-}1.5Ni\text{-}6.4Mo\text{-}5V\text{-}28C \text{----------} \mathbf{2.2}$$

$$A_{c3} = 937.3\text{-}224.5\sqrt{C}\text{-}17Mn+34Si\text{-}14Ni+21.6Mo+41.8V\text{-}20Cu \text{----------} \mathbf{2.3}$$

Elements stabilizing austenite lowers the A_{c1} and A_{c3} temperatures as evidenced by their negative contribution, whereas elements that stabilize ferrite or carbides raises A_{c1} and A_{c3} temperatures and makes a positive contribution (Pawlowski, 2011).

M_s temperature represents the starting temperature for martensite formation from austenite while cooling. All known alloying elements lower M_s temperature except Co and Al which raises it (Abbaschain et al., 2009). The M_s temperature relationship with composition is exemplified in Equation 2.4 given below (Marshall, 1984).

$$M_s = 1305\text{-}61.1\%\ Ni\text{-}41.7\%\ Cr\text{-}33.3\%\ Mn\text{-}27.8\%\ Si\text{-}1667\%\ (C+N) \text{----------} \mathbf{2.4}$$

2.3 RETAINED AND REVERSE AUSTENITE

Retained austenite is the austenite which remains untransformed even after M_s temperature while reverse austenite is the austenite which gets formed from reversion of martensite during the tempering treatment. Retained austenite is not formed in low carbon steels (less than 0.4%C, less carbon leads to higher M_s) (Abbaschain et al., 2009) but by varying the alloy composition, austenite can be retained as depicted by Schaeffler diagram. Reverse austenite is formed as a result of nickel diffusion in low carbon steels and its presence affects the

mechanical properties of steels to a great extent. The addition of Ni suppresses the δ-ferrite formation by widening the austenite region (Park et al., 2004; Lakhtin, 1977). The presence of retained austenite prior to tempering is avoided (Pickering, 1976) but reverse austenite after tempering is good for improving strength and ductility of SMSS (Ma et al., 2012c). The presence of reverse austenite accounts for high toughness, especially at low temperatures, which can been effectively utilized in many kinds of steels such as maraging steels, TRIP steels and 9% Ni steels (Song et al., 2010).

2.4 LITERATURE REVIEW

Takaki *et al.* (1992) studied the changes in morphology of lath martensite by cold working and recrystallization in low carbon steel (SNCM 420). Commercial 0.2% low alloy steel rod of 50mm diameter with chemical composition of 0.21%C, 0.24% Si, 0.57%Mn, 1.59% Ni, 0.50%Cr, 0.16% Mo was hot rolled to 10mm thickness plate and then cold rolled (CR) to 1 mm plate followed by solution treatment at 1200 ^{o}C for 1.8 ks. The solution treated material was subjected to cold rolling up to 80% reduction and was then annealed at 700 ^{o}C followed by water quenching. The microstructure was observed by means of optical microscopy and TEM. The Vickers hardness and tensile tests were also performed. With increase in cold deformation, the fraction of deformed lath martensite increased as depicted by TEM photographs and it resulted in introduction of slip bands and dislocation cell structures. Thus cold rolling destructed the lath martensitic structure and raised the dislocation density of matrix. The hardness of annealed specimen showed an abrupt fall representing softening which was attributed to recrystallization. The recrystallized ferrite grains nucleated from the damaged martensite and recrystallization proceeded at a very fast rate. Recovery proceeded at rapid rate in deformed lath martensite. The grain growth mechanism was barred by precipitates present as they restricted the dislocation movement. The conclusion drawn was that recrystallization enhanced with degree of predeformation as both the nucleation and growth rates enhanced due to rise in dislocation density and destruction of lath martensitic structure. The growth of recrystallized grains was restricted due to presence of precipitates.

Balan *et al.* (1998) made efforts to establish relation between structure and fracture properties and to study the micro-structural changes which take place during tempering treatment for 16Cr-2Ni MSS. 30 kg ingot of the experimental steel was made by vacuum induction melting followed by homogenisation at 1150 ^{o}C. Hot forged and rolled at 1050 ^{o}C

to 16mm thick plate. Blanks of size 16x16x100mm were cut along rolling direction of plate and austenised at 1050 ^{o}C for 2 hrs (S_1). Then sample blanks were tempered at different temperatures between 200 and 600 ^{o}C. Retained austenite was measured using X-ray diffractrometer. Optical microscopy was carried out on specimens etched with glyceregia reagent. Vickers's hardness measurements were carried out. Thin foils for TEM analysis were made from 0.15mm thick disc prepared from heat treated sample blanks by mechanically polishing to 0.05mm thickness and electro polishing using 10% perchloric acid in glacial acetic acid at 10 ^{o}C and 25mV. Microstructure of S_1 showed presence of stringers of delta-ferrite, undissolved carbides, and lath martensite. On tempering between 200-400 ^{o}C, hardness decreased as retained austenite formed on quenching transformed to M_3C carbide which due to depletion of C from martensite made it softer. Secondary hardening took place between 400-500 ^{o}C due to precipitation of Cr_7C_3 and Cr_2C. Even though austenite content was higher than other tempering treatment condition but hardening effect of precipitates dominated the softening effect produced by austenite. Peak secondary hardness was obtained by prolonged tempering. Above 500 ^{o}C hardness decreased steeply. Austenite content decreased to 2% on tempering at 600 ^{o}C. On tempering at 600 ^{o}C, recovered ferritic structure with coarse martensitic interlath was observed. No precipitated austenite was present. Sequence of microstructure change was $M_3C \rightarrow \gamma_{ppt} \rightarrow M_2X$, $M_7C_3 \rightarrow M_{23}C_6$. Dissolution of M_3C led to more carbon content as carbon is an austenite stabilizer, austenite started precipitating. The conclusion drawn was that austenite precipitation was observed while tempering at 400^{0}C which contributed towards secondary hardening.

Leem *et al.* (2001) investigated the volume fraction of retained austenite at room temperature after reverse transformation of martensite to austenite in a Fe-13%, Cr-7%, Mi-3%, Si martensitic stainless steel as a function of heating rate and reversion treatment temperature. The stainless steel (C:0.0094;N:0.0078; Si:2.83; Cr:13.39; Ni:6.78; Mn:0.27; Ti:0.072; Fe: balance ; all in wt%) was prepared in a vacuum induction furnace. The 30kg ingot was homogenized at 1250 ^{o}C for 12h and then hot rolled into 5mm thick sheets. All the specimens were solution treated for 30min and then water quenched. This resulted in 100% fine lath martensitic structure containing high density dislocations. Further specimens were heated between A_s and A_f temperature heating rates from 0.1 ^{o}C/s to 50 ^{o}C/s and holding of 2h at each temperature followed by air cooling or furnace cooling. With regards to austenization process, it was observed that the A_s and A_f temperatures increased with increasing the heating rate upto 10 ^{o}C/s, after which these temperatures were almost constant, regardless of heating

rate. Those reverse transformation occurred by diffusional mechanism below 10 °C/s, while it occurred by a diffusionless shear mechanism above 10 ^{o}C/S. With regards to tempering treatment, it was observed that when the martensitic specimens were heated to temperature range of 575-700VC in diffusional reverse transformation region with heating rate of 0.5 ^{o}C/s (2h holding) followed by air or furnace cooling to room temperature, the amount retained austenite increased with increasing in temperature (in both air and furnace cooling), exhibiting a maximum at around 625 ^{o}C and then decreased with higher temperatures. The air cool specimens had smaller amount of retained austenite than furnace cooled specimens at all reversion treatment temperatures. The smaller amount of retained austenite for the air cooled samples was attributed to more unstable austenite due to introduction of higher thermal stresses and higher concentration of quenched in vacuumed at the μs temperature from higher cooling rate. So it was concluded that the volume fraction of austenite at room temperature (V^{Υ}_{RT}) after the reversion treatment was proportional to both volume fraction of reversed austenite (V^{Υ}_{T}) and the stability of austenite (f^{Υ}_{RT}).

Schino *et al.* (2002) reported the production of ultrafine grains in AISI 301 by martensitic reversion. They reported that reversion of deformation induced martensite (DIM) ($\alpha^{'}$) results in production of ultrafine grained (UFG) structured austenite. Metastable γ was entirely transformed into $\alpha^{'}$ by heavy cold rolling and $\alpha^{'}$ was reverted back to recrystallized austenite (γ_R) during annealing at low temperatures. The $\alpha^{'} \rightarrow \gamma_R$ reversion of martensite induced by cold deformation was analysed at different annealing temperatures and times. It was analysed that reversion rate increased with annealing temperatures and in order to carry out complete reversion at particular annealing temperatures infinitely large times were required. Micrograph along with grain size for sample annealed at 750 ^{o}C for 3 min depicted the presence of ultrafine grains with average size of 2.0 μm. Hence, reverted and recrystallized austenite during annealing results in to formation of ultra-fine grained structure.

Tsai *et al.* (2002) evaluated the effects of austenization temperature and cooling rates on the M_s temperature. In order to understand martensitic transformation and existence of retained austenite in AISI 410 a series of Continuous Cooling Transformations (CCT), isothermal treatments and thermo-mechanical treatment were carried out. Commercial AISI 410 steel bar with 16mm diameter was used as starting material. All thermal treatments were carried out on a dilatometric RDP deformation dilatometer. Before dilatometry, the pieces of steel plates were homoginized at 1200 ^{o}C for 3 days, then quenched into water and then finally the

decarburizing layer was removed. The specimens were machined in form of 3mm diameter cylindrical rods with 6mm length. They were then subjected to continuous cooling treatment, isothermal treatment, thermo-mechanical treatment followed by examination under TEM. M_s temperature decreased with both cooling rate and austenization temperature, but for same cooling rate lower austenization temperature showed lower M_s temperature and vice-versa. The material with higher cooling rate from a higher austenization temperature resulted in lowering down of M_s temperature. The reason suggested by Hsu et al. (1983) was that pinning of clustered vacancies to partial dislocation hindered nucleation of martensite and hence lowered the M_s temperature. The variation in M_s was also analysed by considering the strength of matrices. Carbon was supposed to be the main element to divert the M_s temperature and it had most powerful solid solution strengthening effect than other elements (Cr, Ni, and Si). During precipitation of chromium carbide at higher temperature, lesser amount of carbon was left behind in austenite phase which gave higher M_s temperature. This point suggested about the austenite favouring tendency of carbon atom. For slow cooling rate conditions, martensite laths had enough time to grow without any impingement with other martensite variants. The conclusions which were drawn were that M_s temperature lowered with increase in austenization temperature and with making rapid cooling.

Roucoules *et al.* (2003) proposed a model which could infer some of dominant microstructural processes (work hardening, recovery, and recrystallization) which were dominant while hot rolling of steels. One of most significant aspect of this work was that it predicted changes during static recrystallization. The model proposed was based on equation describing evolution of dislocation density as a function of deformation conditions. The constants for model were obtained from optimization techniques described elsewhere in literature. The analysis of model on stress-strain curves predicted that when only recovery is allowed to take place the work hardening rate increased stress larger than peak stress observed experimentally. The effect of strain, strain rate and temperature on recrystallization was established by measuring the time for 50% recrystallization. Recovery retards work hardening and recrystallization. The interruption of deformation hands the dislocation evolution to recovery and recrystallization. The dislocation within the walls of subgrains governs amount of stored energy required for recrystallization. The stored energy or driving energy for recrystallization is also dependant on misorientation across boundaries. There were only small changes observed in static recrystallization with increasing strain beyond the strain values required to initiate dynamic recrystallization and at such high strain rate

recrystallization was independent of temperature but was influenced by strain rate. The critical strain required for dynamic recrystallization was found to increase with strain rate and decrease with temperature.

Schino *et al.* (2003) conducted present study to establish a recrystallization and grain growth model based on statistical assumptions and involving only two free parameters. The samples of AISI 304 were cold rolled to different thickness reduction of 20%, 40%, 60%, and 80% and were annealed at 1100 ^{o}C for different times. The thermal profiles were measured and interpolated by a polynomial fitting. The samples were analysed in order to determine grain size. The basic assumption of model was that, nuclei at which recrystallization proceeds are homogeneously distributed. The free parameters viz. initial number of nuclei and dislocation density were considered to be dependent on cold reduction rate and independent of heating temperature profile. From a sensitivity study of model it was found out that kinetics of recrystallization was very much dependant on number of nuclei and on dislocation density but least dependant on shape of initial grain size distribution. Although a smaller mean diameter was expected during higher reduction, but results were contrary to expectations. The cold reduction and heating rate produced opposite effect during recrystallization and grain growth. In proposed model no. of nucleation sites (N) and dislocation density (ρ) showed a linear dependency with deformation rate. The important conclusion drawn was that DIM, transformed back to austenite as reversion temperature (700-750 ^{o}C) was lower than the recrystallization temperature.

Park *et al.* (2004) investigated a Super Martensitic Steel (SMSS) with objective to investigate the shape and formation mechanism of reversed austenite and existence of retained austenite (RA) during tempering of F-14Cr-7Ni-0.3Nb-0.7Mo-0.03C SMSS. Additionally, changes in the microstructure, mechanical properties and chemical composition of reversed austenite with variation of tempering temperature and time were also investigated. A hot forged plate of 18mm thickness of material was hot rolled at temperature of 1200 ^{o}C to form 6mm plates. The plates were subsequently cold rolled to 4mm thickness and cut to dimensions of 25mm x 50mm x 4mm to be used as heat treatment specimens. Solution annealing was carried out at 1150 ^{o}C for 1h and water quenched. Tempering was carried out in the range 300-900 ^{o}C with holding time of 1hr. some samples were also tempered at 450 ^{o}C for time range of 1-100hr.

After Solution annealing acicular austenite existed from the interphase of lath boundaries. This acicular austenite retained austenite created by quenching the specimen after solution annealing.

Further during tempering between 300-900 ^{o}C the strength and hardness values increased in the range 300-450 ^{o}C (maximum being at 450 ^{o}C), then decreased in the range 450-600 °C (minimum being at 600VC) and then increased in the range 600-900 °C. The increase in hardness upto 450 ^{o}C was attributed to the hardening effect of precipitates and decrease in hardness between 450-650 ^{o}C was related to the increased volume fraction of reversed austenite (maximum being at 650 ^{o}C). The hardness increase above 650 ^{o}C resulted from transformation of reverse austenite to fresh martensite again during cooling.

Further investigations were carried out at tempering temperature of 450 ^{o}C which gave the best combination of strength and hardness. Now the effect of folding time at this temperature was observed. It was noted that with increase in holding time more strength and hardness increased because of formation of carbides ($M_{26}C_6$).

After tempering above 550 ^{o}C it was observed that acicular retained austenite was not observed at 650 ^{o}C for 1h. However, new plate like reversed austenite was observed.

This reversed austenite was formed by nickel diffusion during tempering. The nickel content of reversed austenite appeared to be 9.7%; however, Ni content of the matrix around reversed austenite was 4.17%. The original chemical composition of nickel was 6.69%. Thus, nickel content in reversed austenite increased and Ni content in surrounding matrix decreased. This indicated the reversed austenite was formed by nickel diffusion.

Chia *et al.* (2005) verified the experimental results with those obtained from Hall-Petch equation regarding effect of grain size on flow stress for β-Ti-15.2 at% Mo. They examined that parameter σ_I (Lattice friction stress) increased with a strain ε and decrease in temperature T whereas K_{H-P} is independent of strain and temperature and verified the effect of d on σ and ρ in a β-Ti alloy and evaluated that σ was inversely proportional to $d^{-1/2}$.There occurred an increase in ρ with ε and decrease in d and gave flow stress as,$\sigma = (0.5\text{-}0.6)M\mu b\rho^{1/2}$, where M (Tylors's factor) = 3. The value of ρ for a given ε and d are relatively independent of temperature from 300 to 650K. There were three mechanisms for increase in dislocation density with decrease in grain size. The results in present paper were in accord with Li's grain boundary ledge mechanism.

Ping *et al.* (2005) did quantitative microstructural characteristic of 13Cr-8Ni-2.5Mo-2Al Martensitic Precipitation Hardened Stainless Steel during aging using TEM. Vaccum induction melting and electroslag re-melting techniques were applied to prepare above mentioned steel. Bars of 50mm diameter were prepared by forging followed by solution treatment at 925 ^{o}C for 1 hr and water quenching. Aging at different temperatures (450-620 ^{o}C) for 4 hours was done followed by overaging at 450^{o}C for 500 hrs to observe the kinetics of precipitate coarsening. Square rods with dimensions of 0.2mmx0.2mmx10mm were cut out from bar sample and electropolished. Maximum hardness was observed at 510 ^{o}C aging. Overaging resulted in rise in hardness but it's a strict function of time of overaging. With time, hardness increased but significantly when time varied from 1 to 4 hr and insignificantly from 4 to 500 hrs. High magnification bright field TEM showed β-NiAl intermetallic compound (2-4nm) with B2 structure and spherical morphology with high number density and inter compound distance of less than 10nm. During aging (not overaging) no size coarsening took place. Above 510 ^{o}C, carbides precipitated were also observed along with above mentioned precipitate. Carbides were not present below this temperature. In aged sample at 510 ^{o}C (for 4 hrs), concentration variation of Cr and Mo around the precipitates took place. Diffusivity of Mo was slower than Ni and Al therefore its segregation at precipitate interface impeded growth of particle. Mo enrichment played an important role in determining the growth of NiAl precipitate as Mo is bigger in diameter than other alloying elements, its diffusivity is less. The conclusions were that the precipitate size and concentration increased with aging temperature but there number density got decreased. Small amount of carbides are formed in martensitic matrix at higher annealing temperature even reverse austenite was also observed.

Hedstrom *et al.* (2007) investigated the lattice strain evolution and accompanying strain-induced martensitic transformations in metastable stainless steel AISI 301 during deformation by using high-energy X-ray diffraction for samples having different initial cold-rolling reductions and the in-situ measurements were complemented with ex situ microstructural characterization. Alloy (17.55 Cr, 7.67 Ni, 1.23 Mn, 0.55 Si, 0.31 Mo, 0.25 Cu, 0.1 Co, 0.095 C, 0.022 N and 0.008 Nb, with other elements less than 0.1) was multi passed cold rolled from initial thickness of 1mm to 2% (A), 23% (B), 36% (C), 42% (D). Samples were prepared by cutting 3 mm discs, mechanically polishing, ending with 1 μm diamond paste, and then final thinning by electropolishing on a Struers dual-jet electropolisher. For in situ high-energy X-ray diffraction experiments, tensile samples were cut along the rolling

direction from the four steel sheets using pulsed Nd-YAG laser cutting. The strain rate during plastic deformation was 104 s^{-1} and the applied strain was recorded with an extensometer. The load was continuously recorded from a load cell and diffraction patterns were collected every 30 s during the in situ loading by an area detector. Both α and ε martensite were formed but at high applied strains the transformation from austenite to martensite occured in step-wise bursts. This stepwise behaviour was a consequence of autocatalytic martensitic transformations, initiated by growth of a-martensite embryos. The transformation from austenite (γ) to ε-martensite occurred in a parabolic transformation behavior when the samples were initially cold-rolled. Stepwise transformation behavior of the strain-induced martensitic transformation in a metastable stainless steel.

Kalu and Waryoba (2007) modified the JMAK model used for determining kinetics of recovery, recrystallization and grain growth by making it to incorporate microstructure data instead of relying on microstructure. Limitation of convention model which was based on measurement of recrystallized fraction from microstructure were that its accuracy depended on contrast of micrograph taken and it wasn't suitable for in homogeneously deformed microstructure such as due to drawing. The main limitation was regarding determination of recrystallized fraction. The OFHC wires drawn were drawn at room temperature and specimens of drawn wire were isothermally annealed 250, 400, 500 ^{o}C for duration ranging from 10s to 1 hr and were immediately water quenched. Microstructural investigations were performed using optical microscope, Orientation Imaging Microscopy (OIM), and Evnviornmental Scanning Electron Microscopy (ESEM). The plot between fraction recrystallized and annealing time gave a sigmoidal curve. The change in slope of lines (JMAK exponent) had been drawn by modified JMAK model represented a change in restoration process from recrystallization to grain growth. The modified JMAK model used microhardness data to predict the restoration kinetics of recovery, recrystallization, and grain growth. The fraction recrystallized was replaced with fraction transformed and it was measure of softening while annealing. The modified JMAK model showed a relation between hardness and annealing time. The onset of recrystallization was earlier in samples annealed at higher temperatures. The modified JMAK model offered more detailed information on restoration kinetics compared to standard JMAK analysis. The conclusion drawn was that the hardness measurement was able to measure the fraction transformed during recovery, recrystallization and grain growth.

Park and Park (2007) investigated the effect of heat treatment parameters on the corrosion resistance and phase transformations of 14Cr-3Mo martensitic stainless steels in relation to the dissolution and precipitation of carbides. The alloy (Fe-0.3C-14Cr-3Mo-1.5Ni-0.12N, all in wt%) specimens of size 1mm x 3mm x 10mm were austenitized at 1000 ^{o}C and 1050 ^{o}C above A_{c3} temperature for 5min to completely dissolve carbon in the austenite phase and cooled at the different cooling rates (0.5, 1.0, and 2.0 K/s) to room temperature.

It was observed that the austenitized specimen at higher temperature had a lower M_s temperature when the cooling rate remained constant. As the austenitizing temperature rose, the amount of carbon atom in the matrix was increased, which depressed the martensitic transformation. Further, an increase in cooling rate reduced the amount of interstitial carbon atoms within the austenite phase and decreased M_S temperature.

The corrosion resistance of the alloy was found to improve at higher austenitizing temperatures. However, it was deteriorated at specific austenitizing temperatures of 1000 ^{o}C and 1050 ^{o}C when cooling rates was 10K/s. the deterioration of corrosion resistance was caused by the impaired balance between the matrix and the retained austenite. This phase distribution used to decide the rank of corrosion resistance, because Cr-Carbides created Cr-depleted zone and the retained austenite impaired the balance of the corrosion resistance in the matrix (mainly martensite).

Further, the amount of retained austenite increased by increasing the austenitizing temperature and cooling rates because these led to increase in dissolved carbides. This increased the volume of carbon in the matrix leading to depressed M_s and thus higher retained austenite.

Calliari *et al.* (2008) investigated the microstructure and properties of Ni-Mo martensitic stainless steels subjected to different heat treatments (annealing, quenching and tempering) to improve the mechanical properties and corrosion behaviour of these steels. The steel ingots were produced in an electric arc furnace, hot rolled, and after annealing, were wrought in 5.5mm rods. From the rods, samples were cut, oil quenched and tempered at various temperatures (150-780 ^{o}C).

The microstructure in annealed condition consisted of randomly globular carbides in a ferrite matrix. The best compromise between temperature and holding times had been obtained by annealing at 750 ^{o}C for 2h, suitable to maintain the final hardness to values lower than 270HB. Higher temperatures produced even lower hardness, as 200HB, but required slow cooling rates, which was unsuitable for industrial applications. After quenching, maximum

hardness corresponded to 1050 ^{o}C, higher than the standard temperature applied to martensitic stainless steels.

The mechanical properties after tempering were satisfactory, though the best results for each property were obtained in different tempering temperature ranges. The tensile strength was more than 1700 MPa till tempering temperatures of 580˚ C (better than commercial martensitic stainless steels), but ductility was low in the tempering temperature range 480-550˚C. Corrosion resistance, characterized with potentiodynamic tests and weight loss tests, was considerably superior then commercial martensitic steel grades (AISI 420) only for tempering temperature higher than 580 ^{o}C.

Thus, it was concluded that the said steel could be potentially used in a large variety of applications, in particular where excellent mechanical properties and good corrosion resistance were needed.

Cao *et al.* (2008) studied the stored energy and thermal stability of OFHC pure Cu processed by ECAP following the $B_c$route up to 16 passes. They observed an increase in stored energy up to the 4th cycle after which it saturated at 0.95±0.05 J/g. ECAPed Cu stored energy was 20% more than that stored by cold-rolled copper. They also observed ECAP has low thermal stability due to high vacancy concentration, which can be enhanced by giving annealing treatment. Stored energy was found due to contribution by dislocation at boundaries, dislocation within grain and vacancy concentration. The contribution due to the first two can be made out directly from the micro-structural observation while the third contributor was calculated from literature. The activation energy was calculated from the Differential Scanning Calorimeter (DSC) curves by using Kissinger (Kissinger et al. 1957) or Chen & Spepen (Chen et al. 1991) methods. The activation energy for restoration process of recovery and recrystallization was calculated as 77±6 KJ/mole by Kissinger process and 80±6 KJ/mole by Chen & Spepen process. The conclusions drawn for paper were that ECAPed Cu has high stored energy and low activation energy than the Cold Rolled (CR) copper.

Karimi *et al.* (2009) investigated the martensite to austenite reversion behaviour and precipitation taking place during annealing treatment. Hot rolled AISI 301 steel (0.11%C, 0.66%Mn, 6.91%Ni, 16.2%Cr, 0.27%Mo, 0.67%Si, 0.53%Cu, 0.06%Al, 0.1%Co, 0.03%P, <0.03%S, 0.008%Nb, 0.005%N) were cold rolled to sheet. The specimen cut out of cold rolled sheet were subjected to isothermal annealing treatments at temperatures between 600-900^{0}C for different times from 1 to 100 min. For annealing treatments between 600-750^{0} C

for different annealing times no substantial reversion was noticed, but for higher annealing temperatures 800-1000 ^{o}C a significant reversion was seen even at annealing time of 10 min using XRD analysis. This ambiguity against martensitic reversion is proposed due to recovery and relaxation of matrix adjacent to martensitic laths leads to martensite growth. Another mechanism may be due to carbide precipitation which leads to C depletion in austenite matrix at higher temperature and rising of M_s temperature. The fully reverted austenitic structure was seen at annealing temperatures of 800 ^{o}C and 850 ^{o}C for 10 sec and formation of nano grained structure was seen while annealing at 800 ^{o}C for 10 sec. The conclusions drawn were that annealing for lower time periods also led to fully reversion austenitic structure and grain refinement.

De-ning *et al.* (2010) investigated the influence of tempering process on microstructural evolution and mechanical properties of 00Cr13Ni4Mo Super Martensitic Stainless Steel (SMSS). The principle objective was to achieve excellent combination of toughness and strength for pipeline steel used in oil/gas industry.

The steel was produced in a vacuum induction melting furnace. Cast ingots were hot forged to a square billet with section area of 80*80mm and hot rolled to round bars of 25mm diameter. The specimens were subjected to solution treatment at 1040 ^{o}C for 1 hour followed by water quenching to get a fully martensitic structure. The solution treated specimens were tempered in range 520-720 ^{o}C for 3 hour followed by air cooling.

The amount of retained austenite gradually increased with tempering temperature and reached a maximum value at 600 ^{o}C (constant holding of 3 hour). For tempering temperatures beyond 600 ^{o}C up to 720 ^{o}C, the amount of retained austenite decreases (reversed austenite that transformed at these temperature retransformed to fresh martensite during cooling above 600 ^{o}C) leading to decrease in percentage elongation. Higher percentage elongation of steel tempered at 600 ^{o}C was attributed to the presence of more retained austenite.

Further, the specimens were tempered at 600 ^{o}C for different durations (3-12hours). In all the samples a complex structure of lath martensitic and retained austenite was formed. It was observed that increased holding (3h to 12h) resulted in increased percentage elongation form 18% to 21%. This owed to increase in volume fraction of retained austenite (maximum 14% at 12h of holding) because of transformation of martensite to retained austenite with increased holding. With increased holding, grains of R.A. elongated and % of R.A. also increased. In the holding time range from 3h to 6h, the dominant factor was increase in percentage of R.A.

phase due to which hardness decreased and withholding time form 6h to 12h both factors were equally dominant resulting in almost constant hardness.

R.A. was responsible for toughness and percentage elongation while lath martensite was responsible for high tensile strength. With increased holding amount of R.A. increased (transformed form martensite) at the expense of lath martensite. Due to this strength decreased. Also because of increased holding there was decrease in dislocation density, which reduced the strength. Thus the optimum combination of strength and toughness (950MPa tensile strength, 832MPa yield strength, 18% elongation and 30HRC hardness) was obtained at tempering temperature of 600 °C with 3h holding.

Lee and Lee (2010) studied the formation of fine ferritic grains during asymmetrical rolling of super cooled austenitic and analysed the effect of rolling reduction and cooling rate after rolling on tensile properties. Low carbon steel was prepared in vaccum induction furnace and was given solution annealing treatment at 1200 ^{o}C for 12 hrs. The homoginized ingot was hot rolled to 30 mm thick plate and was cut into pieces. These pieces were again hot rolled to final thickness of 4mm followed by heating at 900 ^{o}C for 10 min and air cooling to temperature of 750. Shear rolling was performed at 750 ^{o}C using uneven rolls with diameter ratio of 1.5 and reduction ratios of 30, 40, 50, and 60%. The rolled specimens were cooled at various rates ranging from 3-15 ^{o}C/sec while some were even water quenched to preserve ferritic structure. At reduction ratio of less than 50%, ferritic grains were mostly formed at prior austenite grain boundaries and at shear bands in austenitic grains but finer ferrite grains were formed for higher reduction ratio. For low reduction ratio, dynamically formed ferrite content was very much limited. The microstructure at lower rolling reduction was of coarse ferrite and pearlite while at higher rolling reduction it was of fine ferrite and cementite particles. Lower cooling rate introduces Luder's strain while at higher cooling rates grain size got finer and austenite present transformed to martensite. Formation of finer grain size and martensite phase also resulted in enhancing tensile strength. The conclusion drawn were that ferrite is formed in substantial amount only during high reduction ratio and its size or fraction had nothing to do with cooling rate but it got finer with higher reduction ratio. Higher cooling rate transformed austenite to martensite while lower transformed it to pearlite.

Nestorovic *et al.* (2010) assessed the influence of Thermo Mechanical Treatment (TMT) on anneal hardening mechanism and structural changes of cast Cu-6.6 wt. % Ag alloys. The pure Cu and Ag based Cu alloy were casted into sandy clay mould of dimension 65x25x180 mm

followed by homogenization at 800 ^{o}C for 24 h with furnace cooling. Sample of size 65x25x7mm were cut from them and were subjected to TMT. After that Vicker's hardness electrical conductivity were measured and microstructure was analysed. The hardness of Cu alloy was reported to be higher due to solid solution strengthening. The hardness values showed decreases for particular annealing temperature due to occurrence of recovery and recrystallization, but annealing temperature at which recrystallization initiates was bit higher for Cu alloy than pure Cu. During annealing, electrical conductivity of alloy increased up to 350 ^{o}C due to precipitation of solute element Ag from supersaturated matrix. With increasing the annealing time, recrystallization gets suppressed due to anneal hardening effect. The conclusion drawn was that alloy element addition had a pronounced effect on recrystallization temperature.

Song *et al.* (2010) studied the formation of reversed austenite using TEM and mechanism of its formation was discussed. MSS (0.051C-12.34Cr-3.86Ni-0.45Mo-0.5Mn-0.022P-0.004S, in wt. %) was normalized at 1060 ^{o}C for 2h and then water quenched followed by tempering at 570, 590, 610 ^{o}C for 2 hrs followed by argon gas cooling. When the microstructure of alloy tempered at 570 ^{o}C was observed, no traces of reverse austenite were there (as A_s < TT); only carbides precipitates were present along martensitic laths. The dark size image shows that size of precipitates was very small (<100nm). The nucleation of carbides on lath boundaries was expected as martensite lath boundaries were energy favourable sites which provided path for relatively rapidly diffusion of solute. TEM images of alloys tempered at 590 ^{o}C for 2 hrs showed the existence of both reverse austenite and carbide precipitates ($M_{23}C_6$). The precipitates and reverse austenite has a cube-cube orientation relationship with each other and its lattice parameters were 3 times that of reverse austenite. These $M_{23}C_6$ precipitates were pretty rich in Cr content even than that of alloy composition which caused Cr depletion. The reverse austenite formed was rich in Ni but carbide was found to be rich in Cr content which resulted in Cr depletion from boundaries. Moreover carbides or precipitates formed had limited Ni solubility which also caused Ni atoms to diffuse to nearby reverse austenite. In previous literature also no carbon atom enrichment was reported in reverse austenite. Then the authors considered the carbon atoms present provided the nucleation sites for reverse austenite and diffusion of Ni atom will control the growth of reverse austenite. The transformation behaviour of reverse austenite to martensite was determined by its stability. Quantitative measurement of austenite stability was measure of critical driving force required to transform austenite particle. During tempering at 610 ^{o}C, growth in carbides and austenite

was observed at martensite laths. Along with reverse austenite formation at martensite lath, it also got formed within the lath boundaries (only reverse austenite). Similar results as in case of tempering at 590 ^{o}C were observed. Carbides were in excess of Cr content while retained austenite was rich in Ni content. The point was concluded was that the growth of reverse austenite was controlled by Ni diffusion and at the elevated tempering temperature, reverse austenite not only got formed at martensite laths but it also get formed within the martensite laths.

Wang *et al.* (2010) studied the influence of delta ferrite on impact properties of MSS. The experimental alloy was based on American Society for Testing of Materials (ASTM) CA6NM steel, a 13%Cr-4%Ni low carbon martensitic stainless cast steel. The alloy was melted in an electric furnace and vaccum oxygen decarburization (VOD) furnace consecutively and was poured into sand mold of 200mmx200mmx200mm. The blocks with dimension of 12mmx35mmx55mm were machined by EDM for subsequent heat treatments and Charpy V-notch impact tests. To determine effect of delta ferrite on ductile to brittle transition temperature (DBTT) of this steel, impact tests for these samples were carried out at different temperatures ranging from -196-60 ^{o}C. The volume fraction of δ-ferrite decreased monotonously with rise in normalizing time but sample which was normalized at much higher temperature (1350 ^{o}C) and for longer time (20 hrs) exhibited maximum delta ferrite phase. Results showed that presence of δ-ferrite certainly lowers the transition temperature range. At 0 ^{o}C, load displacement curves showed drastic variation. Maximum load, crack initiation and propagation energy decreased with increase in δ-ferrite content. Delta ferrite presence in whatever shape (network morphology, platelet-like discontinuous) shows a monotonically decrease in impact strength with its rise in fraction. According to Griffith fracture theory, material's critical fracture strength is proportional to its strength (microhardness showed hardness of martensite phase was more than delta ferrite phase) so cracks easily initiated in delta ferrite than in martensitic matrix. Therefore cracks first initiated in delta ferrite (mode of fracture was ductile dimple). These cracks propagated and reached martensitic phase as 'pre-cracks'. Pre-cracks could easily propagate in martensitic phase. The conclusions were that the presence of δ-ferrite phase decreases both crack initiation and propagation energy in transition temperature range without varying upper and lower shelf energy of material.

Zheng *et al.* (2010) conducted studies on 12Cr-Ni steels containing carbon ranging from 0.004-0.034% wt to investigate the effect of carbon content on microstructure and mechanical properties of these stainless steels. The alloy steels were prepared in a vacuum induction furnace and cast as 50 kg ingots. The ingots were hot forged into 50mm thickness, which were then hot rolled into 6mm thickness plates by 7 passes. Subsequently they were air cooled to ambient temperature conditions.

It was observed that microstructure of hot rolled 12Cr-Ni stainless steel consisted mainly of martensite and a small amount of banded ferrite. Banded ferrite was composed of equiaxed sub-grains whose size was approximately 1μm. Banded ferrite was formed from delta ferrite. Dynamic recovery of delta ferrite occurred during hot rolling resulting in the formation of sub-grains. The ultra-low carbon martensite in the steel containing 0.004% C after hot rolling and air cooling was characterized by dislocation cells structure. The formation of dislocation cells structure was attributed to high M_f temperature and low interstitial atoms content. Therefore, cell wall with high dislocation density was formed as a result of dislocation motion and tangle. On the other hand, the martensite in steel containing 0.034%C consisted mainly of typical martensite laths because of low M_f temperature and high interstitial atom content which hindered dislocation motion.

It was observed that the increase in yield strength, tensile strength and decrease in percentage elongation with increase in carbon content was attributed to the following reasons: Increased C content increased the super saturation of martensite leading to strong effect of solution strengthening, Increased C content lowered the M_s and M_f temperatures and thus increased the dislocation density, Increased carbon content resulted in a decrease in the volume fraction of ferrite phase resulted in decrease in elongation.

Benchabane *et al.* (2011) studied the recrystallization kinetics of pure copper (99.999%) deformed by cold rolling by using differential scanning calorimeter (DSC) under non-isothermal conditions and calculated two kinematic parameters 1) activation energy of recrystallization process by using three different methods 2) Avarmi coefficient (n) using Matusita method. The peaks of DSC curves showed that energy stored during cold working is released during annealing as recrystallization takes place. The differential scanning calorimeter measurements gave DSC run thermographs of deformed pure copper for different heating rates. The exothermic peaks showed the amount of heat released from the deformed Cu for different heating rates. Activation energy required for recrystallization was calculated using three methods a) Kissinger b) Boswell c) Ozawa method which came out to be 58.33

KJ/mol which was same as reported earlier in literature. Evaluation of Avarmi's exponent of recrystallization (n) by Matusita equation gave a value of 1.4, which was lower than what was listed in literature. The reasons cited for this discrepancy were1) recrystallized nuclei were non-randomly distributed 2) tendency of grain growth retarded with an increase in recrystallization, which was due to non-uniform distribution of stored energy in cold worked matrix.

Isfahany *et al.* (2011) analysed the effect of austenizing and tempering treatment on mechanical and electrochemical corrosion resistance and plotted a relation between properties and microstructure. Steel was produced in vaccum induction furnace and cast as cylindrical ingot reined by electroslag refining. Hot forging was done b/w 900 ^{o}C and 1000 ^{o}C followed by annealing at 700 and air cooling. Block of suitable size was cut along longitudinal direction. Samples were austenised at 980, 1015, 1050 ^{o}C (for 30, 60, 120 min) followed by tempering at 200 for 1 hr. In order to determine second hardening temperature range again tempering was done in range of 200-700 ^{o}C. Hardness, microstructure, tensile test, charpy test were performed. Microstructure analysis showed that in annealed condition microstructure consisted of ferrite and carbide ($M_{23}C_6$) and amount of carbides decreased with increasing austenisation temperature from 980 to 1050 ^{o}C. Austenization temperature had little effect. Microstructure of tempered sample at 200 ^{o}C showed $M_{23}C_6$, at 500 showed M_7C_3, and at 700 ^{o}C showed $M_{23}C_6$. After austenization, highest hardness and strength was observed at 1050 ^{o}C due to homogeneous distribution of lath martensite. With rise of austenisation temperature, impact energy increased, carbide dissolution started, carbide content in martensite matrix increased which produces the lattice distortion together with amount of twin boundaries and dislocations within the microstructure. Tempering between 400-500 ^{o}C led to secondary hardening due to formation of M_7C_3 within martensite lath. In 500-700 ^{o}C range softening starts happening as M_7C_3 transform to $M_{23}C_6$. Impact strength was maximum at tempering temperature of 200 ^{o}C due to presence of retained austenite and lowest amount of carbide. Impact strength started decreasing in 200-500 ^{o}C range and attained minimum value for 500 ^{o}C. After 500 ^{o}C impact strength become maximum for 700 ^{o}C tempering temperature. The conclusion was that maximum hardness, strength and toughness were attained at austenizing temperature of 1050 ^{o}C and while tempering secondary hardening took place in tempering temperature of 400-500 ^{o}C. In present steel optimum combination of strength and ductility could be achieved by austenizing at 1050 ^{o}C and tempering at 200 ^{o}C for 60 min

Ma *et al.* (2011) added Nb to a super martensitic stainless steel (N: 0.01; C: 0.01; Cr: 13; all in wt %) and subjected the steel to normalizing and tempering heat treatments. The objective of the work was to investigate the effect of high Nb addition (0.1%) on solid state transformations, microstructure and the consequent mechanical properties of these SMSSs in the normalized and tempered state. Two laboratory steel samples (SMSSs and Nb SMSSS) were made in the form of ingots, using vacuum induction furnace. The ingots were hot rolled at 1200^0C into plates. Normalizing was carried out at 1050^0C for 0.5h, followed by 2h tempering heat treatment at temperatures ranged from 550^0C to 700^0C. After tempering, the samples were quenched in oil. The heating rate of tempering is about 60^0C/min. The dilatometer technique was performed to study the solid state transformation of these steel samples. The mechanical properties were evaluated by means of tensile and impact tests. It was observed that addition of 0.1% Nb to low interstitial SMSSs decreases the amount of Cr-rich precipitates, as Nb preferentially combines with residual nitrogen and carbon to form nano-scale Nb rich precipitates (5-15nm) during tempering. While the well dispersed Nb rich nano-scale precipitates contribute to significantly to enhance strength, an optimum volume fraction of retained austenite contributes to enhanced ductility and toughness. Nb retards the kinetics of reversed austenite formation. The effect of higher tempering temperature is to increase the volume fraction of retained austenite. The modified SMSSs exhibited yield strength of 930MPa, which was 30% higher (710MPa) than the reference steel without Nb addition, with enough elongation (close to 20%) and charpy toughness (160 J) after tempering at 600^0C.

Yu-Rong *et al.* (2011) investigated the microstructure and mechanical properties of Cr13 Super Martensitic Stainless Steel (SMSS) subjected to heat treatment quenching followed by tempering. In this study two types of low martensitic stainless steels (steel no.1: C: 0.019; Mn: 0.40; Si: 0.16; Cr: 11.69; Ni: 4.94; Mo: 2.04; Fe: balance; all in wt %) and (Steel no.2: C: 0.02; Mn: 0.41; Si: 0.17; Cr: 11.86; Ni: 5.14; Mo: 2.17: W: 1.00; Cu: 1.39; Fe: balance all in wt %) were produced in a vacuum induction furnace. The ingots were forged into bars of diameter of 15mm. All specimens were quenched in the temperature range of 900-1100 °C for 0.5h and then oil quenched. Quenching was followed by tempering in range 550-750 °C for 2h. It was observed (in both steel no.1 and steel no.2) that microstructure after quenching in range 900-1100 °C consisted of lath martensite and retained austenite. Volume fraction of R.A. ranged from 0.3% to 0.49%. With increase in quenching temperature, the martensite

platelets coarsened and original austenite grain size increased (16.8-56.88μm). Grain growth was slow in the quenching temperature ranges 900-1000 °C (because of pinning effect of carbides and other second phase particles) and 1050-1100 °C (due to fully dissolution of carbides and other second phase particles in austenite) however it was rapid in range of 1000-1050 ^{o}C (because of re-dissolution of carbides in austenite). The size of austenite grains of both steels remained same after quenching at the same temperature.

Tempering (done in range 550-750 °C) had little effect on austenite grain growth but the amount of R.A. firstly increased and then decreased with increase in tempering temperatures; the maximum amount of R.A. being at 650 ^{o}C. The microstructure of both steels after tempering at 650 ^{o}C consisted of fine tempered martensite of width 100-200nm with reversed austenite. After same heat treatments steel no.2 had bigger (23%) volume fraction of reversed austenite than steel no. 1 (8%). The reversed austenite located along the boundaries of original austenite crystals and lath boundaries displayed good toughness. In addition the tempered martensite consisted of very fine (width of 100-200nm) martensite with high dislocation density. Comparing the mechanical properties of both steels after same heat treatment (quenching followed by tempering), the tensile strength, hardness and elongation of steel no.2 was better than that of steel no.1. This indicated that addition of W and Cu can significantly improve the material properties of super martensitic stainless steel by retaining more austenite in microstructure.

Bojack *et al.* (2012) conducted in-situ analysis of the phase transformations during re-austenization in a tempered 13Cr6Ni2Mo SMSS using three in-situ techniques namely Thermo-Magnetic Technique (TMT), Dilatometry and High Temperature X-Ray Diffractrometry (HT-XRD).

The SMSS was delivered in the double-tempered condition (4h at 635 ^{o}C and 2h at 550 ^{o} C) with a microstructure consisting of martensite, retained austenite and very small fraction of carbides, nitrides and carbonitrides.

From dilatometry, the austenite formation in SMSS was found to take place in two steps. The Ni-rich regions transformed to austenite first, due to their lower A_{C1} temperature. The second stage of austenite formation then takes place at higher temperatures due to the lower local Ni-content. The two stages could not be observed with magnetic measurement, because they occurred above the Curie temperature.

The martensite fraction obtained from the magnetic experiment was more accurate than the one from dilatometry experiment. Since only the length changes contributed to the

observation of martensite phase fraction, the anisotropic character of the transformation affected the results of dilatometry more than those from the magnetometer experiments. Furthermore, the austenite fraction could be calculated directly from the magnetic results using the Koistinen-Marburger equation with $\alpha_{km} = 0.018K^{-1}$ and $T_{km} = 220\ ^{o}C$.
Enhanced martensite formation at the sample surface was detected by XRD, which was assumed to be due to the increased relaxation of transformation stresses at the sample surface. Also, 4 vol % retained austenite was detected after cooling from the austenitization temperature, which was due to the thermodynamic stability of austenite at room temperature in the composition.

Nakada *et al.* (2012) investigated the effect of prior deformation and heating rate on the formation of dual phase structure obtained by partial reversion of cold rolled martensite in a low carbon steel (C:0.15; Mn:1.00; all in % wt). Low carbon dual phase steels comprise of ferrite and martensite structure. These steels have god tensile strength and deformability. In the present work, the author tried to obtain further improvement in tensile strength (for good strength to wt ratio) without loss of ductility. Grain refinement of ferrite matrix is an effective method to strengthen DP steels without a significant loss of elongation. The research focused on using martensite as a starting structure to form fine-grained DP structure. In this study, steel plates were initially solution treated (at 1273K) and were then water quenched to obtain a full martensitic structure. These were then cold rolled to achieve 20%, 40% and 60% thickness reduction. The cold rolled samples were heated to 1023 K at two different heating rates (0.083k/s and 100K/s respectively) and held there for 300s, followed by water quenching. Additionally, CR materials were isothermally tempered at 723-923 K for various durations to quantify the recrystallization w.r.t tempering parameter $\lambda = T (\log t + C)$. It was observed that increasing the rolling reduction extent or lowering the heating rate enhanced the recrystallization of martensite matrix on heating before the onset of reversion, although the undeform med martensite never caused recrystallization irrespective of the heating rate. The results showed that in less deformed materials (with C.R. up to 20% or less), only reversion of martensite to austenite occurred (as recrystallization temperature) in such cases was above the reversion temperature. Such steels showed a balance of good tensile strength and ductility. In highly deformed materials (with CR more than 20%), both recrystallization and reversion occurred resulting in dual phase structure comprising of recrystallized ferrite martensite. These steels had excellent tensile strength with reasonably good ductility. Thus, it

was concluded that in less deformed steels, only reversion process occurred whereas in highly deformed materials both reversion as well as recrystallization took place.

Perdahcioglu and Geijsealaers (2012) proposed a model which can describe the different aspects of mechanically induced martensitic transformation on physical basis. The novelty of approach was that the magnitude and direction of transformation strain were completely determined on macroscale as a function of transformation only. When the material is under stress, the additional driving force was applied to potential martensite variants for transformation. The martensite formed was considered to be function of applied stress and transformation during stress application will take place with dissipation of mechanical energy due to inelastic deformation of material. The aim was to use calculated driving force resolved on variants to predict the amount of transformation. There always exist a transformation barrier which had to be crossed to initiate transformation and when driving force on variant reaches the barrier transformation took place. The two interpretations for this transformation were that either the M_s rose due to applied force or for getting transformation there needs to be application of certain force. It has been proved experimentally that different potential martensite variants required different transformation energy or they had different critical barrier energy. During martensitic transformation a significant amount of additional inelastic strain was gained. The conclusions drawn were that knowing mechanically driving force resolved on variants and critical energy barrier enable to compute the total transformation strain and by computing the martensitic fraction enable the amount and direction of transformation strain to be determined analytically.

Ye *et al.* (2012) investigated the effect of Cu addition (0, 1.5 and 3; all in wt. %) to a 15% Cr Super Martensitic Stainless Steel (SMSS). The study focused on the comparison of solid solution and precipitation behaviour and its effect on microstructure and mechanical properties of 0-Cu, 1.5-Cu and 3-Cu SMSS. These three types of SMSSs were designed and melted with extra low impurity contents in vacuum induction furnace. The ingots were cast and hot forged into round bars of 15mm diameter. Solution annealing was carried out at 1050 ^{o}C for 1.5h followed by oil quenching. Tempering was carried out at a temperature range from 550^{0}C to 750 ^{o}C for 1h.

The study revealed that after quenching (during solution annealing), lath martensite and retained austenite were formed, and there were more than one lath martensite packets with different orientation in one austenite grain. There was no significant difference in the

microstructure obtained in the three type of steels, but the width of lath martensite of 3-Cu was smaller than that of 1.5-Cu and 0-Cu. The results showed that Cu can contribute to grain refinement because of precipitation of Cu-rich phase along dislocation and grain boundaries. This led to a strong pinning effect on grain boundary migration and prevented grain growth.

During tempering, the microstructures of the three steels had changed from the thick lath martensite to fine tempered martensite. Also it was observed that Cu acted as a austenite stabilizing element and promoted the formation of reversed austenite. The reversed austenite was formed by diffusion process of alloying elements during tempering, particularly nickel. So the microstructure after tempering was tempered martensite, retained austenite and reversed austenite. The volume fraction of austenite at 650 ^{o}C was maximum in all three steels and above this it decreased due to the transformation from reversed austenite to martensite during the cooling process. Comparing the two steels, the volume fraction of austenite (55.9%) in 3-Cu was higher/maximum than 1.5-Cu, demonstrating addition of Cu promotes the austenite formation. As a result, the elongation of 3-Cu was highest of these steels.

The study concluded that Cu can act as a solute in the matrix under quenching condition and can precipitates as Cu-rich nanometer phase in SMSS, leading to solid solution strengthening and precipitation strengthening. Cu also contributes to grain refinement. The increase of Cu content not only improves the ductility but also increases the hardness and strength of SMSS after tempering. Cu alloyed SMSS exhibits greatly improved mechanical properties.

Prat *et al.* (2013) investigated the effect of Laves phase formation and their growth on creep strength of 9% Cr alloys. The composition of newly designed alloy was adjusted to allow formation of Fe_2W Laves phases during creep at 650 ^{o}C. The growth kinetics of Laves phases was modelled using software and simulation results were compared with experimental investigation. The investigated alloy was produced by vaccum induction furnace followed by hot rolling and forging at temperature of 1150 ^{o}C and was air cooled. Standard heat treatments were performed including austenization for 0.5hr, subsequent air cooling and tempering at 780 ^{o}C for 2 hrs with posterior air cooling. Quantitative analysis of precipitates was done and there mean diameter was calculated even though they were not spherical but were assumed so. The microstructural analysis by TEM showed nano sized Nb-MX particles with spheroidal shape and V-MX precipitates with plate like shape. For both alloys laves phase of approximately hexagonal shapes were observed after certain time of creep testing and TEM-EDS analysis showed that main element in them were W, Fe and small amount of

Cr and conforming that laves phases in present steel were of Fe_2W type. The irregular shaped Laves phases were always present close to $M_{23}C_6$ and on martensite lath boundaries or sub-grain boundaries. Distribution of laves phases was very much heterogeneous and they were always found to present in clusters which decreased the strengthening of heat resistant alloy and clustered regions were preferential sites for damage initiation and accumulation ahead of cracks. The conclusions drawn were that Laves phases of type Fe_2W precipitate out near to $M_{23}C_6$ with distribution completely heterogeneous. The clustering of precipitates decreases the strength of heat resisting alloy.

Wang *et al.* (2013) studied the martensitic transformation behaviour of deformed super-cooled austenite and formation of nanostructured lath martensite in medium-carbon Si-Al-rich alloy steel. The forged bars of alloy with section dimension of 25 mm x 25 mm were completely annealed by heating to 920 ^oC for 1 h and furnace cooling to room temperature. The thermomechanical process was carried out on a thermomechanical simulator. After compressive deformation at 600 and 300 ^oC by 50% reduction with a strain rate of $0.01s^{-1}$, samples were unloaded and cooled down to room temperature. Microstructure was examined by OM, XRD, and TEM. Dilation temperature curves showed a depression in M_s temperature with deformation and it also showed a variation in strength. The deformation temperature decrease resulted in decrease of M_s temperature and the martensite lath thickness also decreased. The conclusion drawn was that with decrease in austenite grain size, M_s temperature decreases and corresponding explanation was given on basis of martensite nucleation thermodynamics.

2.5 GAPS IN LITERATURE

Literature review carried out for the present work clearly brings forth the fact that microstructure of SMSSs has an imperative effect on their mechanical properties. MSSs from which SMSSs have been developed consist of martensite, un-dissolved carbides and δ-ferrite (Sedriks, 1996; Balan et al., 1998; Tsai et al., 2002; Choi et al., 2007; Wang et al., 2010; Isfahany et al., 2011).

There exists a huge ambiguity on the role of δ-ferrite in these steels. Some researchers believe it to be a soft phase which enhances ductility and toughness while others believe that it deteriorates impact properties due to lack of cohesion between delta ferrite and surrounding matrix (Carrouge et al., 2004; Wang et al., 2010; Zheng et al., 2010). One of the main reasons for this confusion is the difficulty in studying the effect of δ-ferrite and carbides individually.

δ-ferrite being rich in Cr content than the surrounding matrix has higher tendency for carbide formation within its vicinity. Majority of the work reported in literature attributes the negative effect to the carbides and little attention has been paid on the real effect caused by the difference between delta ferrite and matrix properties (Rho et al., 2000).

After studying the literature, it has been observed that in order to possess high strength in combination with good ductility, the volume fraction of retained austenite plays a decisive role and needs to be controlled by appropriate heat treatment/tempering process for any given chemistry of SMSSs (Leem et al., 2001; Ping et al., 2005; Li et al., 2008; Song et al., 2010; Yu-rong et al., 2011). Major effort has been devoted on effect of alloying additions on properties of SMSSs and it was limited to retained austenite content (Klotz et al., 2008; Zheng et al., 2010; Ma et al., 2011; Ma et al., 2012b; ; Ma et al., 2012c; Tobata et al., 2012**;** Ye et al., 2012**)**. Quite correctly, even though this grade of SS is heat treatable, unlike austenitic SSs, limited attempts have been made to investigate the effect of thermo-mechanical processing routes. Most of the work related to thermo-mechanical routes has been inclined towards tempering treatment (Balan et al., 1998; Isfahany et al., 2011; Ma et al., 2012b). High temperature tempering has been considered to be a requisite condition for obtaining optimal combination of ductility, toughness and stress corrosion resistance along with maximum possible strength (McDowell et al., 1966; Pickering, 1976; Sedriks, 1996). Even though tempering results in toughness and ductility escalation but it happens at the cost of strength values (De-ning et al., 2010; Isfahany et al., 2011; Yu-rong et al., 2011; Bojack et al., 2012). Further, the precipitates (mainly $Cr_{27}C_6$) formed along the martensitic laths or the prior austenite grain boundaries (Ma et al., 2012a) while tempering, deplete the grain boundaries of Cr content making it vulnerable to corrosion (Raghvan, 2006; Choi et al., 2007; Ma et al., 2012a). Also, the tempering treatment demands for long soaking periods. As a result, it has become important to develop a new thermo-mechanical route which could lead to optimum combination of properties in SMSSs. Thus, there is a need to develop a new thermo-mechanical route for super martensitic stainless steels which can produce an optimum combination of properties, involving shorter soaking periods making it feasible for industrial applications.

CHAPTER 3
DESIGN OF THE STUDY

3.1 INTRODUCTION

This chapter presents the overall design of the study. It describes the objective of present research, the methodology, experimental procedure adopted, and the details of machines and equipment used for carrying out the research work.

3.2 METHODOLOGY

One of the most important tasks in the present work has been identification of controllable and uncontrollable parameters and conducting a series of experiments to find out the combination of parameters which have greatest influence on the desired objective function.

Phase I: This phase is aimed at determining the important parameters which play a vital role in the present work. The parameters such as extent of cold rolling, temperature and holding time periods for heat treatment, critical temperatures for the alloy under investigation etc. have been established through an extensive literature review and experimentation. The operating range of each process parameter has been finalised after its detailed study from the previous research work.

Phase II: In this phase, a series of experiments have been carried out in order to extract valuable information regarding the alloy. The experiments have been conducted with due concern in the operating range of process parameters (established in the previous phase) and the resulting outputs have been analysed.

Phase III: This phase discusses the results obtained, the reasons thereof, and draws important conclusions. It also discusses the limitations of the present work and its future scope.

3.3 ESTABLISHMENT OF OBJECTIVE FUNCTION

The review of literature for the present dissertation work revealed that extensive work has been reported with regards to improvement in properties of Super Martensitic Stainless Steels through alloy addition (i.e. by changing the alloy composition). However, very limited work has been reported on improvement in properties of SMSSs through the heat treatment route (thermo-mechanical treatment).

The overall objective of the present study is to analyse the effect of a new thermo-mechanical treatment route on the microstructure and mechanical properties of a Super Martensitic Stainless Steel. The thermo-mechanical treatment comprised of cold working followed by isothermal annealing for a short period of time to study its effect on the recrystallization behaviour, phase transformations, morphology and the resulting mechanical properties.

The overall objective of the present work consisted of several sub-problems/ issues. The key issues taken up during the present research work are:

- To determine the conditions for austenite stability and reversibility in the given SMSS.
- To evaluate the effect of isothermal annealing on the recrystallization kinetics, phase reversion and morphological/ microstructural changes for cold rolled and for annealed cold rolled specimens.
- To account for competition between recrystallization and reversion during isothermal annealing process.
- To evaluate the effect of cold rolling and isothermal annealing on the yield strength and ductility of SMSS alloy under investigation.

3.4 MATERIAL SELECTION

The present work investigates a newly developed Super Martensitic Stainless Steel. The Fe-11%Cr-7%Ni alloy selected for the study has composition as shown in Table 3.1.

Table 3.1 Composition of the SMSS Alloy

Element	C	Cr	Ni	Mn	Si	Fe
% Weight	0.023	11.3	7.6	1.3	0.62	Balance

The above stated composition was selected in order to obtain martensitic microstructure while air cooling from high temperature uniphase austenite. Nickel acts as an austenite stabilizing phase, therefore its content is raised from 4-6 wt. % (as in conventional martensitic stainless steels) to above 7 wt. % (in SMSS). The formation of δ-ferrite detracts

from maximum achievable strength, therefore δ-ferrite forming element chromium is targeted at slightly lower end of 13-16wt. % (as in conventional martensitic stainless steels) specification to near 11% wt. (in SMSS). This is requisite requirement of Chromium for retaining corrosion resistance. The cheapest austenite forming addition is carbon, but its %wt. has been lowered to near 0.02% wt., as higher carbon content would decrease the toughness and weldability, impair corrosion resistance and require higher solution-treatment temperatures.

3.5 INPUT PARAMETERS

The main input variables whose effect has been investigated in the present work are discussed as follows.

3.5.1 Cold Rolling

Plastic deformation which is carried out in a temperature region and over a time interval such that the strain hardening is not relieved is called cold rolling (cold working) (Dieter, 1988). With the increase in extent of cold working, the dislocation density goes on increasing which by virtue of their interaction results in higher state of internal stress. The energy expended in deforming a metal is stored in lattice as internal strain energy while most of energy transforms into heat energy. The cold worked dislocation cell structure is mechanically stable but it is not thermodynamically stable. With temperature rise, the cold worked state becomes more and more unstable and starts reverting towards the strain-free condition. This process of reversion from the cold worked state is given the name of annealing and it comprises of fairly distinct processes of recovery, recrystallization, and grain growth. For compositions, representing the martensitic/ super-martensitic stainless steel range, it has been concluded that 80% thickness reduction during cold working results in almost prefect destruction of lath martensite structure through intrusion of many slip bands and through the lattice distortion. Above 80%, the fraction of distorted martensite and dislocation density levels off (Takaki et al., 1992). The extent of cold rolling decides the fraction of recrystallized matrix while undeformed martensite is hardly recrystallized (Takaki et al., 1992; Natori et al., 2005; Tsuchiyama et al., 2010; Nakada et al., 2012).

3.5.2 Isothermal Annealing Temperatures

Intercritical heat treatment temperatures lie within the range of lower critical temperature (LCT) and upper critical temperature (UCT) for a given metal or an alloy. It is expected that in this very range of temperature, there exists a competition between recrystallization and reversion phenomenon. Therefore, the lower and upper critical temperatures (LCT and UCT) were considered as very important parameters for tailoring the microstructure of the alloy under investigation. In-situ high temperature phase transformation studies performed on the alloy under investigation in an earlier work (Kumar et al., 2013) and also on a similar SMSS alloy (Bojack et al., 2012) found the austenite formation start and finish temperatures (A_s and A_f) for the alloys to be lying between the upper and lower critical temperatures for the respective SMSS alloys. The lower critical temperature and the upper critical temperatures for the alloy under investigation as obtained by Kumar et al. (2013) were found to be 750ºC and 950ºC respectively and the same will be used for the present investigation.

3.5.3 Isothermal Annealing Time Periods

In the present work, the objective is to understand the effect of cold rolling and annealing process on the phase transformations and recrystallization of SMSS alloy to establish a new route of thermo-mechanical processing which can result in desired mechanical properties. Literature (De-ning et al., 2010; Isfahany et al., 2011; Bojack et al., 2012) reveals that tempering treatment performed on lath martensitic structure of SMSS (in earlier studies) required an elongated time period, without producing substantial restoration of properties viz. ductility and toughness. The aim in the present work is to obtain a heat treatment route in which recrystallization proceeds for very short holding period at the heat treatment temperature. As a result, very short soaking time periods have been selected in the present study. Such short time periods can be very fruitful for industrial applications for producing high strength SMSS along with optimum combination of ductility.

3.6 EXPERIMENTAL SETUP

This section provides an overview of the various machines and equipment used in the conduct of present study. The experimental set up included various sophisticated machines and equipment for alloy preparation, cutting to specific sizes, facilities for heat treatment, characterization and mechanical testing of the material.

A brief outline and description of the characteristic features of these machines and equipment is described below.

3.6.1 Precision Cutter

Precision cutter is convenient preparation equipment in a laboratory and is designed for precision cutting of wide variety of materials. Samples can be cut with minimum damage and deformation. Precision cutter (Make: Metkon Microcut, 125 Low speed) used in the present work is suitable for precision cutting of hard materials. The machine is equipped with diamond saw blade and a resin blade to meet the demand of cutting of varying specimens. Many specimen clamping grippers are equipped with this machine and it can realize the positioning cutting at best angle for the work piece. It can also realize work piece processing without being watched.

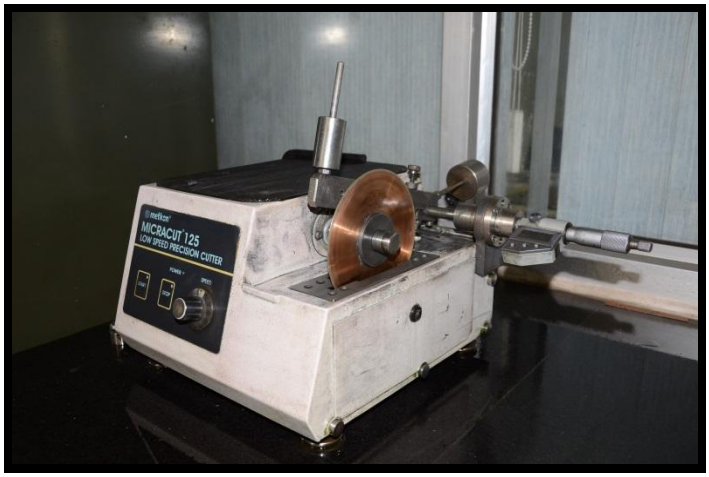

Fig 3.1 Low Speed Precision Cutter

3.6.2 Muffle Furnace

Muffle furnace is a front loading box type oven or kiln for high temperature applications such as fusing glass, creating enamel coating, ceramics soldering and brazing of articles. The inner chamber is made of stainless steel and heaters are clamped to its outside and operated at low heat. Glass wool insulation is used between the two walls. Temperature control is provided by a capillary thermostat which possesses excellent durability and accuracy. Heaters are made of 80/20 nichrome wire, uniformly wound on the muffle. The safety fuse limits the temperature from exceeding the value of set temperature. Mild steel control box is fitted at the bottom of the furnace and consists of indicating lamps, On/Off switch, digital temperature controller along with Cr/Al thermocouple sensor. The furnace is electrically operated at 230 Volts (AC), Single Phase, and 50 Hz supply. The muffle furnace used in the present work is shown in Figure 3.2.

Fig. 3.2 Muffle Furnace

3.6.3 Ultrasonic Cleaner

Ultrasonic cleaning is used widely for removing problem of contamination from all form of hard surfaces such as metals, plastics, and ceramics. The present work uses an Ultrasonic Cleaner (Make: Elmasonic S30H) with temperature capacity of 30ºC and time limit of 30 minutes. Its unique properties can be harnessed to clean items of all shapes, sizes and technical complexity, penetrating holes and cavities that are impossible to reach using ordinary cleaning methods. Ultrasonic-cleaner works on the principle that piezoelectric transducers attached to the cleaning tank generate ultrasound waves that vibrate the cleaning fluid at very high velocity, creating a process called cavitation. Millions of tiny bubbles implode within the solution and penetrate into every orifice of the item being cleaned, removing dirt, oil, grease, pigments, polishing compounds, flux agents, fingerprints, soot, wax etc. within seconds.

Fig 3.3 Ultrasonic Cleaner

3.6.4 Hardness Testing Machine

Vickers Hardness Tester is a key piece of equipment that is vital to metallographic research. In Vickers micro-hardness test procedure, indentation is made with a range of loads using a diamond indenter which is then measured and converted to a hardness value. For this purpose, test samples are carefully and properly prepared by grinding and polishing. Two types of indenters are generally used for Vickers test family; a square base pyramid shaped diamond indenter for Vickers hardness testing and a narrow rhombus shaped indenter for Knoop hardness testing. The Vickers hardness test method requires a pyramidal diamond with square base having an angle of 136° between the opposite faces. Upon completion of indentation, the two diagonals are measured and the average value is considered.

Fig 3.4 Vickers Micro-hardness Tester

Vickers Hardness Number is obtained by dividing the applied load in kilogram-force by surface area of indentation. Figure 3.4 shows the hardness tester used in the present work (Make: Leica VMHT Auto of type 302803).In the present study, the micro-hardness tester was operated at a low load of 50 gram-force for a dwell time of 10 s and with an indenter speed of 30 μm/s.

3.6.5 Tensile Testing Machine

Tensile testing can be used to ascertain several mechanical properties. A specimen is deformed, usually to fracture, with a gradually increasing tensile load that is supplied

uniaxially along the long axis of the specimen. The standard tensile test specimen is dog-bone shaped. In a tensile test, the primary use of the tensile test machine is to prepare the stress-strain curve. After the diagram is generated, a pencil and a straight edge or a computer algorithm can be used to calculate the yield strength, young's modulus, ultimate tensile strength and total elongation.

Fig. 3.5 Universal Tensile Testing Machine

Tensile testing takes several minutes to be performed and is destructive (the test specimen is permanently deformed and usually fractured). Figure 3.5 shows the setup of tensile testing machine (Make: Instron 8862) used in the present work. It has a capacity of 100 kN.

3.7 EXPERIMENTAL PROCEDURE

A recently developed Super Martensitic Stainless Steel has been used for investigation in the present work. Though material processing of this alloy was directly not a part of the present research work, but still an overview regarding its preparation is being presented along with the experimental procedure.

3.7.1 Material Processing

The SMSS alloy of stated composition (Table 3.1) was prepared in the form of an ingot using a 5 kg induction furnace in vacuum. The ingot was homogenized at 1200ºC for 25 hours and was hot forged and hot rolled at 1200ºC to 13 mm thick plate. Now, coupons of size 200 x 30

mm were cut and machined to clean the top oxidized scales (formed during hot rolling) before further processing.

3.7.2 Cold Rolling

The SMSS alloy coupons were now cold rolled for thickness reduction. The coupons were cold rolled and reduced to 2.5 mm thickness from 13 mm (original thickness) in multiple passes (with water intercooling). Thus, the total thickness reduction achieved was 80%. Multi-pass unidirectional cold rolling with same thickness reduction per pass was performed in a two-high rolling mill under oil lubrication (shown in Figure 3.6).

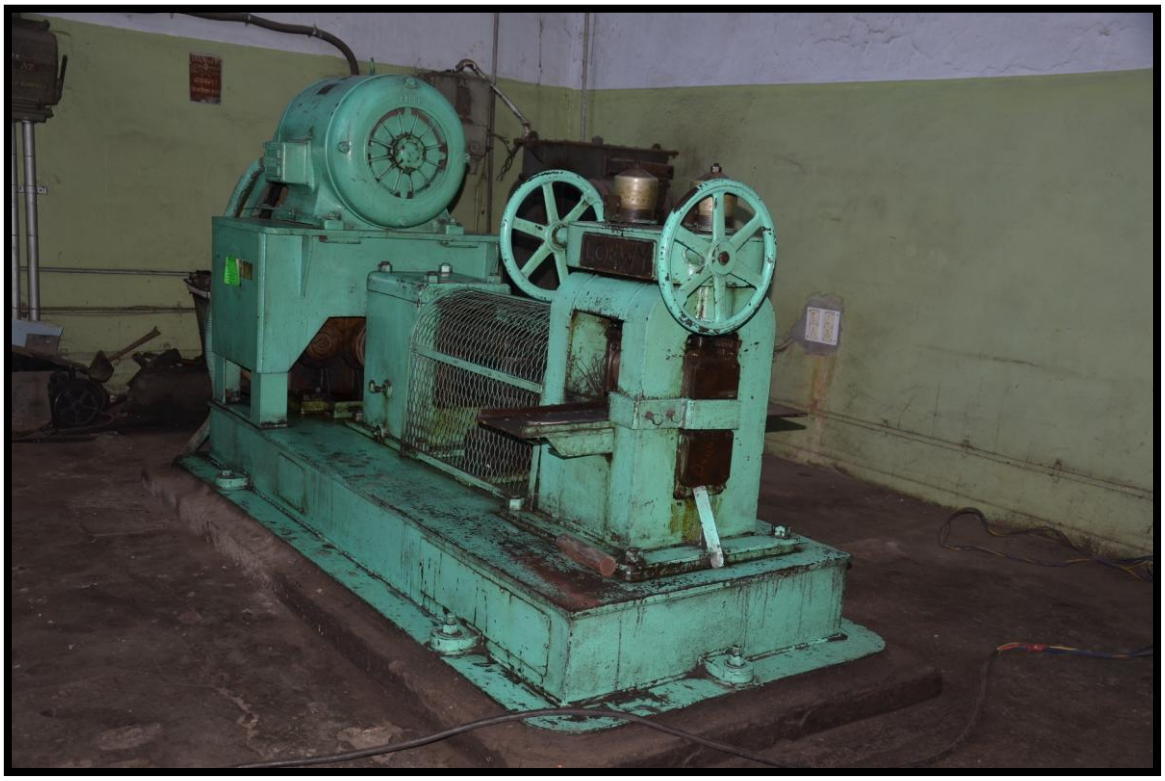

Fig. 3.6 Two-high Rolling Mill

3.7.3 Sizing and Solution Annealing

From one of the cold rolled coupons, three small coupons were cut. The first coupon was designated as 'CR_1' (cold rolled and solution annealed by quenching), the second coupon was designated as 'CR_2' (cold rolled and without solution annealing), and the third small coupon was designated as CR_3 (cold rolled and solution annealed by air cooling).

The sample, CR_1 was subjected to solution annealing treatment. For this, it was heated to 1060ºC, soaked there for 1 hour and was then water quenched. The purpose of CR_1 was just

to act as a reference sample to compare the stability of austenite phase when SMSS is subjected to quenching (CR_1) and to air cooling (CR_3).

CR_2 samples were not given any additional post treatment (solution annealing) to modify the effects induced due to cold rolling. However, for CR_3 samples, an additional post treatment was provided (to the cold rolled material) in the form of solution annealing at 1060ºC for 1 hour followed by air cooling (to finish out all effects of processing).

CR_2 coupon was cut into 16 samples of the same size. The samples were designated alphabetically as shown in Table 3.2. In the nomenclature used, the alphabets represent the temperature and the subscript numerals represent the soaking time periods to which the samples were subjected.

For CR_3, only four samples (A_1, A_2, A_3, and A_4) were cut. Prior studies (Nakada et al., 2012; Kumar et al., 2013) have shown that cold rolled SMSSs subjected to solid solution (air cooled) contain undeformed martensite. The studies showed that SMSS with undeformed martensitic structure does not show any recrystallization in the temperature range 750-950ºC for soaking time periods up to 1 minute. Due to this less tendency of SMSS (air cooled) containing undeformed martensite to show recrystallization, the air cooled samples (CR_3) were only investigated for a larger time period (2 minutes) at all temperatures. The samples were designated as shown in Table 3.3.

Table 3.2 Annealing Treatment Parameters for CR_2 Samples

Time (min) ⇨	**1.00**	**1.50**	**2.00**	**2.50**
Temperature (°C) ⇩	**SAMPLE DESIGNATION**			
750	U_1	$U_{1.5}$	U_2	$U_{2.5}$
800	V_1	$V_{1.5}$	V_2	$V_{2.5}$
850	W_1	$W_{1.5}$	W_2	$W_{2.5}$
900	X_1	$X_{1.5}$	X_2	$X_{2.5}$

Table 3.3Annealing Treatment Parameters for CR_3Samples

SAMPLE DESIGNATION	**Temperature (°C)**	**Time (min)**
A_1	750	2.00
A_2	800	2.00
A_3	850	2.00
A_4	900	2.00

3.7.4 Annealing Treatment

The CR_1 sample was only given solution annealing in such a way that it was raised to a temperature of 1060ºC and was water quenched from this temperature. Each sample cut out from CR_2 and CR_3 coupons were heated to a particular intercritical temperature and soaked there for a stipulated time period as shown in Table 3.2 and Table 3.3. The temperature chosen for investigation were inter-critical temperatures lying in range of 750-950ºC. The annealing treatment was carried out in a muffle furnace.

3.8 SAMPLE PREPARATION FOR METALLOGRAPHY

After the heat treatment, all samples were prepared for metallographic examination. In order to prepare samples for material characterization, some basic steps need to be followed carefully. These include mounting, planar grinding, rough polishing, final polishing, etching, and microscopic analysis. These steps are discussed in brief as follows:

A) Mounting

Mounting of samples is usually done in order to facilitate their easier handling. Mounting is done with either copper or bakelite. Copper is mostly used as a mounting material but it also exhibits a limitation. While ultrasonic cleaning, copper gets removed and settles down over the specimen.

Specimens were hot mounted at a temperature of 160ºC by following the procedure similar to powder metallurgy. The edges of the mounted samples were rounded to minimize the damage to grinding/polishing discs. The mounting press (Make: Bainmount METCO) is shown in Figure 3.7(a). The samples used in the study and the mounted sample are shown in Figure 3.7 (b) and Figure 3.7 (c) respectively.

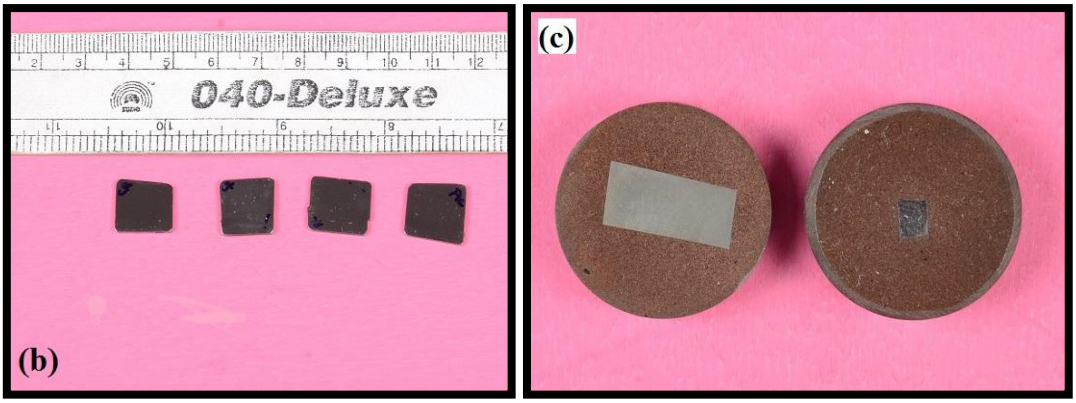

Fig 3.7 (a) Mounting Press (b) Samples (c) Mounted Samples

B) Grinding

Grinding is required to planarize the specimen. The surface to be examined by microscope is polished with abrasive papers of successive finer grades such as 80, 120, 220, 320, 400, 600, 800, 1000, 1200, 2000 mesh abrasive paper. Each time the sample is rubbed on SiC paper, it produces scratch marks and therefore polishing is continued till the scratches from earlier stages (SiC paper) have been obtained in uniform one direction. Then, the direction of scratching or rubbing is switched perpendicular to previous scratches on the next paper with finer grade. Again this is repeated until all scratches get oriented uniformly in one direction. The over-heating of sample is avoided as it may cause modification in the microstructure. Further, the pressure needs to be adjusted wisely as high pressure applied can lead to introduction of deep scratches and low pressure applied can result in elongated time consumption. Starting from the coarse grade paper (80 grit size), the procedure was carried up to fine grade paper (2000 grit size).

Fig. 3.8 Emery Papers

C) Polishing

The next step in preparation of sample is polishing on a horizontal rotating wheel. Polishing wheels are covered with a soft cloth (velvet, canvas, suede or selvet etc.) which needs to be impregnated with polishing medium (alumina or colloidal). The polishing medium is spread on to the rotating disc and specimen is held on the rotating disc in order to obtain a scratch free surface with mirror like polishing. Precautionary measures such as washing the specimen and also the polishing cloth thoroughly with water prior to initiating polishing should be done. This would divert any chances of introduction of contaminant or abrasive particles (from abrasive paper during grinding) which may lead to more deep scratches. Polishing medium is spread on to a well washed cloth and as soon as the specimen starts to stick or friction starts to act between the specimen and cloth, water is poured on to the rotating wheel. Polishing machine (Make: BANIPOL METCO, Model No: PMV018) of 0.37 kW capacity was used in the present work. Polishing machines are shown in Figure 3.9.

Fig 3.9 Polishing Machines

D) Etching

Etching is done in order to reveal the microstructure of the metal/alloy system through selective chemical attack as the constituents mostly show similar reflectivity, causing difficulty in distinguishing them. Etching occurs by electrolytic action at structural variations on the sample surface. Chemical etchants produce either a metallographic contrast as grains etch at different rates because of variation in their crystallographic orientation which produces steps at grain boundaries and reflectivity difference or by grain or phase-boundary etching, which produces grooves. The sample must be thoroughly cleaned before etching. A satisfactory etchant must be selected and prepared, and etchant may be applied using a cotton bud wiped over the surface for a few times (necessary precautions must be taken while etching, as there is only a hair line difference between etching and over-etching). Chemical

etchant needs to have three main components: a corrosive agent (such as hydrochloric, sulphuric, phosphoric, or acetic acid), a modifier (such as alcohol or glycerine) that reduces ionization, and an oxidizer (such as hydrogen peroxide, Fe^{3+}, or Cu^{+}).

The etchant used in the present work has a composition comprising of HCl (5ml) + $FeCl_3$ (1g) + C_2H_5OH (12ml). The specimen is immediately washed with alcohol after applying etchant and dried. Numerous small pits appear on the etched specimen due to localized chemical attack which preferentially occurs in regions of high local disorder (high concentration of dislocations). The presence of pits obscures the main feature to be observed up to a certain extent.

3.9 MICROSTRUCTURAL EVALUATION

Microstructural analysis is used in research studies to determine the microstructural changes that occur as a result of varying parameters such as composition, heat treatment processing etc. Through microstructural analysis, the processing-structure-property relationships are developed. Material characterization of each sample has been done on the material characterizing machines as discussed below. The various material characterization techniques used in this study are described as follows.

A) Optical Microscopy

Optical microscope is used for the purpose of magnifying small samples by using visible light and system of lenses. The image from an optical microscope can be captured by normal light sensitive cameras to generate micrographs. Metallic materials are usually opaque and therefore investigations of plane cross-sections by incident light prevail in metallography. While amplitude objects become visible owing to differences in light absorption and thus appear in different grey shades or even colours, phase objects only differ in the refractive indices which cannot be recognized without additional provision. Starting from the cross-section preparation, to etching of the specimen, and setting up of microscope, all steps should be carefully optimized in order to get maximum information from a microscopic study. The optical microscope used in the study is shown in Figure 3.10. In the present work, optical microscopy has been largely utilized to check if the samples have been appropriately prepared (i.e. do not contain pits, scratch marks etc.) for SEM, XRD and EBSD analysis.

Fig 3.10 Optical Microscope

B) ***Feritscope***

Feritscope is the easiest and a non-destructive method for measuring the ferrite content accurately. When the probe of feritscope is placed on the surface of specimen, the reading is displaced automatically and is stored in the instrument. In order to obtain comparable measurement results, the instrument is calibrated using standards that can be traced to internationally recognize secondary standards. Influences including the shape of part to be measured (strong curvature, thickness of ferrite containing coating, etc.) can be taken into account through corrective calibrations with customer specific calibration standards or through corrective factors included. Feritscope measurements are based on magnetic induction method. A magnetic field generated by the instrument's coil begins to interact with the magnetic portion of the specimen. A change in magnetic field induces a voltage proportional to the magnetic content (i.e. ferrite content and martensitic content) in the secondary coil. Feritscope (Fisher Feritscope MP 30E-S) has been used in the present study and shown in Figure 3.11.

Fig. 3.11 Feritscope

C) X-Ray Diffraction

X-ray diffraction technique is one of the most powerful techniques for qualitative and quantitative analysis of nano-crystalline materials. There are various techniques which can be used for determination of phase type, their volume fraction, grain size measurements, and other minute details. These include transmission electron microscopy (TEM), scanning electron microscopy (SEM) and X-ray diffraction (XRD). Apart from grain size measurement, information obtained includes type and nature of crystalline materials present, structural make-up of phases, degree of crystallinity, and amount of amorphous content, micro- strain, and size and orientation of crystallites. In non-crystalline materials, microstructure is inhomogeneous with grain sizes being widely distributed. Thus grain size alone becomes inadequate in describing microstructure. In order to overcome this problem, XRD has recently included dislocation density and different type of crystal defects to provide valuable information about material under investigation. In the present work, XRD analysis of different samples was conducted on the X-Ray Diffraction machine (Make and Model: D8 Discover Brucker) shown in Figure3.12. The 2θ start and end angles are 38º and 105ºrespectively with scan speed of 2s/step and increment of 0.02θ/step. Cu K□ of 0.154nm wave length along with fast position sensitive detector has been used for diffraction experiments.

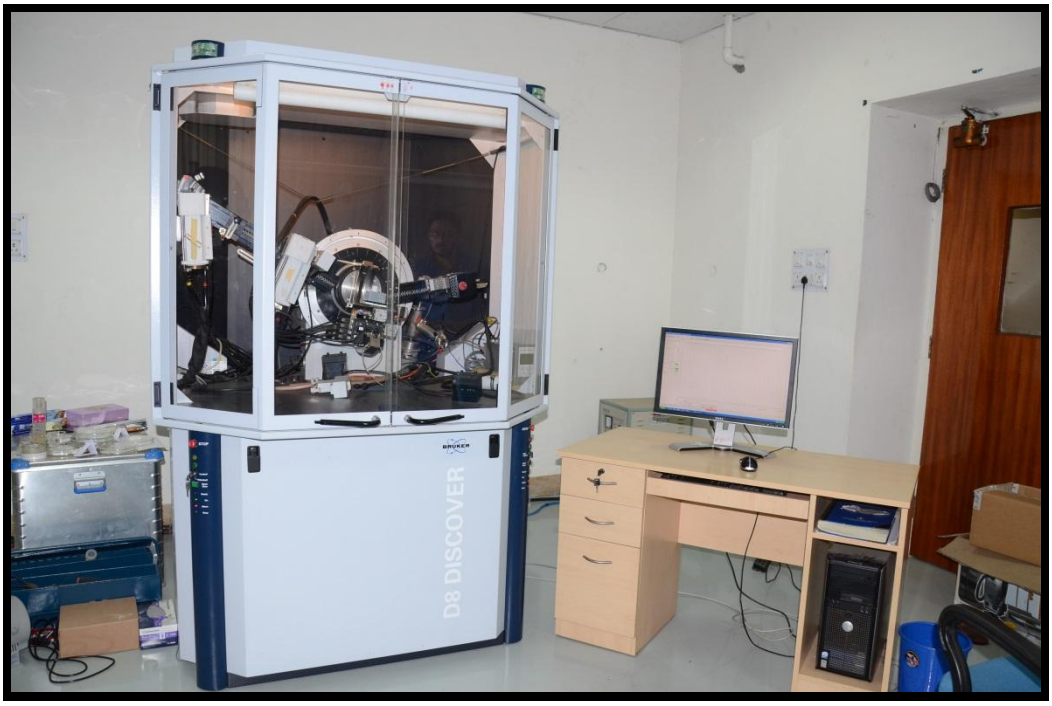

Fig 3.12 X-Ray Diffraction Machine

D) Electron Back Scatter Diffraction

Electron Back Scatter Diffraction (EBSD) is also known as Backscatter Kikuchi Diffraction (BKD) or Electron Back Scatter Patterns (EBSP). It is generally an add on package to Scanning Electron Microscopy (SEM). EBSD is used to examine the crystallographic orientation of many materials, applied to crystal orientation mapping, defect studies, phase identification, grain boundary and morphology studies, regional heterogeneity investigations, material discrimination and micro-strain mapping etc. Additionally, the technique enables three-dimensional (3D) reconstruction of microstructure from consecutive surface sections that are created by mechanical serial sections.

Fig 3.13 SEM with facility for EBSD

EBSD is conducted using a scanning electron microscope equipped with an EBSD detector containing at-least a phosphor screen, compact lens and low light CCD camera. Automated EBSD at present is limited to characterize only conductive materials in which grain size is larger than several tens of nanometre in diameter and several square millimetres in area. The surface should be reasonably flat and free from foreign layers. Figure 3.13 shows the SEM set-up (Nova Nano SEM 430) having provision of EBSD.

3.10 Property Evaluation

The mechanical properties evaluated in the present study included hardness, yield strength and ductility. The measurement procedure for these properties is being discussed below:

A) Micro-Hardness Measurement

The micro-hardness measurements on the Vickers Hardness (HV) Scale were taken for all samples (i.e. cut out of CR_2 and CR_3) after inter-critical annealing treatment. The mean of five hardness values was plotted against the tempering parameters and temperatures. Two different graphs were plotted for CR_2 samples and CR_3 samples against mean hardness value. The average of 5 micro-hardness readings was taken to minimize the chances of error.

B) Tensile Property Evaluation

A flat dog-bone shaped specimen of 25 mm gauge length as per the ASTM standard E-8M was machined from cold rolled (CR) plate and was given isothermal annealing at 800ºC for 2 minutes.

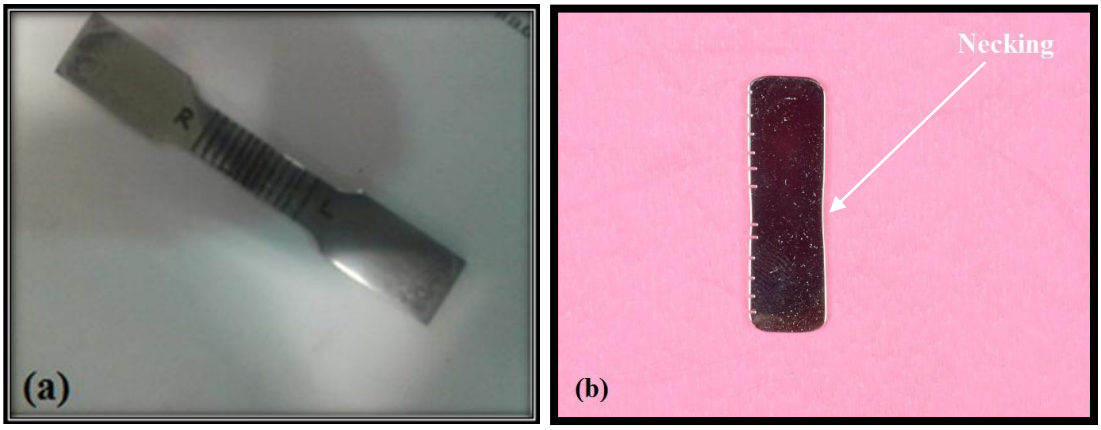

Fig. 3.14 Tensile Testing Specimen (a) before tensile test (b) after tensile test showing gauge length specimen and cutting grip section

Tensile tests were conducted at room temperature under displacement control at a strain rate of 1 x 10^{-3} s^{-1} using a tensile testing machine (Make: Instron 8862 System) of 100 kN capacity in the region of uniform elongation. Elongation was measured by an extensometer of 25mm gauge length. The uniformly elongated specimen (i.e. up-to necking) was again analysed in EBSD after being polished by following the steps described in earlier sections.

3.11 Summary of the Chapter

This chapter puts forward the design of the present study. The chapter describes the composition of the material under investigation and the overall objective of the thesis work. It describes the main input controllable variables to be used, and discusses the experimental set-up details and experimental procedure to be followed. Finally the chapter describes the procedure for sample preparation for metallography, microstructural analysis and mechanical properties evaluation.

CHAPTER 4
RESULTS AND DISCUSSION

4.1 INTRODUCTION

This chapter deals with the theoretical calculations done by using empirical formulae and presents the results of various experiments performed on the basis of calculated values. The micrographs and diffraction curves obtained have been thoroughly analysed to draw conclusions regarding the austenite reversion and also to account for the competition between reversion and recrystallization process in super martensitic stainless steels during the isothermal annealing process. The behaviour of the SMSS under investigation has been studied under two main conditions during isothermal annealing treatment (CR_2 Samples: have been provided only cold working before isothermal annealing; CR_3 Samples: have been provided cold working followed by annealing/ air cooling to relieve the effects of cold working, subsequent to these steps, isothermal annealing has been provided). The overall objective of the present study has been to analyse the effect of a new thermo-mechanical treatment route on the microstructure and mechanical properties of a Super Martensitic Stainless Steel.

4.2 ALLOY CHEMISTRY

Martensitic Stainless Steels are generally susceptible to toughness deterioration mainly caused by grain boundary embrittlement due to chromium carbide precipitation and delta ferrite formation. This carbide formation results in creation of chromium-depleted zones in vicinity of carbides at grain boundaries, thereby leading to inter-granular stress corrosion cracking in the steel (Nakamichi et al., 2008; Ma et al., 2012a). During solidification from higher temperatures or while welding in heat affected zones, the martensitic steels tend to lose their strength and toughness due to formation of δ-ferrite (Wang et al., 2010; Takano et al., 2008; Carrouge et al., 2004). But still, there exists an ambiguity on the effect of delta ferrite on impact properties. Some researchers believe that delta ferrite deteriorates impact properties of material because of lack of cohesion between delta ferrite and surrounding matrix; while others believe that it is relatively a soft phase which increases the ductility and toughness of material. Generally, retention of austenite in the microstructure at room temperature has been reported to be very effective to confer ductility and toughness, though at the cost of strength (Song et al., 2010; Wang et al., 2010; Zheng et al., 2010; Ma et al.,

2011). Super martensitic stainless steels have primarily been developed to overcome some of the (above mentioned) limitations of martensitic stainless steels. The present work investigates a Fe-Cr-Ni super martensitic stainless steel (SMSS). The chemical composition of alloy has been presented in Table 3.1. Ni content had been raised as it acts as austenite stabilizing phase while Cr content was lowered up to minimum permissible value in order to avoid δ-ferrite formation. The chromium and nickel equivalents (which form the two axes of Schaeffler Diagram) can be calculated using Equation 1.1 and Equation 1.2 (Pickering, 1976; Sedriks, 1996).

$$\% Ni_{eq} = 1.00(\%Ni) + 1.00(\%Co) + 30.00(\%C) + 25.00(\%N) + 0.50(\%Mn) + 0.30(\%Cu) \quad \text{----------Eq. 1.1}$$

$$\% Cr_{eq} = 1.00\ (\%Cr) + 2.00(\%Si) + 1.50(\%Mo) + 5.00(\%V) + 5.50(\%Al) + 1.75(\%Nb) + 1.50(\%Ti) + 0.75\ (\%W) \quad \text{----------Eq. 1.2}$$

The Ni_{eq} and Cr_{eq} values calculated using Equation 1.1 and Equation 1.2 came out to be 8.94 and 12.54 respectively. These values falls very close to the martensitic and martensitic-austenitic phase field boundaries of the Schaeffler diagram shown in Figure 1.3. This shows the probability of austenite retention at room temperature.

4.3 MICROSTRUCTURE OF SMSS ALLOY

The microstructures observed in the SMSS alloy in the hot rolled condition and the cold rolled state is being discussed in the following sub-sections.

4.3.1 SMSS in Hot Rolled State

The as-received hot rolled plate showed lath martensitic microstructure as depicted in Figure 4.1 (a). The structure of martensite can either exist in lath form or in lenticular shape that is internally twinned. The formation of lath or lenticular structure is controlled by transformation temperature (M_s) which indirectly depends on composition. Carbon has the most powerful solid solution strengthening effect on austenite than other alloying elements and is considered to be the main alloying element in steels to influence M_s temperature. High M_s temperature steels or steels with less than 0.4% C carbon content have a lath structure (Tsai et al., 2002; Abbaschian et al., 2009). The lath martensite packets observed in the

present study shown in EBSD Map in Figure 4.1 (b) describes the presence of multi-variant lath formation in which laths are oriented in different directions.

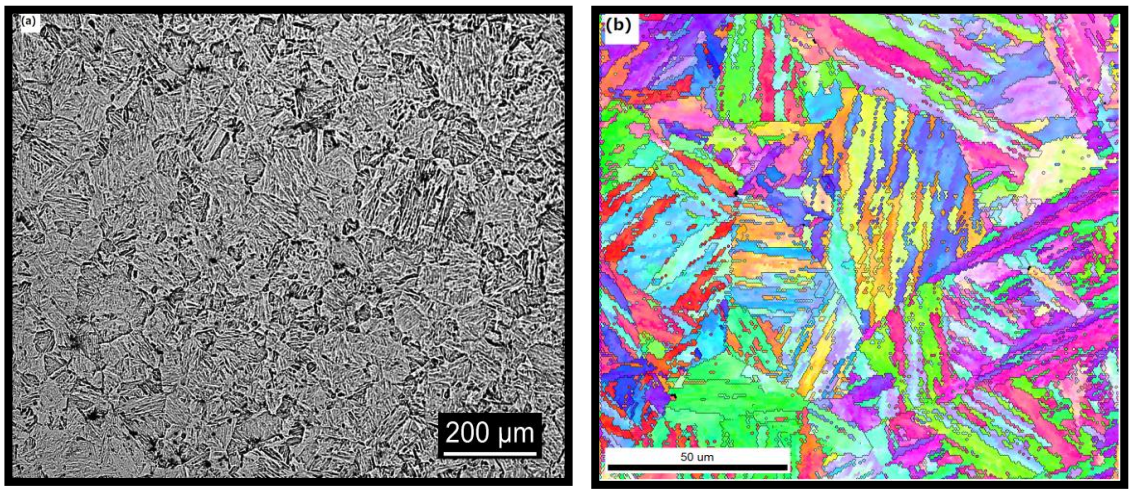

Fig. 4.1(a) Microstructure showing Lath Martensitic Structure in Hot Rolled Plate (b) EBSD Map

4.3.2 SMSS in Cold Rolled state

Figure 4.2 shows the micrograph of 80% cold rolled material. The microstructure reveals that the lath martensite structure has heavily deformed grains elongated along the rolling direction. This microstructure is in agreement with the work of Takaki et al. (1992) which stated that 80% deformed material was almost composed by a 'damaged martensite' in which the lath structure has been destructed directly through the intrusion of slip bands and indirectly through the lattice distortion.

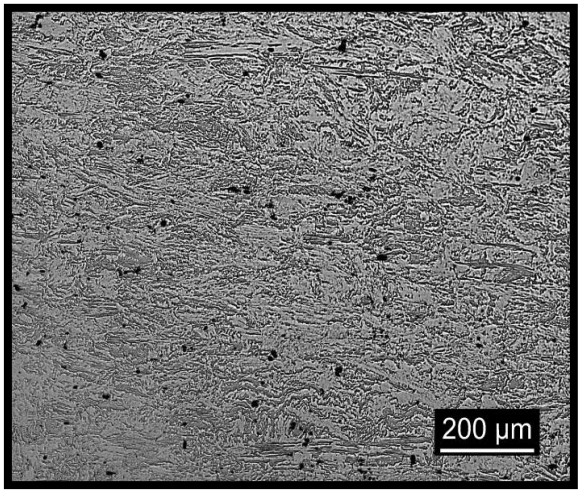

Fig 4.2 Microstructure showing Distorted Lath Martensitic Structure in Cold Rolled Plate

4.3.3 Phase Analysis of Hot Rolled and Cold Rolled SMSS

XRD analysis carried out for the SMSS alloy in the hot and cold rolled state showed the presence of very small volume fraction of retained austenite as shown in Figure 4.3.

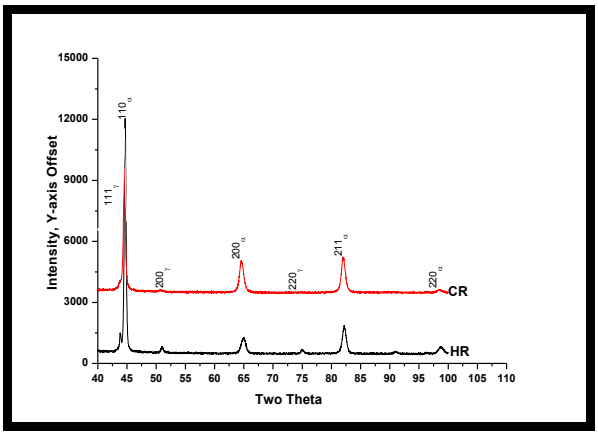

Fig. 4.3 XRD Analysis of Hot Rolled and Cold Rolled Coupons

The hot rolled coupon indicated higher austenite content than the cold rolled coupon. The cold rolling of hot rolled plate would have resulted in deformation induced transformation of austenite to martensite, which is a well-known phenomenon (Marshall, 1984; Tomimura et al., 1991). The deformation induced transformation of Fe-Cr-Ni stainless steels is a complex subject in which FCC austenite (γ) may transform to BCC martensite (α') or HCP martensite (ε) at any temperature below M_{d30} temperature. ε-martensite is commonly found in conjunction with α'-martensite and still attempts are being made by researchers to make out whether ε-martensite is an intermediate phase formed as a result of strain generated by γ→ α' transformation (Marshall, 1984). The chemical composition again plays a crucial role in increasing or decreasing the microstructural stability before the imposed deformation (Rocha and Oliveira, 2009). The stability of austenite to deformation induced transformation is linked to austenite stabilizing elements (C, N, Mn and Ni) through a relation between $M_d(\alpha')$(30/50) temperature and wt% of alloying elements (Marshall, 1984). This relation is exemplified in Equation 4.3.

$M_d(\alpha')$ (30/50) = 413-9.5% Ni-13.7% Cr-8.1% Mn-9.2% Si-18.5% Mo-462% (C+N)

---------- **Eq. 4.3**

M_d (α') (30/50) temperature represents the lowest temperature where 50% of deformation induced martensite (α') is formed with a true strain of 30%. It can also be interpreted in a way that lower is the M_{d30} temperature; the greater will be stability of alloy under investigation (Rocha and Oliveira, 2009). The M_d (α') (30/50) temperature calculated using Equation 4.3 for the alloy under investigation comes out be 160°C. This shows that deformation induced

transformation of austenite to martensite can be very readily achieved in the present alloy. Though the calculated M_d (α') (30/50) comes out to be 160°C (much above the cold rolling temperature) but still some austenite has been observed in the microstructure of the alloy. **The small amount of austenite present even after 80% cold rolling can be attributed to local alloy enrichment in some pockets of the microstructure. As a result, the M_d (α') (30/50) temperature at these sites (of local alloy enrichment) drops down, which can even be way below room temperature.** As a result austenite phase remains stable at these sites even under conditions of severe cold rolling, and thus explaining our observation of austenite stabilization against deformation induced martensitic transformation.

4.4 AUSTENITE STABILITY IN SOLUTION ANNEALED SAMPLES

The present work has classified the cold rolled samples into three categories. The first category has been designated as 'CR_1' (cold rolled and solution annealed by quenching), the second category has been designated as 'CR_2' (cold rolled and without solution annealing), and the third category has been designated as CR_3 (cold rolled and solution annealed by air cooling).

The sample, CR_1 was subjected to solution annealing treatment. For this, it was heated to 1060ºC, soaked there for 1 hour and was then water quenched. CR_2 samples were not given any additional post treatment (solution annealing) to modify the effects induced due to cold rolling. The sample, CR_3 was also subjected to solution annealing treatment. For this, it was heated to 1060ºC, soaked there for 1 hour and was then air cooled. The purpose of CR_1 was just to act as a reference sample to compare the stability of austenite phase when SMSS is subjected to (i) quenching (CR_1) and (ii) to air cooling (CR_3). In both these categories of samples, solution annealing has been given (though with different types of cooling) with the purpose to eliminate the effects induced because of cold rolling and finally choosing that category (either of CR_1 or CR_3) for further investigations which showed greater amount of austenite after solution annealing.

This section discusses the austenite stability in solution annealed samples (CR_1 and CR_3 samples).

Ma et al. (2012b) reported that martensitic lath microstructure can be produced even by air cooling of SMSS from solution treatment temperature at austenite field due to its adequate hardenability.

The 'CR_3' sample, cold rolled and air cooled from 1060°C of solution annealing temperature showed similar results i.e. martensitic microstructure. Austenite presence was difficult to be

established from optical microscopy as shown in Figure 4.4(a). Feritscope analysis quantified it to be about 17%.

The cold rolled and water quenched coupon (CR_1) produced recrystallized microstructure of lath martensite as depicted in Figure 4.4 (a); again the retained austenite presence was quantified to be about 3.1% through feritscope analysis. The EBSD Inverse Pole Figure (IPF) Map shown in Figure 4.5 revealed the lath martensitic microstructure. Retained austenite phase between laths of martensite was difficult to be detected as it was present in very small volume fraction.

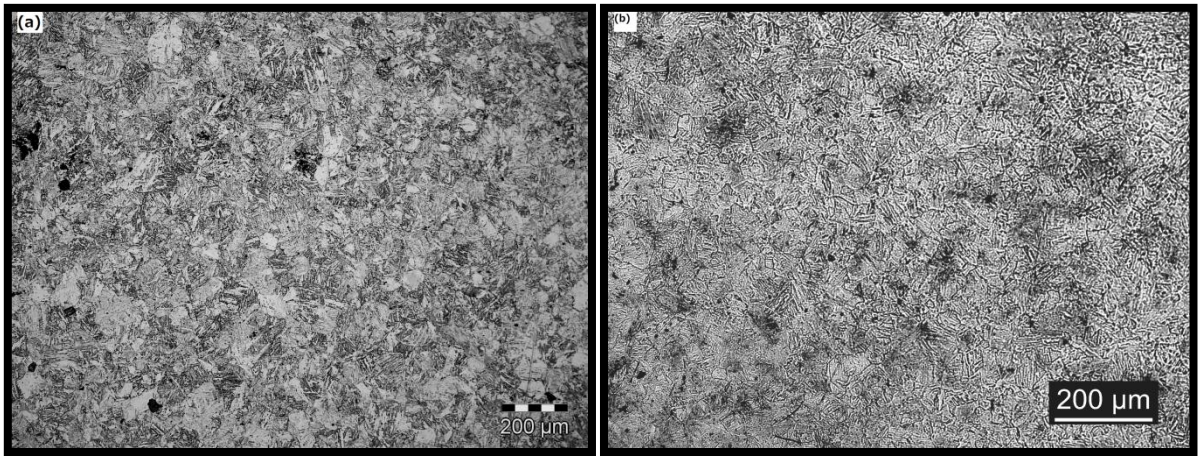

Fig 4.4 Microstructure of (a) cold rolled, solution annealed, water quenched coupon (b) cold rolled, solution annealed, air cooled coupon

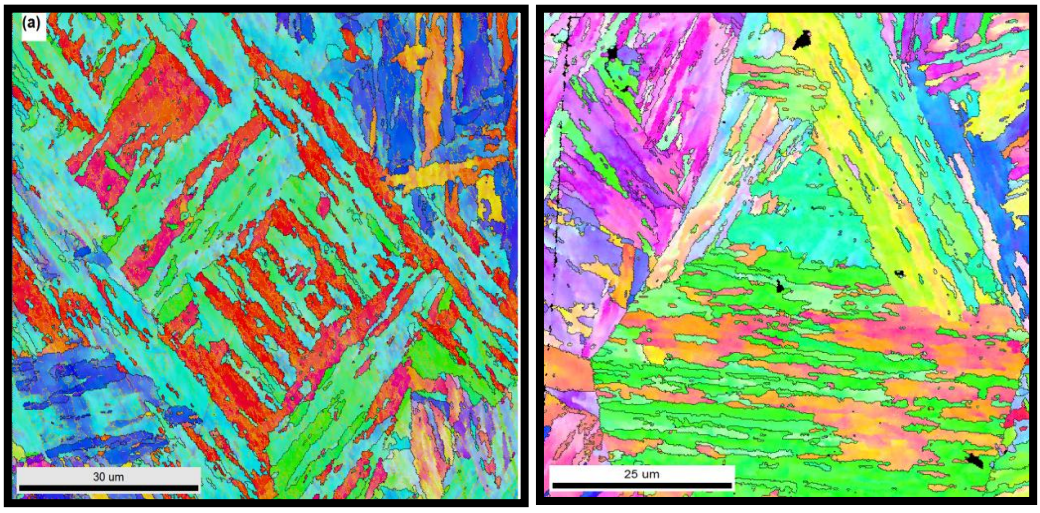

Fig 4.5 EBSD Inverse Pole Map of (a) cold rolled, annealed and water quenched specimen (b) cold rolled, annealed and air cooled depicting martensitic lath structure

The typical lath martensitic structure comprised of laths packets. Laths had formed in different directions (as shown in Figure 4.5). A group of laths form a block and a couple of

blocks form a packet. A schematic of lath martensite structure is shown in Figure 4.6 which also depicts laths, blocks and packets. Such stratified lath martensitic structure is formed due to multi-variant martensitic transformation of coarse austenitic grains (Takaki et al., 2004).

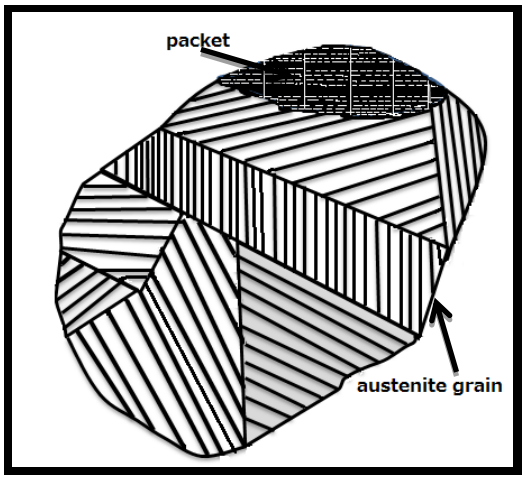

Fig 4.6 Morphology of Martensite

The size (mainly width) of martensite laths depends on the cooling rate. As depicted in Figure 4.5, lath size differs for both the conditions of solution annealing viz air cooling and water quenching. **Martensite laths formed at slow cooling rate (i.e. in case of air cooling, CR_3 samples) had enough time to grow without impingement with other martensite variants, while for higher cooling rate conditions of water quenching (CR_1 samples), much more uniform fine laths of martensite could be obtained.** The same observation had been reported in Tsai et al. (2002) work.

The presence of austenite, both in cold rolled air cooled (CR_3) and cold rolled water quenched (CR_1) samples is in agreement with alloy chemistry discussed in Section 4.2. However, since austenite stability has been observed to be more in CR_3 samples (17 % austenite as compared to 3.1 % in CR_1 sample), thus these samples (CR_3) would be considered for further investigations along with (CR_2) samples for establishing the thermo-mechanical route to meet the main objective of the work.

4.5 ESTABLISHING THE HEAT TREATMENT TEMPERATURES

This section establishes the heat treatment temperatures: the temperatures for austenite reversion and also the temperature for start of martensite formation.

4.5.1 Austenite Reversion Temperature

Since the alloy is amendable to microstructural changes by heat treatment, one can modify the microstructure by heat treatment; hence it became pertinent to establish austenite reversion temperature. The results of in-situ high temperature phase transformation studies carried out on the same material in an earlier work (Kumar et al., 2013) and on a similar SMSS (13Cr6Ni2Mo) alloy (Bojack et al., 2012) were used to find the austenite transformation (lower and upper critical) temperatures for the alloy under investigation. Kumar et al. (2013) reported that the beginning/start of martensite to austenite isothermal phase transformation indication was observed at 750^0C (Ac_1), which increased further with rise in temperature. The martensite peaks completely disappeared at annealing temperature of 950^0C (Ac_3) indicating uniphase austenite at this temperature. The value of Ac_1 as reported by Kumar et al. (2013) was in almost close agreement to the one established by Bojack et al. (2012) in their in-situ studies carried on SMSS (13Cr6Ni2Mo). In the present work, for all further investigations with regards to heat treatment (isothermal annealing), the heat treatment temperature will be taken in the range of 750-950^{o}C.

4.5.2 Martensitic Transformation Temperature

The start of martensite formation temperature (Ms) for stainless steels can be related to the steel composition by Marshall (1984) equation. The Ms temperature relationship with composition is exemplified in Equation 4.4.

M_s= 1305-61.1(% Ni)-41.7(% Cr)-33.3(% Mn)-27.8(% Si)-1667(%[C+N]) - - - - - - - **Eq. 4.4**

The M_s temperature at which austenite starts transforming to martensite during cooling from higher temperature has been calculated using Equation 4.4 and comes out to be 270^0C. This result is in close agreement with the M_s value calculated by Bojack et al. (2012) for the (13Cr6Ni2Mo) super martensitic stainless steel. Bojack et al. (2012) determined the M_s value experimentally using dilatometry technique and the Ms value was found to be 260^0C.

4.6 ISOTHERMAL ANNEALING

While annealing of plastically deformed (and sometimes even undeformed) metals or alloys, some interesting sequence of events (viz. recovery, recrystallization, and grain growth etc.) take place that control the structure and mechanical properties of the metals/alloys.

In the present work, isothermal annealing treatment was given to the SMSS alloy between austenite start formation temperature (750^{o}C) and austenite complete formation temperature (950^{o}C) with the aim to determine the recrystallization temperature, establishing a competition between reversion and recrystallization, and to study the changes in microstructural morphology for both cold rolled (CR_2) and cold rolled and annealed (CR_3) samples.

4.6.1 Isothermal Annealing of Cold Rolled Annealed (CR_3) Samples

This section discusses the effect of isothermal annealing treatment provided to the cold rolled annealed specimens (CR_3 samples). Before being subjected to this treatment, the microstructure of CR_3 samples mainly comprised of lath martensite and austenite (Figure 4.4).

Figure 4.7 (a), (c), (e), and (g) represent the EBSD inverse pole maps for CR_3 samples subjected to various temperature-time conditions during isothermal annealing. The morphology is observed to be comprising of a mixture of polygonal grains and lath structure. These have been encircled with white and black colour respectively.

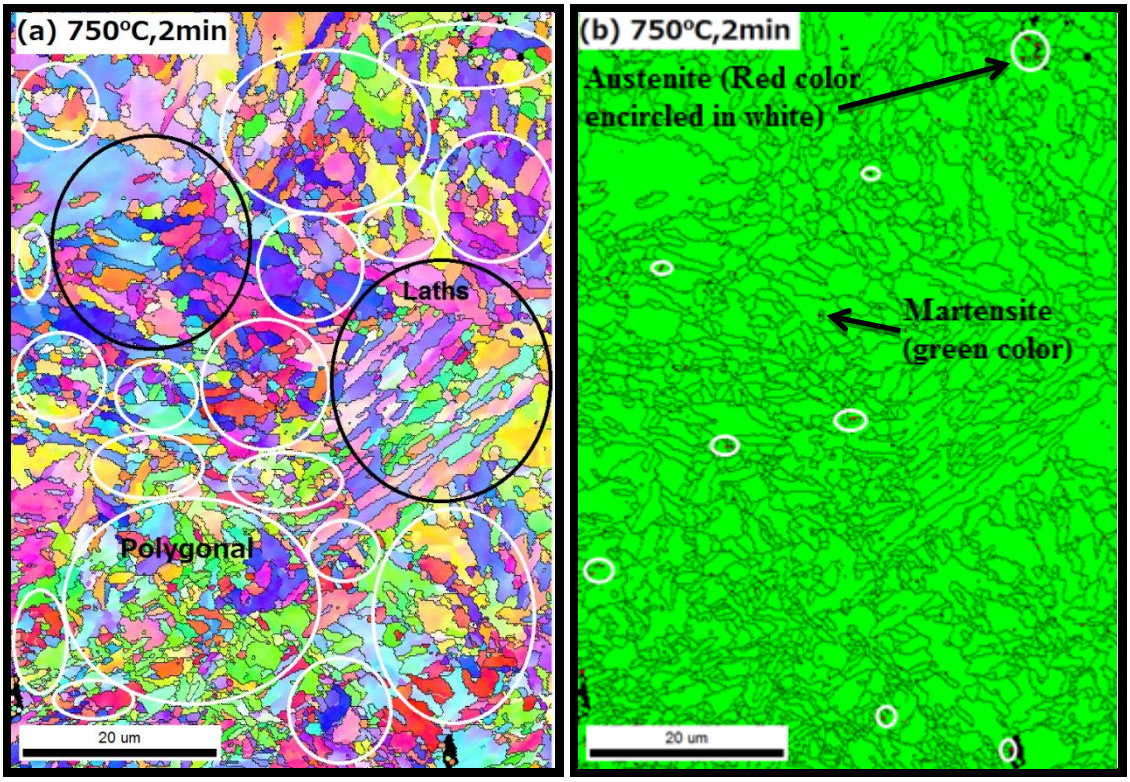

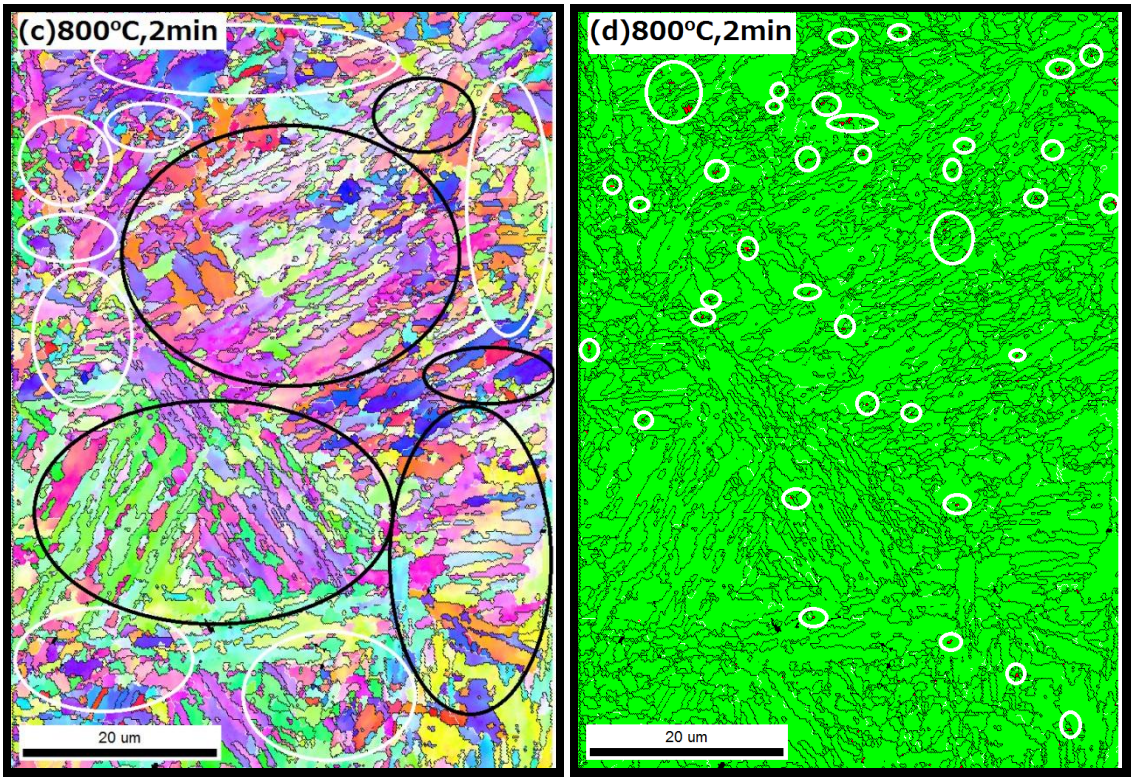
(c)800°C,2min
20 um
(d)800°C,2min
20 um

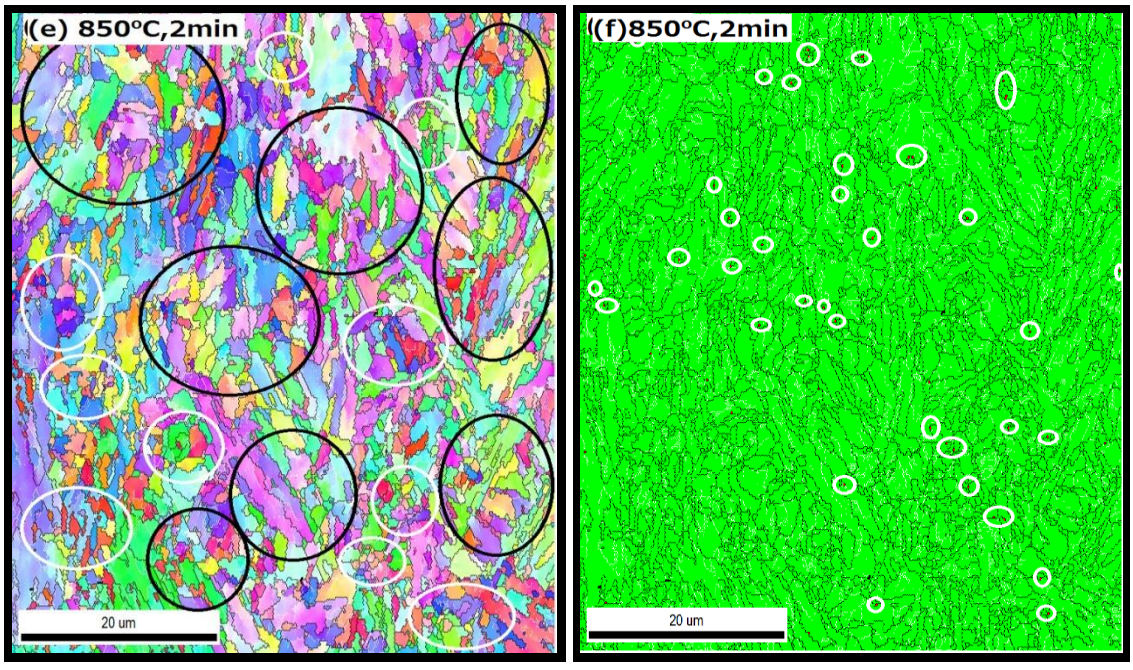
(e) 850°C,2min
20 um
(f)850°C,2min
20 um

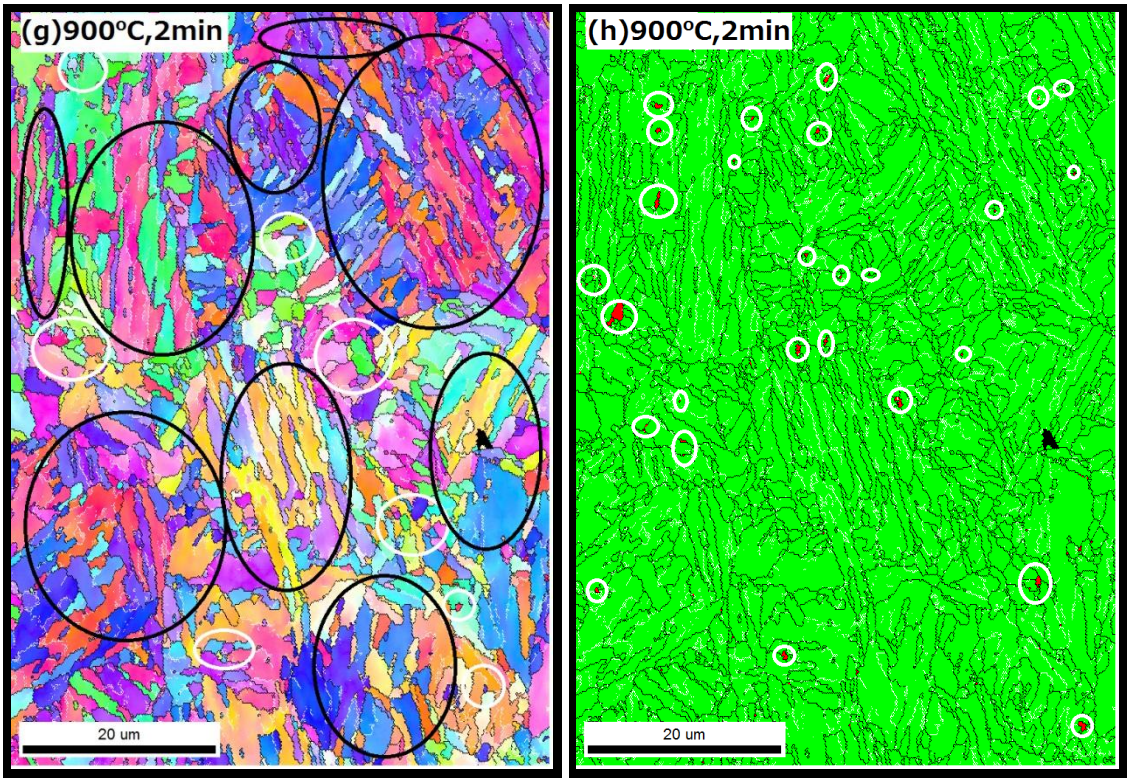

Fig 4.7 EBSD inverse Pole Maps of air cooled and isothermally annealed specimens (a), (c), (e), & (g) and EBSD Phase Maps (b), (d), (f), & (h) under different conditions

It can be observed from the inverse pole maps that with rise in temperature, the polygonal structure started disappearing and lath structure was seen mostly. When isothermal annealing treatment was given at 750^{o}C, lath martensite present in the SMSS alloy partially converted to fine grained austenite phase. On subsequent cooling, this fine grained austenite converted to martensite with polygonal structure. Thus, after isothermal annealing at 750^{o}C, the structure consisted of martensite (both freshly formed polygonal as well as the original lath shaped) and austenite (fine grained austenite formed at 750^{o}C led either to its retention or formation of polygonal grains). At higher isothermal annealing temperatures (> 750 ^{o}C), the transformation was seen to be cyclic ($\alpha \rightarrow \gamma \rightarrow \alpha$). It can be noted from Figures 4.7 (a, c, e, and g), that beyond isothermal annealing temperature of 750^{o}C, the polygonal structure got diminished and lath structure was mostly seen.

Another aspect to be explored in the present work was to find out the phase(s) present in the polygonal shaped grains. The polygonal grains could have been anticipated to be of austenite but EBSD Phase Map shown in Figure 4.7 (b) side-lined any such possibility, as no austenite presence could be seen (none of the polygonal grains area could be seen in red colour, which otherwise was marked for austenite). Other possibility may have been of ferrite grains but the

high hardness values in range of ~ 400 HV (as shown in Figure 4.10 a; Appendix I and II) also pointed towards the presence of martensite phase. Moreover, the composition of the given SMSS alloy is such that only austenite and martensite can be present at room temperature as shown on the Schafler Diagram (Figure 1.7).

The lattice parameter calculated for the martensite phase using Equation 4.5 revealed that martensite formed during austenite to martensite transformation was of BCC structure.

$$\frac{1}{d^2} = \frac{h^2 + k^2 + l^2}{a^2} \qquad \text{----------Eq. 4.5}$$

The h, k, l, d values and the calculated a value (lattice parameter) for different isothermal annealing temperatures is shown in Appendix I and V. The calculated values match closely with the lattice parmeter values for BCC martensite (Rajan et al., 2011).

The Bains Distortion Model suggests that transformation from FCC austenite to BCC while air cooling from isothermal annealing temperature can be brought about by contraction and expansion along the crystallographic planes (Abbaschian et al., 2009; Rajan et al., 2011). Schematic illustration in Figure 4.8 shows that FCC to BCC transformation can either take place by shear deformation of 36% in $[\bar{1}\ 1\ 0]$ direction or by anisotropic deformation in [0 0 1], $[\bar{1}\ 1\ 0]$, and $[\bar{1}\ \bar{1}\ 0]$ directions. The total volume change due to deformation is 4.5 % with 13.9 % expansion in [0 0 1] direction, 7% contraction in $[\bar{1}\ 1\ 0]$ direction and 14% contraction in $[\bar{1}\ \bar{1}\ 0]$ direction. Crystallographic anisotropy caused by lattice displacement is only cancelled out by multi-variant transformation. In multi-variant transformation, a stratified structure is formed which consists of martensitic laths oriented in different directions as shown in Figure 4.7 (a), (c), (e), and (g). The group of laths form blocks and couple of blocks form a packet as shown in Figure 4.6.

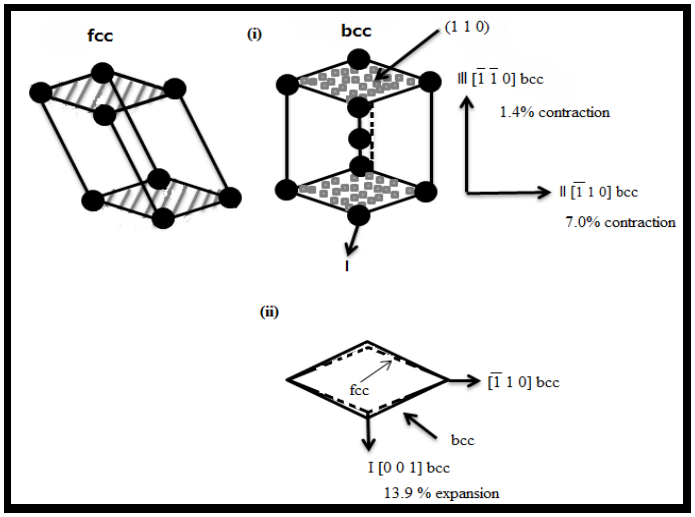

Fig 4.8 Schematic illustration of Lattice Displacement in FCC to BCC Martensitic Transformation

Even though similar amount of austenite was present at all annealing temperatures (as shown in Figure 4.9 (a) by XRD diffraction curves and in Figure 4.9 (b) by quantitative austenite fraction curve, Appendix III), still the highest hardness value was obtained for CR_3 sample annealed at 750^{o}C. This could be attributed to grain refinement from lath martensitic structure to equiaxed grains. The finer equiaxed grains showed restriction to dislocation motion as explained by Hall-Petch equation (Abbaschian et al., 2009). In general, CR_3 samples showed lesser hardness than CR_2 reference sample (500 HV) (refer Figure 4.10 a, and 4.13 a), may be due to annihilation of dislocations.

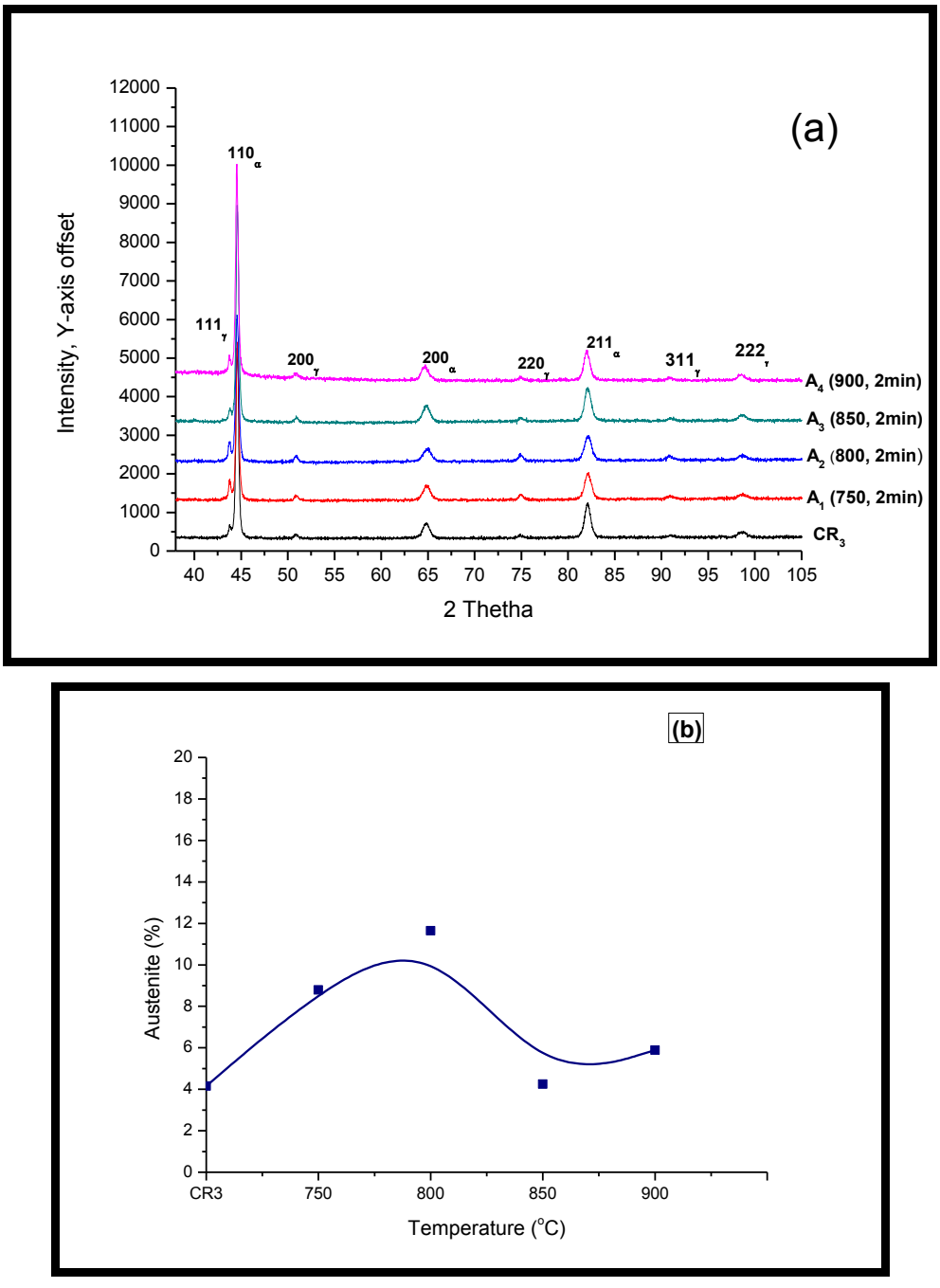

Fig 4.9 (a) XRD Diffraction Curves (b) Austenite variation with Annealing Temperature for CR_3 Samples

At higher isothermal annealing temperatures than 750°C, there was a decline in hardness as shown in Figure 4.10 (a). At annealing temperature of 800, 850, and 900°C, very little austenite could be seen in the phase maps shown in Figures 4.7 (d), (f), & (h) (encircled in white colour). This may point towards initiation of recrystallization which forms fine austenite grains. With grain refinement, transformation mode of austenite to martensite transformation shifted from multi-variant transformation to single or restricted variant transformation. Elastic strain energy required for single variant transformation is 27 times higher than required for multi-variant transformation, hence making austenite grains stable even at room temperature (Takaki et al., 2004).

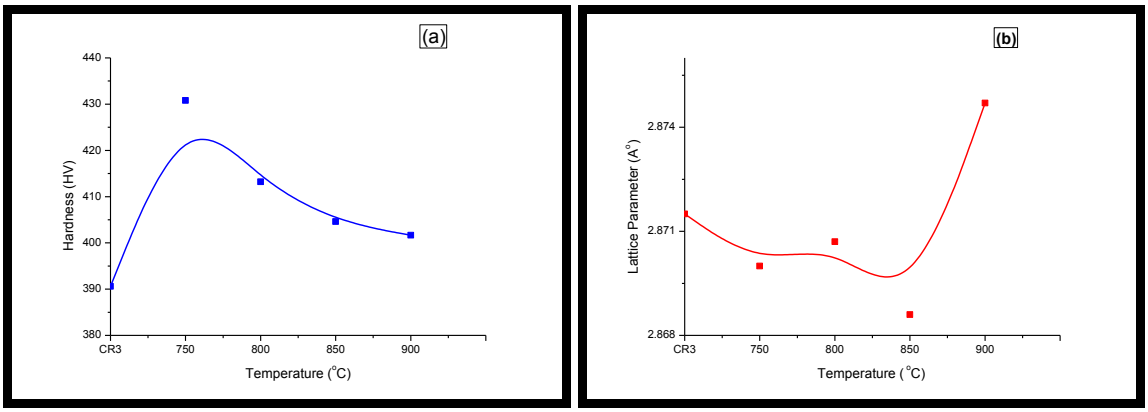

Fig 4.10 Variation of (a) Hardness (b) Lattice Parameter with different temperature for CR_3 samples

4.6.2 Isothermal Annealing of Cold Rolled (CR_2) Samples

Cold worked specimen (CR_2 at room temperature) with deformed lath martensitic microstructure is shown in Figure 4.2. After isothermal annealing, this microstructure was replaced by a new set of strain free grains (while some forming ultra-fine grains) as depicted (by white circles) in Figure 4.11.

The morphology of martensite changed from lath structure to equiaxed grains and was oriented in the same direction. This pointed towards single variant (or variant with same habit plane) transformation. The equiaxed grains as shown in EBSD phase map (with green colour) in Figures 4.11 (b), (d), (f), and (h) are of martensite (even justified by the high hardness values in range of ~ 400 HV as shown in Figure 4.13 a (Appendix IV) and lattice parameters calculations using Equation 4.5, Appendix V). XRD diffraction curves shown in Figure 4.12 (a) also point towards presence of austenite phase along with martensite phase. Quantification of austenite at various isothermal annealing temperatures obtained from XRD analysis is shown in Figure 4.12 b (Appendix VI).

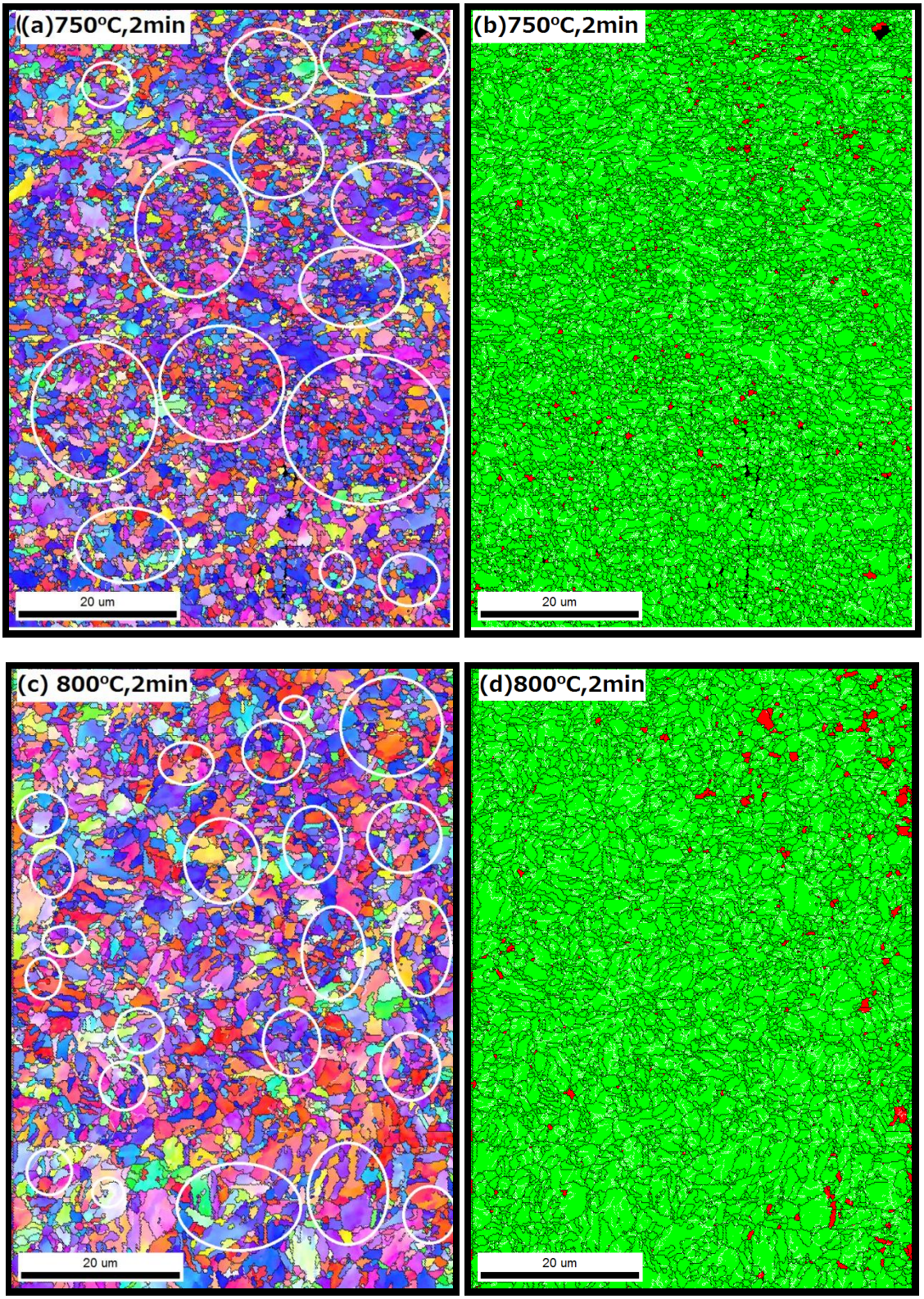
(a)750°C,2min
20 um
(b)750°C,2min
20 um
(c) 800°C,2min
20 um
(d)800°C,2min
20 um

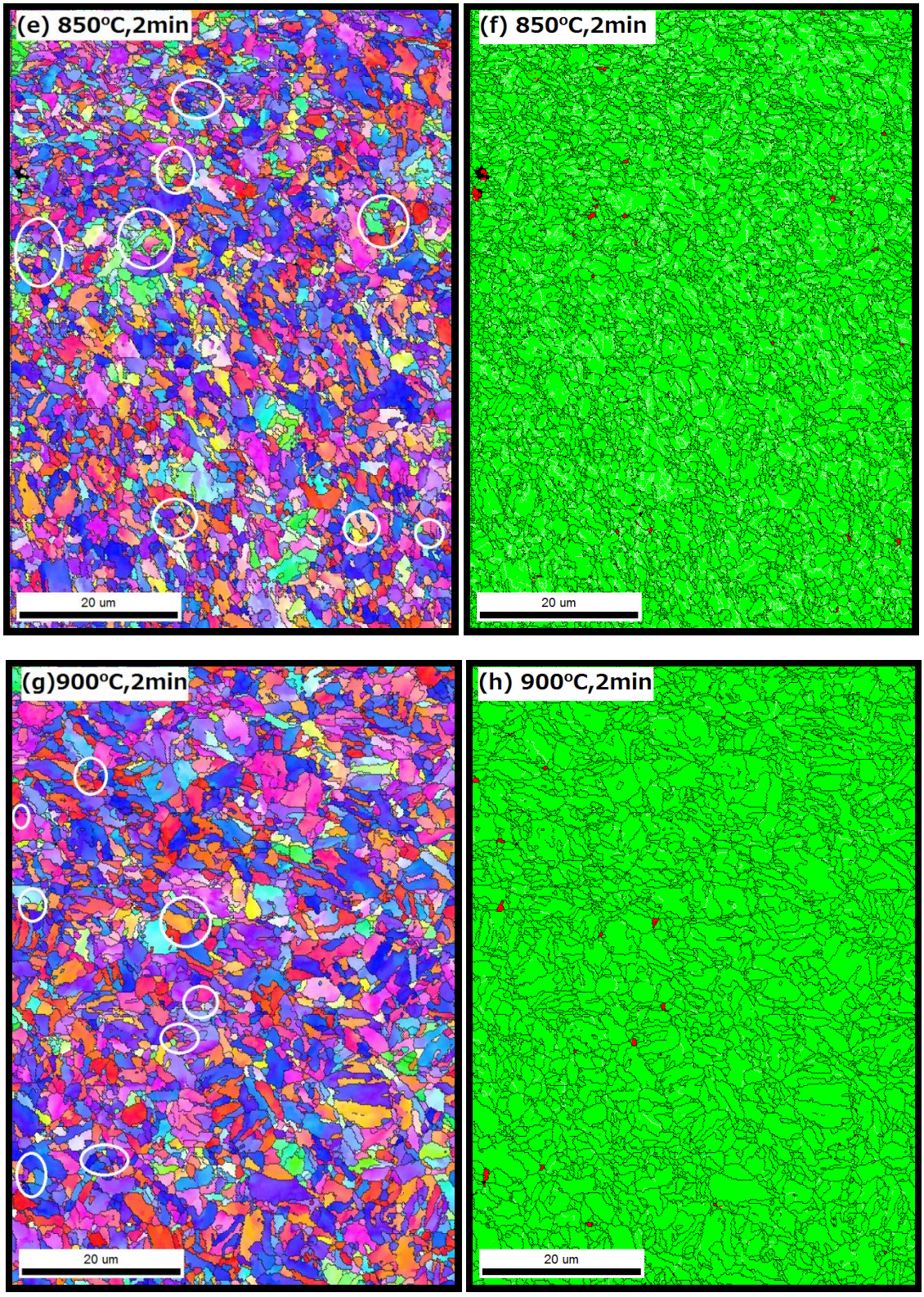

Fig 4.11 EBSD inverse pole of cold rolled and isothermally annealed specimens (a), (c), (e), & (g) and EBSD phase map (b), (d), (f), & (h) of U_2, V_2, W_2, X_2 respectively

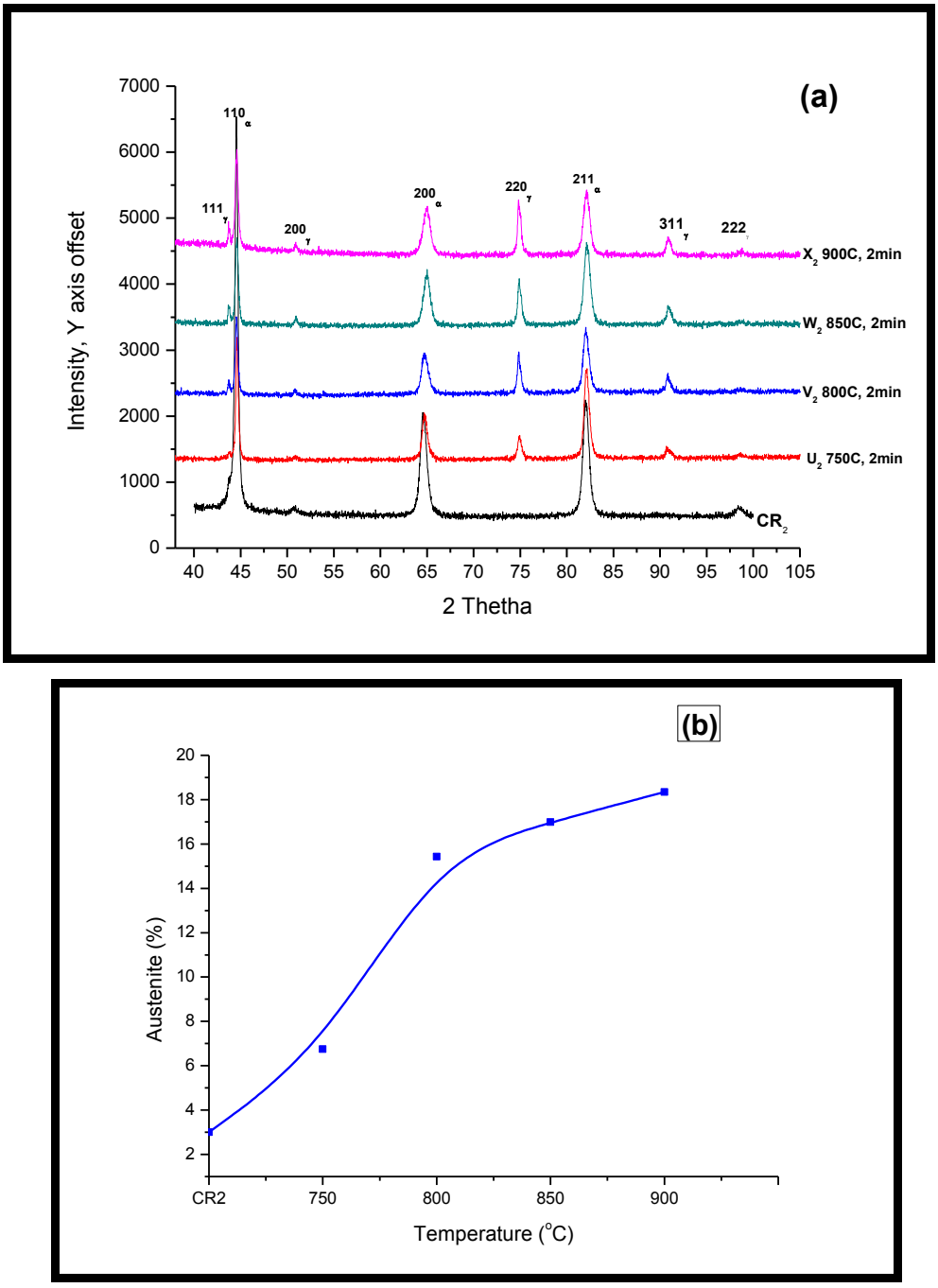

Fig 4.12 (a) XRD diffraction curves (b) austenite variation with annealing temperature

At isothermal annealing temperature of 750^{o}C for 2 min, strain free grains start nucleating at some places which points towards initiation of recrystallization. At 800^{o}C (for 2 min holding) hardness value is minimum for annealing time of 2 min (Figure 4.13 a) which can either be due to maximum austenite content or due to complete recrystallization of distorted lath martensitic structure. Softening effect is linked to recrystallization due to annihilation of dislocations and formation of new strain free grains. For isothermal annealing conditions of 800^{o}C for 2 min (Figure 4.11 d), the austenite is heterogeneously scattered within the martensitic matrix and the deformed lath martensitic microstructure has been replaced by fine

equiaxed grains. The ultra-fine austenite grains formed due to recrystallization of deformed lath martensitic matrix at annealing temperatures of 750°C and 800°C can only transform to martensite by single or restricted variant transformation. As elastic strain energy required for such transformations is very high, it makes the austenite grains thermally stable at room temperature. The ultra-fine grains as shown by white circles in Figures 4.11 (a), (c), (e), and (g) are only retained as shown by red colour in phase maps of Figures 4.11 (b), (d), (f), and (h), mostly visible for sample isothermally annealed at 800°C. However, the austenite fraction values obtained by XRD analysis (shown in Figure 4.12 b) pointed towards maximum austenite content at 900°C. This inconsistency might be due to heterogeneous distribution of austenite within the matrix and limitation of EBSD (as it can only index very smaller area of the sample). At 900°C, larger equiaxed grains were seen as depicted in Figure 4.11 (g). New strain free grains formed while annealing at 900°C (when heated upto 900°C) showed a progressive increase.

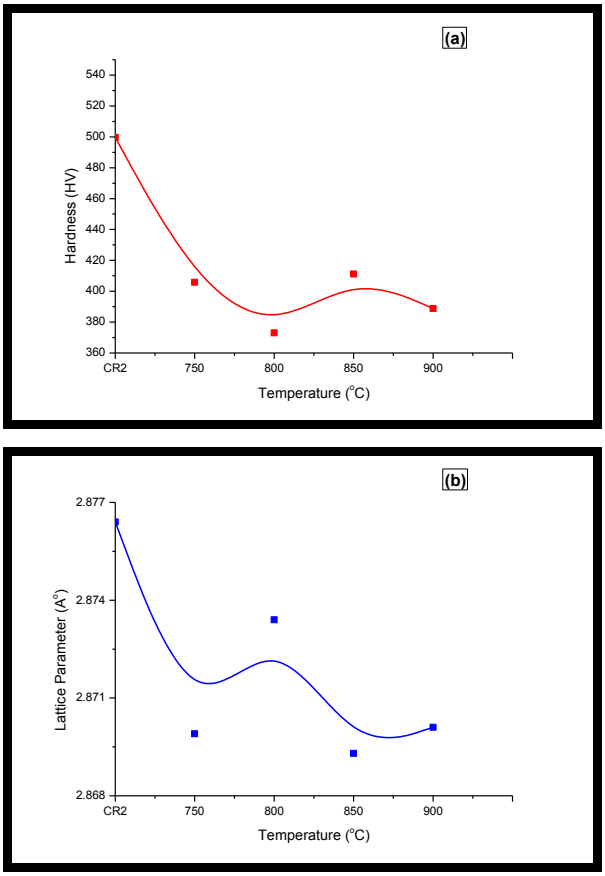

Fig 4.13 Variation of (a) hardness and (b) lattice parameter with annealing temperatures for 2 min period for CR_2 samples

The recrystallization behaviour in the two types of specimens viz. CR_2 and CR_3 was expected to be entirely different as formation of recrystallized grains after isothermal annealing

treatment is largely dependent on the prior matrix substrate. In CR_2 samples, the rate of recrystallization was higher as the energy stored while cold rolling acts as a driving force for recrystallization while in CR_3 samples, the recrystallization was noticeable at higher temperatures.

In cold rolled-annealed samples (CR_3), both modes of martensitic transformation were observed viz. multi-variant transformation and single variant transformation (e.g. at 750^{o}C, both types were observed and at all other annealing temperatures, multi-variant transformation was more predominant). In cold rolled (CR_2) specimens, single variant transformation was more predominant. Further, the single variant transformation is of two types viz. single variant or variants with same habit planes and single or restricted variant transformation mode. The multi-variant transformation was seen in coarse austenite grains; while those grains which were refined due to recrystallization underwent single variant transformation.

The CR_3 samples showed both kind of microstructural morphologies viz stratified lath martensitic structure as well as equiaxed or polygonal martensitic grains while CR_2 samples mostly had equiaxed grains. Moreover, the austenite content retained by CR_2 samples at room temperature was more for most of the annealing temperatures.

4.7 ESTABLISHMENT OF RECRYSTALLIZATION PARAMETERS

In order to get more accurate recrystallization parameters, the isothermal annealing was carried out in the same temperature range for different soaking time periods (for CR_2 samples) as discussed in Section 3.7.3 in Table 3.2. Figure 4.14 (a) shows variation of hardness with tempering parameters (λ). λ was calculated using Equation 4.6 (Appendix VII), where T is annealing temperature in Kelvin, t is annealing time in seconds and C is a constant taken as 20 for low carbon steels (Grange and Baughman, 1956; Nakada et al., 2012). As seen in Figure 4.14 (a), no concrete conclusion regarding recrystallization could be established as steep drop in hardness value was not observed corresponding to different λ values but from Figure 4.14 b (Appendix VIII) hardness for samples annealed at different temperatures and for different times can be compared and it can be used to establish some conclusions regarding recrystallization.

$$(\lambda = T (\log t + C) \qquad \text{---------- Eq. 4.6}$$

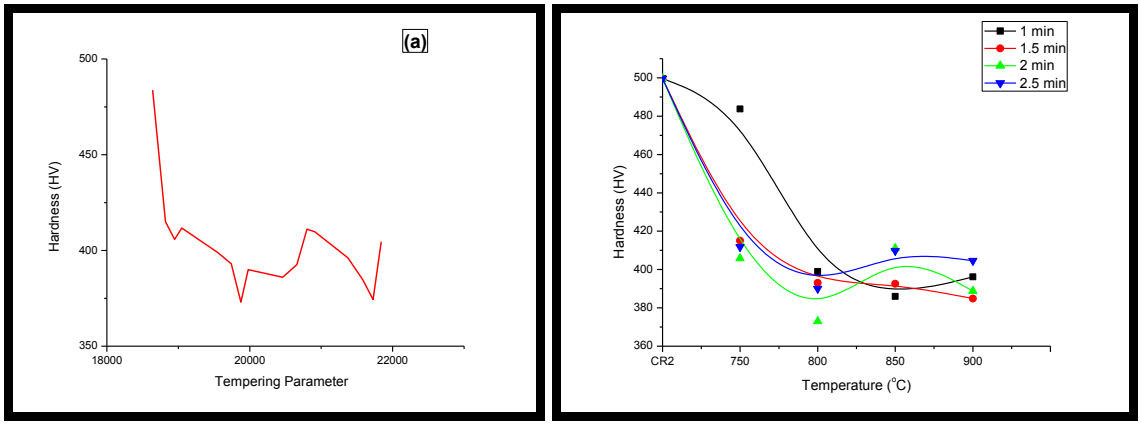

Fig 4.14 Variation of Hardness in CR_2 samples with (a) tempering parameter (b) annealing temperature & time

The hardness of CR_2 specimens was less after isothermal annealing treatment (as compared to their cold rolled state) irrespective of the annealing temperature and time. This may be due to annihilation of dislocations (present in the deformed martensitic lath structure) and/or formation of new strain free grains after the annealing treatment. For annealing temperature of 750^{o}C, annealing time of 1 min was insufficient to produce any recrystallization effect (refer Figure 4.14 b; as hardness value was observed to be much higher) but time periods of 1.5 min and above were sufficient to produce softening effect and hardness values did not show much variation for these annealing times. The hardness values at higher annealing temperatures of 850^{o}C and 900^{o}C were almost similar and showed less scatter irrespective of annealing times. The same hardness value could be only when austenite content was same within the martensite laths. The minimum hardness value was observed at annealing temperature of 800^{o}C with 2 min of holding. This means that either austenite content was highest at this annealing condition or maximum amount of new strain free grains had formed at these annealing parameters due to recrystallization and due to annihilation of dislocations.

4.8 EFFECT OF MICROSTRUCTURE ON TENSILE PROPERTIES

The previous sections discussed the steps to obtain the microstructure to obtain an optimum combination of strength and ductility in the SMSS alloy under investigation. It was discussed that the annealing condition which could provide the maximum softening effect either through availability of austenite or by formation of strain free grains or both would achieve this objective best. Out of the three category of samples considered in the present work, it was seen that the CR_2 samples subjected to isothermal annealing treatment at 800^{o}C and 2 min holding time were the best in meeting the stated objective.

In this section, the tensile properties of CR_2 reference sample (subjected to 80 % plastic deformation) and CR_2 sample given isothermal annealing at 800^oC for 2min (being referred to as V_2) were observed (Appendix IX). This sample (V_2) was selected over all samples given isothermal annealing treatment as it showed more pronounced softening effect and austenite content observed by EBSD Phase Map (Figure 4.11 d). The engineering stress-strain curves for material under these conditions have been being shown in Figure 4.15.

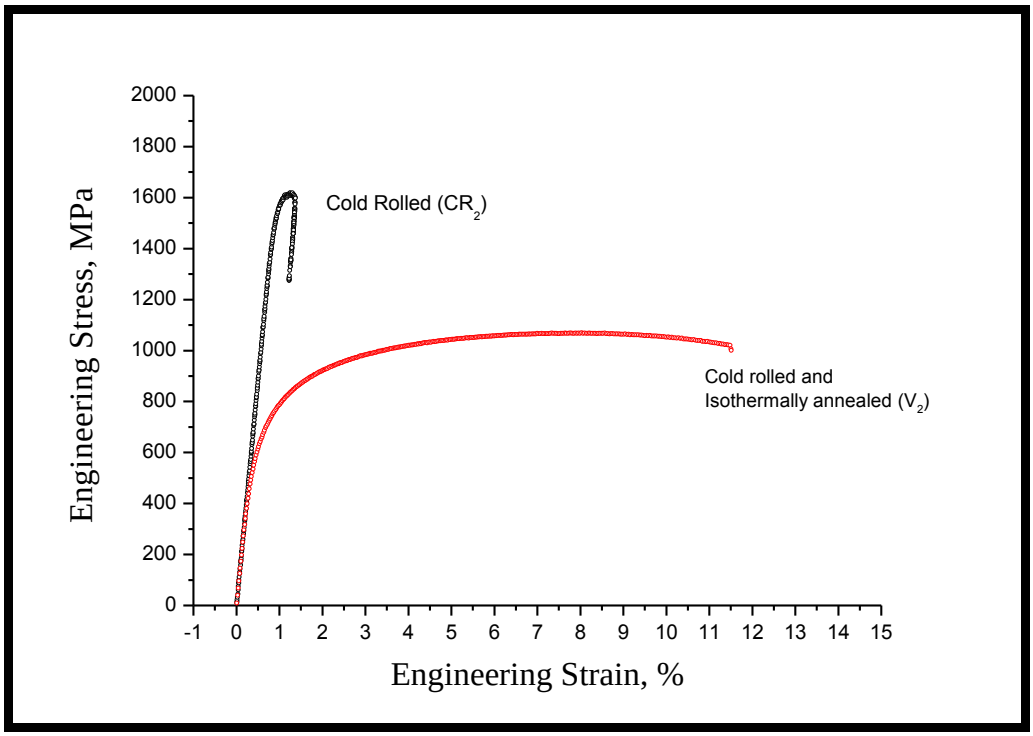

Fig 4.15 Engineering Stress-Strain Curves for CR_2 Reference Sample and V_2 Sample

Here, it may be noted that cold rolled sample at room temperature (CR_2 reference sample) is being used as reference to compare changes in properties as a result of the selected isothermal heat treatment process (V_2 sample). This is because one of the routes to improve the strength of as-received SMSS alloys is to subject them to plastic deformation (here taken as 80 % for all categories of samples). Figure 4.15 shows the strength of reference sample to be high (~1600 MPa) but with extremely poor ductility (~ 1.5 %) up to fracture. The main aim of the present work was to improve ductility to obtain an optimum combination of strength and % elongation. The gain in ductility has been achieved at the expense of loss in strength. The isothermal annealing process which produced a recrystallized microstructure (CR_2 sample annealed at 800^oC with soaking period of 2 min) provided good improvement in ductility (> 12 % up to uniform elongation) with still good value of strength (~1100 MPa).

CHAPTER 5
CONCLUSIONS

5.1 GENERAL

The development of high strength steels characterized by high strength-high ductility combination is a subject of significant interest worldwide. Still, there exists curiosity of further augmenting ductility, toughness, workability, and corrosion resistance. There have been endless efforts made to develop good ductility and toughness without compromising on strength in MSS. Most of the efforts in the last two decades were inclined towards alloy design and following appropriate heat treatment/tempering process for making austenite phase retention possible which helps in improving ductility and toughness. Although this results in considerable improvement in mechanical properties but little emphases is paid on the thermo-mechanical processing routes. It has been reported in literature that thermo-mechanical processing results in formation of fine grains due to recrystallization of cold rolled martensitic matrix. The fine grains of austenite are much stable at room temperature than the coarser grains; hence austenite retention can result in ductility enhancement. Moreover, the strain free grains formed due to recrystallization result in improved ductility due to annihilation of dislocations within them without significantly deteriorating strength. Keeping in mind this exploration, in the present investigation, it was proposed to explore a route for producing high strength (above 1 GPa) along with good ductility martensitic stainless steel.

The δ-ferrite phase whose presence is expected to deteriorate the mechanical properties was removed by lowering the δ-ferrite stabilizing element chromium to its minimum permissible limits obligatory for corrosion resistance properties. Nickel content was raised for austenite phase stabilization within martensitic matrix. The morphological changes in deformed and annealed martensitic phase after isothermal annealing were analysed.

5.2 RESULTS AND CONCLUSIONS

The main results and conclusions drawn from the present investigation are as follows:

General

- The alloy chemistry was such that it lied in the region of austenite and martensite (on Schaeffler diagram). The presence of austenite in hot rolled plate and after solution

annealing treatment showed probability of austenite retention at room temperature in this alloy at the room temperature.

- The A_s temperature for alloy was determined to be 750^{o}C while the A_f temperature was 950^{o}C. The M_s temperature was determined to be 270^{o}C which was well above the room temperature.

SMSS in Hot Rolled and Cold Rolled State

- Multi-variant lath morphology formed after hot rolling with laths oriented in different directions got heavily deformed after 80% cold rolling and elongated along the rolling direction.
- The M_d (α') (30/50) temperature for this alloy was way above the room temperature (160 ^{o}C) and thus showed possibility of deformation induced martensite (DIM) formation in it after cold rolling. The XRD analysis of hot rolled plate and cold rolled coupons showed the conversion of austenite to martensite after cold rolling.

Solution Annealing of Samples

- Laths formed in air cooled samples were slightly wider than laths formed due to water quenching of samples during solution annealing treatment.
- Morphology of martensite comprised of laths, blocks and packets.
- After solution annealing, austenite retention was higher in air cooled samples (17% austenite) than the water quenched sample (3.1% austenite). Thus, during solution annealing, air cooling route is to be preferred for more austenite retention in the alloy.

Isothermal Annealing of Samples

- Isothermal annealing of cold rolled (CR_2) and cold rolled, air cooled and annealed (CR_3) specimens showed changes in microstructural morphology due to recrystallization. In cold rolled specimens, recrystallization was seen at much lower isothermal annealing temperature (recrystallization initiated at ~ 750 ^{o}C) while in cold rolled annealed samples, it took place at higher isothermal annealing temperatures (recrystallization initiated at ~ 900 ^{o}C). Recrystallization effect was much pronounced in cold rolled specimens.
- In cold rolled and annealed specimens (with typical annealed lath martensitic structure), after isothermal annealing, the martensite morphology changed to combination of polygonal grains and lath martensite at isothermal annealing temperature of 750^{o}C for 2

min. With rise in isothermal annealing temperature, the polygonal grains started diminishing and were again replaced by martensitic laths. At isothermal annealing temperature of 900^{o}C for 2 min, complete lath martensitic structure was observed.

- In cold rolled specimens (with deformed martensitic structure), after isothermal annealing at all temperatures, the martensitic morphology changed to equiaxed fine grains. At higher isothermal annealing temperatures of 900^{o}C, grain growth was observed.
- With grain refinement of austenite grains, the mode of austenite transformation changed from multi variant transformation to single variant transformation which either leads to austenite stability (for ultra-fine grains) or formation of equiaxed martensite grains (for fine grains).
- Austenite retained in the microstructure due to single or restricted variant transformation of the ultra-fine austenite grains formed was found to be heterogeneously distributed.

Mechanical Properties with Heat Treatment

- Solution annealing (with air cooling) of cold rolled samples (CR_3) resulted in a decline in hardness from 500 HV (of the reference 80% cold rolled sample, CR_2) to 377 HV probably due to annihilation of dislocation while solution annealing. In cold rolled samples (CR_2), maximum hardness was observed after isothermal annealing at 750^{o}C for 1 min (484 HV) due to formation of martensite with fine equiaxed grains from lath martensite present in cold rolled samples. The minimum value of hardness was observed for the sample isothermally annealed at 800^{o}C for 2 min (373 HV). This was because of the maximum recrystallization achieved at these isothermal annealing parameters.
- In general, cold rolled solution annealed samples (CR_3) showed slightly higher hardness values than cold rolled samples (CR_2), after both were given isothermal annealing treatment at different temperatures for 2 min.
- Isothermal annealing of CR_3 samples at higher annealing temperatures of 800, 850 and 900^{o}C produced almost similar hardness (413, 405, 402 HV respectively) while CR_3 at 750^{o}C showed maximum hardness (431 HV) due to formation of equiaxed grains.
- The cold rolled sample showed extremely poor ductility (~1.5% upto fracture) with enormous ultimate tensile strength (~1600 MPa). The isothermal annealing of cold rolled sample at 800^{o}C for 2 min enhanced the ductility (~ 12% up to uniform elongation) with good ultimate tensile strength of ~ 1100 MPa, thus giving a good combination of properties.

5.3 MAJOR CONCLUSIONS AND RECOMMENDATIONS

- The Fe-11%Cr-7%Ni Super Martensitic Stainless Steel under investigation showed probability of austenite retention at room temperature. M_d (α') (30/50) temperature was above room temperature which meant that austenite present in the hot rolled plate was thermodynamically unstable leading way to formation of deformation induced martensite during cold rolling.
- Cold rolled specimens exhibited a lower recrystallization temperature than cold rolled and annealed samples as the energy stored during cold rolling acted as a driving force for recrystallization.
- In cold rolled annealed specimens, two types of transformations from austenite were observed viz. multi variant transformation and single variant transformation. The single variant transformation either changed martensite morphology from lath structure to equiaxed grains or assisted in austenite retention. However, in cold rolled specimens, only single variant transformation was dominant.
- The isothermal annealing route for cold rolled specimens could provide reasonable ductility whilst maintaining good strength value in the super martensitic stainless steel. The poor strain hardenability shown by isothermally annealed cold rolled specimen (V_2) is attributed to the poor dislocation storing capacity of the fine grains formed.

5.4 SCOPE OF FUTURE WORK

In the present work, the recrystallization fraction achieved in the material at the selected heat treatment parameters has been assessed only by indirect means viz. through hardness measurements. The recrystallization fraction can be calculated exactly using the empirical relation put forward by Kalu and Waryoba (2007). The average grains size has been (roughly) assessed by using EBSD Inverse Pole Maps. The grain size can be appropriately determined through quantitative analysis which can be further used for numerical assessment and for relating with mechanical properties. The present study can be extended to focus more on competition between reversion and recrystallization. Investigations can be carried out to estimate the heat treatment parameters which can maximize the recrystallization fraction and reversed austenite content to improve ductility further whilst restoring good strength values.

REFERENCES

- Abbaschian, R., Abbaschian, A. and Reed-Hill, R. E. (2009), 'Physical Metallurgy Principles', *CENGAGE Learning, USA*, ed. 4th, pp. 209–638.
- Balan, K. P., Reddy, A. V. and Sarma, D. S. (1998), 'Austenite precipitation during tempering in 16Cr-2Ni martensitic stainless steels', *Scripta Materialia*, Vol. 39(7), pp. 901–905.
- Benchabane, G., Boumerzoug, Z., Gloriant, T. and Thibon, I. (2011), 'Microstructural characterization and recrystallization kinetics of cold rolled copper', *Physica B*, Vol. 406, pp. 1973–1976.
- Bojack, A., Zhao, L., Morris, P. F. and Sietsma, J. (2012), 'In-situ determination of austenite and martensite formation in 13Cr6Ni2Mo supermartensitic stainless steel', *Materials Characterization*, Vol.71, pp. 77–86.
- Calliari, I., Zanesco, M., Dabala, M., Brunelli, K. and Ramous, E. (2008), 'Materials and Design Investigation of microstructure and properties of a Ni–Mo martensitic stainless steel', *Materials and Design*, Vol. 29, pp. 246–250.
- Callister, W. D. (2007), 'Material Science and Engineering: An Introduction', *John Wiley and Sons, Inc., New York*, ed. 7th, pp. 152, 195-201.
- Cao, W. Q., Gu, C. F., Pereloma, E. V, and Davies, C. H. J. (2008), 'Stored energy , vacancies and thermal stability of ultra-fine grained copper', *Material Science and Engineering A*, Vol. 492, pp. 74–79.
- Carrouge, D., Bhadeshia, H. K. D. H., and Woollin, P. (2004), 'Effect of d ferrite on impact properties of super martensitic stainless steel heat affected zones', *Science and Technology of Welding and Joining*, Vol. 9, pp. 377–89.
- Chia, K., Jung, K., and Conrad, H. (2005), 'Dislocation density model for the effect of grain size on the flow stress of a Ti–15.2 at. % Mo β-alloy at 4.2–650 K', *Materials Science and Engineering A*, Vol. 409, pp. 32–38.
- Choi, Y., Kim, J., Park, Y., and Park, J. (2007), 'Austenitizing treatment influence on the electrochemical corrosion behavior of 0.3C–14Cr–3Mo martensitic stainless steel' *Materials Letters*, Vol. 61, pp. 244–247.

- De-ning, Z., Ying, H., Wei, Z. and Xu-dong, F. (2010), 'Influence of Tempering on Mechanical Properties of 00Cr13Ni4Mo Supermartensitic Stainless Steel', *Journal of Iron and Steel Research, International*, Vol. 17(8), pp. 50-54.
- Dieter, G. E. (1988), 'Mechanical Metallurgy', *McGraw-Hill Book Company, London*, ed. 4th, pp. 156–235.
- Grange, R., A. and Baughman, R., W. (1956), 'Hardness of Tempered Martensite in Carbon and Low Alloy Steels', *Transaction of the ASM*, Vol. 48, pp. 165-197.
- Gunn, R.N., (1997), 'Duplex stainless steels', *Abington publishers, USA*, 1st ed., pp. 50-52.
- Habibi, A., and Ketabchi, M. (2012), 'Enhanced properties of nano-grained pure copper by equal channel angular rolling and post-annealing', *Materials and Design*, Vol. 34, pp. 483–487.
- Hedstrom, P., Lienert, U., Almer, J., and Oden, M. (2007), 'Stepwise transformation behavior of the strain-induced martensitic transformation in a metastable stainless steel', *Scripta Materialia*, Vol. 56, pp. 213–216.
- Humphreys, F. J. and Hatherly, M. (2004), 'Recrystallization and related Annealing phenomenon', *Elsevier Ltd., Oxford, UK*, ed. 2nd, pp. 1–171.
- Isfahany, A. N., Saghafian, H., and Borhani, G. (2011), 'The effect of heat treatment on mechanical properties and corrosion behavior of AISI420 martensitic stainless steel', *Journal of Alloys and Compounds*, Vol. 509, pp. 3931–3936.
- Kalpakjain, S. and Schmid, S.R. (2009), 'Manufacturing Processes', *Dorling Kindersley Pvt. Ltd., India*, ed. 5th , pp. 87–97.
- Kalu, P. N., and Waryoba, D. R. (2007), 'A JMAK-microhardness model for quantifying the kinetics of restoration mechanisms in inhomogeneous microstructure', *Material Science and Engineering A*, Vol. 464, pp. 68–75.
- Karimi, M., Najafizadeh, A., Kerampur, A., and Eskandari, M. (2009), 'Effect of martensite to austenite reversion on the formation of nano/submicron grained AISI 301 stainless steel', *Materials Characterization*, Vol. 60, pp. 1220-1223.
- Klotz, U. E., Solenthaler, C., Uggowitzer, P. J., (2008), 'Martensitic-austenite 9-12% Cr steels-Alloy design, microstructural stability and mechanical properties', *Material Science and Engineering A*, Vol. 476, pp. 186–194.
- Klueh, R. L., Hashimoto, N., and Maziasz, P. J. (2005), 'Development of new nano-particle-strengthened martensitic steels', *Scripta Materialia*, Vol. 53, pp. 275–280.

- Krauss, G., (1980), 'Principle of Heat Treatment of Steels', *American Society for Metals, United States of America*, ed. 1964, pp. 13–88.
- Kumar, R. B., Sharma, S., Munda, P., and Minz, R. K. (2013), 'Structure and microstructure evolution of a ternary Fe-Cr-Ni alloy akin to super martensitic stainless steel', *Material and Design*, Vol. 50, pp. 392-398.
- Lakhtin, Y. (1977), 'Engineering Physical Metallurgy', Mir Publishers, Moscow, ed. 1st, pp. 279-303.
- Lee, K., and Lee, H. (2010), 'Grain refinement and mechanical properties of asymmetrically rolled low carbon steel', *Material Processing Technology*, Vol. 210, pp. 1574–1579.
- Leem, D., Lee, Y., and Jun, J., Choi, C. (2001), 'Amount of retained austenite at room temperature after reverse transformation of martensite to austenite in an Fe ± 13 % Cr ± 7 % Ni ± 3 % Si martensitic stainless steel', *Scripta Materialia*, Vol. 45, pp. 767–772.
- Li, X. Y., Song, Y. Y. and Li, Y. Y. (2008), 'Effect of reverse Austenite on the cryogenic tensile prperties of 0Cr13Ni4Mo Martensitic steel', *Advances in cryogenics engineering*, Vol. 54, pp. 145–150.
- Lo, K. H., Shek, C. H., and Lai, J. K. L. (2009), 'Recent developments in stainless steels', *Materials Science and Engineering A*, Vol. 65, pp. 39–104.
- Marshall, P. (1984), 'Austenitic Stainless Steels Microstructure and Mechanical Properties', *Elsevier Applied Science Publishers, England*, ed. 1st, pp. 23–27.
- Ma, X. P., Wang, L. J., Liu, C. M., and Subramanian, S. V. (2011), 'Role of Nb in low interstitial 13Cr super martensitic stainless steel', *Materials Science and Engineering A*, Vol. 528, pp. 6812–6818.
- Ma, X. P., Wang, L. J., Liu, C. M., and Subramanian, S. V. (2012b), 'Microstructure and properties of 12Cr5Ni1Mo0.025Nb0.09V0.06N super martensitic stainless steel', *Materials Science and Engineering A*, Vol. 539, 271–279.
- Ma, X. P., Wang, L. J., Qin, B., Liu, C. M., and Subramanian, S. V. (2012a), 'Effect of N on microstructure and mechanical properties of 16Cr5Ni1Mo martensitic stainless steel', *Materials and Design*, Vol. *34*, pp. 74–81.
- Ma, X., Wang, L., and Subramanian, S. V. (2012c), 'Studies on Nb Microalloying of 13Cr Super Martensitic Stainless Steel', *Metallurgical and Material Transaction A*, Vol.43, pp. 4475–4486.

- McDowell, D. W., Jr., B. S. and Charles Mayne, B. S. (1966), 'Stainless Steels', *American society for metals*, *Metals park*, ed. 1st, Lesson-1-3.
- Nakada, N., Arakawa, Y., Park, K., Tsuchiyama, T., and Takaki, S. (2012), 'Dual phase structure formed by partial reversion of cold-deformed martensite', *Materials Science and Engineering A*, Vol.553, pp. 128–133.
- Nakamichi H., Sato, K., Miyata Y., Kimura M., and Masamura, K. (2008), 'Quantitative analysis of Cr-depleted zone morphology in low carbon martensitic stainless steel using FE-(S)TEM', *Corrosion Science*, Vol. 50, pp. 309.
- Nestorovic, S., Markovic, I., and Markovic, D. (2010), 'Influence of thermomechanical treatment on the hardening mechanisms and structural changes of a cast Cu–6.6 wt. % Ag alloy', *Material and Design*, Vol. 31, pp. 1644–1649.
- Natori, M., Fatamura, Y., Tsuchiyama, T., Takaki, S. (2005), 'Difference in recrystallization behaviour between lath martensite and deformed ferrite in ultralow carbon steel', *Scripta Materialia*, Vol. 53, pp. 603-608.
- Padilha, A. F., Plaut, R. L., and Rios, P. R. (2003), 'Annealing of Cold-worked Austenitic Stainless Steels', *ISIJ International*, Vol. 43(2), pp. 135–143.
- Park, J., and Park, Y. (2007), 'The effects of heat-treatment parameters on corrosion resistance and phase transformations of 14Cr–3Mo martensitic stainless steel', *Materials Science and Engineering A*, Vol. 451, pp. 1131–1134.
- Park, E. S., Yoo, D. K., Sung, J. H., Kang, C. Y., Lee, J. H., and Sung, J. H. (2004), 'Formation of reversed austenite during tempering of 14Cr-7Ni-0.3Nb', *Metals and Materials International*, Vol. 10(6), pp. 521–525.
- Pawlowski, B. (2011), 'Critical points of hypoeutectoid steel - prediction of the pearlite dissolution finish temperature A_{c1f}', *Journal of Achievements in Material and Manufacturing Engineering*, Vol. 49(2), pp. 331–337.
- Perdahcioglu, E. S., and Geijselaers, H. J. M. (2012), 'A macroscopic model to simulate the mechanically induced martensitic transformation in metastable austenitic stainless steels', *Acta Materialia*, Vol. 60, pp. 4409–4419.
- Ping, D. H., Ohnuma, M., Hirakawa, Y., Kadoya, Y., and Hono, K. (2005), 'Microstructural evaluation in 13Cr-8Ni-2.5Mo-2Al martensitic precipitation-hardened stainless steel', *Material Science and Engineering A*, Vol. 394, pp. 285–295.
- Pickering, F.B. (1976), 'Physical metallurgy of stainless steel developments', *International Metals Review*, Vol. 21, pp-227–268.

- Pickering, F. B. (1978), 'Physical Metallurgy and the Design of Steels', *Applied Science Publishers Limited, London*, ed. 1st, pp. 226–266.
- Prat, O., Garcia, J., Rojas, D., Sauthoff, G., and Inden, G. (2013), 'The role of Laves phase on microstructure evolution and creep strength of novel 9% Cr heat resistant steels', *Intermetallics*, Vol. 32, pp. 362–372.
- Raghvan, V. (2006), 'Physical Metallurgy: Principles and Practice', *PHI Learning private Limited, New Delhi*, ed. 2nd, pp. 161, 176-179.
- Rho, B. S., Hong, H. U., Nam, S. W. (2000), 'The effect of delta ferrite on fatigue cracks in 304L steels', *International Journal of Fatigue*, Vol. 22, pp. 683-690.
- Rocha, M. R. and Oliveira, C. A. S. (2009), 'Evaluation of the martensitic transformations in austenitic stainless steels', *Materials Science and Engineering A*, Vol. 517, pp. 281–285.
- Rajan, T. V., Sharma, C. P. and Sharma, A. (2011), 'Heat Treatment principles and techniques', *PHI Learning private limited, New Delhi*, ed. 2nd, pp.
- Roucoules, C., Pietrzyk, M., and Hodgson, P. D. (2003), 'Analysis of work hardening and recrystallization during the hot working of steel using a statistically based internal variable model', *Material Science and Engineering A*, Vol. 339, pp. 1–9.
- Schino, A. D., Barteri, M. and Kenny, J. M. (2002), 'Development of ultrafine grain structure by martensitic reversion in stainless steel', *Materials Science Letters*, Vol. 21, pp. 751–753.
- Schino, A.D., Abbruzzese, G. and Kenny, J. M. (2003), 'Recrystallization and grain growth in Austenitic Stainless Steels: a statistical approach', *Material Science Technology*, Vol. 19, pp. 119-121.
- Sedriks, A. J. (1996), 'Corrosion of Stainless Steels', *John Wiley and Sons, Inc.*, New York, ed. 2nd, pp. 1–3, 14–23, 41–59, 146.
- Singh, V. (2008), 'Physical Metallurgy', *Standard Publishers Distributors*, Delhi, ed. 1st, pp. 624–637.
- Song, Y. Y., Li, X. Y., Rong, L. J., Ping, D. H., Yin, F. X., and Li, Y. Y. (2010), 'Formation of the reversed austenite during intercritical tempering in a Fe–13%C–4% Ni–Mo martensitic stainless steel', *Materials Letters*, Vol. 64(13), pp. 1411–1414.
- Takaki, S., Fukunaga, K., Junaidi, S., and Tsuchiyama, T. (2004), 'Effect of grain refinement on Thermal Stability of Metastable Austenitic Steel', *Materials Transaction*, Vol. 45, pp. 2245-2251.

- Takaki, S., Iizuka, S., Tomimura, K., and Tokunaga, Y. (1992), 'Influence of cold working on recovery and recrystallization of lath martensite in 0.2% C steels', *Material Transactions, JIM*, Vol. 33, pp. 577-584.
- Takano, K., Sakakibara, M., Matsui, T., and Takaki, S. (2008), 'Effect of alloying elements and microstructure on corrosion resistance and hardness of martensitic stainless steel', *J Iron Steel Inst Jpn*, Vol. 86, pp. 123–30.
- Tobata, J., Ngo-Huynh, K., Nakada, N., Tsuchiyama, T., Takaki, S. (2012), 'Role of Silicon in Quenching and Partition Treatment of Low-carbon Martensitic Stainless Steels', *ISIJ International*, Vol. 52, pp. 1377–1382.
- Tomimura, K., Takaki, S. and Tokunaga, Y. (1991), 'Reversion mechanism from deformation induced martensite to austenite in metastable austenitic stainless steels', *ISIJ International*, Vol. 31, pp. 1431–1437.
- Tsai, M. C., Chiou, C. S., Du, J. S. and Yang, J. R. (2002), 'Phase transformation in AISI 410 stainless steel', *Materials Science and Engineering*, Vol. A332, pp. 1–10.
- Tsuchiyama, T., Natori, M., Nakada, N. and Takaki, S. (2010), 'Conditions for grain boundary bulging during tempering of lath martensite in ultra-low carbon steel', *ISIJ International*, Vol. 50, pp. 771–773.
- Wang, P., Lu, S. P., Xiao, N. M., Li, D. Z., and Li, Y. Y. (2010), 'Effect of delta ferrite on impact properties of low carbon 13Cr–4Ni martensitic stainless steel', *Materials Science and Engineering A*, Vol. 527(13–14), pp. 3210–3216.
- Wang, T. S., Zhang, M., Wang, Y. H., Yang, J., and Zhang, F. C. (2013), 'Martensitic transformation behaviour of deformed supercooled austenite', *Scripta Materialia*, Vol. 68, pp. 162–165.
- Wu, W., Hwu, L. Y., Lin, D. Y., and Lee, J. L. (2000), 'The Relationship between Alloying Elements and Retained Austenite in Martensitic Stainless Steel Welds', *Scripta Materialia*, Vol. 42, pp. 1071–1076.
- Ye, D., Li, J., Jiang, W., Su, J., and Zhao, K. (2012), 'Effect of Cu addition on microstructure and mechanical properties of 15 % Cr super martensitic stainless steel', *Materials and Design*, Vol. 41, pp. 16–22.
- Yeddu, H. K., Razumovskiy, V. I., Borgenstam, A., Korzhavyi, P. A., Ruban, A. V, and Argen J. A. (2012), 'Multi-length scale modelling of martensitic transformations in stainless steels', *Acta Materialia*, Vol. 60, pp. 6508–6517.

- Yu-rong, L., Dong, Y., Qi-long, Y., Jie, S., Kun-yu, Z., Wen, J. (2011), 'Effect of Heat Treatment on Microstructure and Property of Cr13 Super Martensitic Stainless Steel', *Journal of Iron and Steel Research International*, Vol. 18(11), pp. 60–66.
- Zheng, H., Ye, X. N., Li, J. D., Jiang, L. Z., Liu, Z. Y., Wang, G. D., and Wang, B. S. (2010), 'Effect of carbon content on microstructure and mechanical properties of hot-rolled low carbon 12Cr-Ni stainless steel', *Materials Science and Engineering A*, Vol. 527, pp. 7407–7412.